

This is the peer reviewed version of the following article: Bosence, D. and Gallois, A. (2022), How do thrombolites form? Multiphase construction of lacustrine microbialites, Purbeck Limestone Group, (Jurassic), Dorset, UK. *Sedimentology*, 69: 914-953, which has been published in final form at <https://onlinelibrary.wiley.com/doi/10.1111/sed.12933>. This article may be used for non-commercial purposes in accordance with Wiley Terms and Conditions for Use of Self-Archived Versions. This article may not be enhanced, enriched or otherwise transformed into a derivative work, without express permission from Wiley or by statutory rights under applicable legislation. Copyright notices must not be removed, obscured or modified. The article must be linked to Wiley's version of record on Wiley Online Library and any embedding, framing or otherwise making available the article or pages thereof by third parties from platforms, services and websites other than Wiley Online Library must be prohibited.

PROF. DAN BOSENCE (Orcid ID : 0000-0001-8541-4138)

Article type : Original Article

How do thrombolites form? Multiphase construction of lacustrine microbialites, Purbeck Limestone Group, (Jurassic), Dorset, UK

DAN BOSENCE* and ARNAUD GALLOIS*

*Department Earth Sciences, Royal Holloway University of London, Egham, Surrey, TW20 0EX, United Kingdom (E-mail: d.bosence@rhul.ac.uk)

Associate Editor – Jim Hendry

Short Title – Jurassic lacustrine thrombolites

ABSTRACT

This paper examines how non-marine thrombolites are formed through a complex, multiphase process of microbial framework construction, erosion, cementation, recrystallization and episodes of internal sedimentation. Recognition of such phases of thrombolite construction provides a framework for the interpretation of the fluctuating environmental conditions leading to their formation. Microbialite frameworks are examined in detail from the Purbeck Limestone Group and their affinities and palaeo-environmental significance assessed. Three types of thrombolite, one stromatolite and a leolite are described and interpreted. The thrombolite frameworks include: a peloidal mesoclotted type, a thrombolite constructed by the filamentous alga *Cladophorites* and a type with concentrically laminated micritic mesoclots. Physical and chemical erosion led to extensive early cavity formation within the frameworks. Early calcite rim cements with associated spherulites then developed over the microbial frameworks and these were reworked into cavities. Frameworks were also replaced by chalcedonic quartz and calcite spherulites. Internal sediments

This article has been accepted for publication and undergone full peer review but has not been through the copyediting, typesetting, pagination and proofreading process, which may lead to differences between this version and the [Version of Record](#). Please cite this article as [doi: 10.1111/sed.12933](https://doi.org/10.1111/sed.12933)

This article is protected by copyright. All rights reserved

comprise peloids, intraclasts and brackish-water molluscs and ostracods, together with their debris. The thrombolites grew in moderate-energy to high-energy shallow, lacustrine, microbial mounds whereas stromatolites occurred in deeper-water settings. A brackish-water, lacustrine setting is indicated by the preserved macro-biota, microbes, absence of charophytes and syndepositional evaporites, and negative stable carbon and oxygen isotope ratios. Strontium isotopes suggest that the carbonate-rich waters were fed from erosion of Mid-Lower Jurassic limestones on the western basin margin with possible mixing with waters from nearby uplifted Upper Jurassic limestones and with Late Jurassic seawater. The research indicates that non-marine thrombolites have a complex, multiphase origin resulting in a diverse succession of textures and structures relating to microbially induced and influenced construction, dissolution, cementation, recrystallization and mineral replacement which have not been previously recorded and indicate the major differences between marine and non-marine thrombolites.

Keywords Algal limestone, England, microbialite, Purbeck, thrombolite, Upper Jurassic.

INTRODUCTION

The aims of this paper are to address:

- 1 How thrombolites are formed through a combination of biotic microbial framework construction, erosion, internal sedimentation and early diagenetic alteration.
- 2 What thrombolites can tell us about the environment of formation of non-marine, Mesozoic carbonate mounds.

The rationale for the study is that thrombolites are enigmatic, often poorly described and understood carbonate rocks. They have an irregular and commonly disorganized internal structure that is challenging to describe. For example, the review by Riding (2000) states that they have a “blotchy, generally unlayered, mesoscale fabric” that ranges in form from “diffuse to distinct, and from primary to secondary”. Pache *et al.* (2001) describe Miocene thrombolites as “extremely heterogeneous in thin section”. Many, particularly those formed in Cambrian and Lower Ordovician rocks, are described as having a microbial framework composed predominantly of coccoid communities (Kennard & James, 1986), some as agglutinated structures (e.g. Riding *et al.*, 1991) and

others as bioturbated stromatolites (e.g. Walter & Heys, 1985). The term thrombolite clearly covers a diversity of microbial and diagenetic fabrics and their precise structure has frequently evaded comprehension or a clear definition. However, thrombolites are typically formed of peloids (of various origins), calcified microbial sheaths/filaments, associated early cements and numerous cavities variably filled with cements and sediments. They form one end-member of three types of microbialite, with variations in between, proposed by Schmid (1996) and later modified by Dupraz & Strasser (1999) from clotted thrombolites (after ‘clotted fabric’ of Aitken, 1967; p. 1171) to laminated stromatolites (Kalkowsky, 1908; in Riding, 2011) to dense leiolites (lacking distinctive macrofabrics, Braga *et al.*, 1995), terms that are all used in this paper (Fig. 1).

Central to an understanding of thrombolite construction is the structure and role of mesoclots (Kennard & James, 1986). This is an equivalent term to ‘clots’ of Aiken (1967), introduced by Kennard & James (1986) to avoid confusion with the micro-scaled clotted textures such as ‘Spongiostromata’ (Pia, 1927) and ‘grumeleuse’ (Cayeux, 1935). Shapiro (2000) further clarified these terminological issues and introduced scale-dependant descriptors (illustrated by Flügel, 2004) as micron to millimetric ‘microstructure’ [*cf.* Spongiostromata of Pia (1927) together with peloids, filaments etc.], a millimetric to centimetric ‘mesostructure’ (*cf.* mesoclots of Kennard & James, 1986), a decametric to metric ‘macrostructure’ (domes, columns etc.) and ‘megastructure’ for the overall microbial buildup (for example, biostome, bioherm, mound) and this scheme is followed in this paper.

In this examination of Late Jurassic thrombolites a new approach to their study is taken that is informed by work on other, bioconstructed carbonate rocks, namely shallow-marine coral and coralline algal reefs. Here, complex rock fabrics result from multiple phases of bio-construction, erosion, encrustation, internal sedimentation and early cementation (Ginsburg & Schroeder 1973; Bosence 1984). Whilst some of the processes differ, a similar method of examination, together with the principle of multiphase construction, can be applied to both types of carbonate rocks. Following this approach, this paper unravels, for the first time, the different phases involved in the formation of thrombolites which provides clues to the evolving environmental conditions that are required to produce these complex carbonate rocks. This approach makes some progress in resolving the current enigma that the fabrics of non-marine thrombolites appear not to be diagnostic of different environments (e.g. Della Porta, 2015). Rather similar fossil microbes and microbialites have been described from subaqueous freshwater, brackish, marine and hypersaline environments from the Proterozoic through to the present day.

This paper is based on particularly well-exposed rocks of the Purbeck Limestone Group (PLG), Upper Jurassic, Dorset, UK (Fig. 2) cropping out along the UNESCO World Heritage Site of the Jurassic Coast. Previous research on the microbialites (or algal limestones) of the PLG extends back to the early 19th century and is reviewed in Appendix S1.

METHODS

This work is based on 22 detailed logs from the coastal sections and inland quarries (mainly on Isle of Portland) (Fig. 1). From these, 300 samples were collected of which 228 were slabbed and 237 thin sections were prepared as detailed and precisely located by Gallois (2016), and Gallois *et al.* (2018). A subset of 63 thin sections were from the microbialite facies, the focus of this paper. Thin sections for scanning electron microscopy (SEM) study were polished then etched in 1% HCl for 30 seconds and carbon coated for study on a Hitachi S3000 (Hitachi, Tokyo, Japan) at Royal Holloway University of London (RHUL). Selected thin sections were studied using cathodoluminescence (CL) but CL did not show features in addition to those from standard thin section and SEM observation and are not illustrated. Energy dispersive X-ray analysis (EDS) was undertaken on a FEI Quanta 650F (FEI Company, Hillsboro, OR, USA) at CGG (Compagnie Générale de Géophysique), North Wales, and a Jeol JSM 6610 (Jeol Limited, Tokyo, Japan) at the University of Liverpool. Carbon and oxygen stable isotope analyses were undertaken on drilled bulk samples from a fresh quarry face at Perryfield Quarry, Isle of Portland. Initially holes were drilled to about 1 cm into the face, the drill and hole were cleaned with compressed air and 2 to 3 g of fresh unweathered sample was drilled. Analyses of 300 to 500 µg of powder, dissolved in orthophosphoric acid were undertaken on an IsoPrime Multiprep and dual inlet mass spectrometer system (Elementar, Langensfeld, Germany) at RHUL with a precision of 0.12‰ for $\delta^{13}\text{C}$ and 0.03‰ for $\delta^{18}\text{O}$. Standards used were NBS-19, LSVEC and RHUL internal calcite. Strontium isotopes were measured on the thermal ionization mass spectrometer (VG 354; Thermo Fisher Scientific, Waltham, MA, USA) at RHUL with mean $^{87}\text{Sr}/^{86}\text{Sr}$ values for SRM 987 of 0.710244 and error of ± 0.000030 .

STRATIGRAPHIC SETTING OF MICROBIALITES

The Purbeck Limestone Group (PLG) is exposed in quarries and cliffs on the northern and southern limbs of a string of anticlines along the south coast of Dorset (Fig. 2). These structures were formed during Cenozoic compression of the area that inverted former hangingwall basins to the Ridgeway

and Purbeck faults (Fig. 2) (Underhill & Stoneley, 1998). The faults are soft linked by a relay ramp centred around the Lulworth area (Fig. 2). The quarry faces on the Isle of Portland provide the best exposed vertical sections through the mounds of the PLG (Figs 2 and 3A to E). The lowest part of the PLG [the Mupe Member of the Lulworth Formation of Westhead & Mather (1996)] comprises three similar metre-scale lacustrine depositional sequences separated by microkarstic erosion surfaces (Gallois *et al.*, 2018). These surfaces of emergence are overlain by transgressive palaeosols, passing up to sub-lacustrine mounds and intermound facies (Fig. 3A). Mound growth is commonly, but not always, around former trees rooted in the underlying palaeosols. Subsequent growth is preferentially on upper surfaces and comprises the Thrombolite sub-facies of Gallois *et al.* (2018). These accumulations grow upwards and outwards and are then cut by the succeeding erosion surface (Gallois, 2016). These three depositional sequences have traditionally (see review by Ensom, 2002) been referred to as the Caps, comprising, in stratigraphic order, the Skull Cap, the Hard Cap and the Soft Cap (Fig. 3E). Plan views are best displayed in the coastal outcrops east of Lulworth Cove including the Fossil Forest (Arkell, 1947; West, 2018a; Gallois *et al.*, 2018), together with bedding surfaces in old quarries on the Isle of Portland (Francis, 1984). A thorough re-investigation of the Caps, their carbonate mounds and their associated facies of south Dorset was undertaken by Gallois (2016) and Gallois *et al.* (2018) and this paper is an extension and refinement of these studies. They describe mounds that are constructed by the Microbialite facies (Thrombolite and Stromatolite sub-facies) and a Burrowed boundstone facies (for details see Gallois *et al.*, 2018). Intermound, bedded strata comprise the Intraclastic peloidal packstone-grainstone facies of Gallois *et al.* (2018) (Fig. 3). The occurrence and main features of the Thrombolite sub-facies are described by Gallois *et al.* (2018) but are examined in detail in this current paper and their Stromatolite sub-facies is not discussed further.

The microbialites of the PLG are complex structures built by three different types of microbial/algal filaments (below) and by 12 different components that are described in Table 1 and illustrated in Figs 4 to 12. Interpretations are discussed below. Whilst for convenience of description the components of the thrombolites are divided into depositional and diagenetic features (Table 1) some of these cut across this somewhat artificial classification and involve both processes in their formation. The subsequent section describes how these components build the five types of microbialite framework recognized within the mounds of the Purbeck Caps.

DEPOSITIONAL STRUCTURES AND TEXTURES

Filaments

Filaments are abundant within mesoclots in the thrombolites and in some places form a dense framework. These tubular features have a variable in internal diameter (15 to 85 μm), have a distinct, dense micrite wall and are characterized by lateral, as opposed to dichotomous, branching (Fig. 4A to C). The size, morphology and the common lateral branching appear to be similar to that of the modern genus *Cladophora* (Fig. 4D). This freshwater to marine green alga that has many similarities to the fossil taxa *Cladophorites* (Fig. 4C) known from Cenozoic freshwater limestones in Germany and France (Riding, 1979, Arp, 1995, Freytet, 1997). The commonly occurring Purbeck filaments that are major constructional element of the thrombolites are therefore assigned to *Cladophorites* Reiss (1921), even though the younger Cenozoic examples have somewhat larger diameter filaments (Riding 1979, Arp, 1995). These filaments, together with the reported observation of rare internal cross-partitions, led to their previous identification as *Pycnoporidium* (Yabe & Toyama, 1928) and a comparison with the Recent *Cladophora* by Bosence (1987; Appendix S1). However, a more extensive examination in the current study has failed to confirm the cross-partitions within the filaments, so they are hereby assigned to *Cladophorites*. Previously, both Brown (1963) and Pugh (1968) identified *Ortonella*, *Girvanella*, *Cayeuxia* and *Hedströemia* in the Caps of the basal PLG that were incorrectly assigned at that time to the codiacean green algae, but these taxa have not been recognized in this study's re-examination of this material (for details see Appendix S1). These earlier records are now considered to be incorrect identifications and therefore have led to mis-interpretation of a hypersaline environment of deposition for the microbialites (or Caps) by these, and by subsequent authors (e.g. West, 1975).

Very rarely, much finer filaments are found intertwined within the *Cladophorites* thallus (Fig. 4E). These vary from 2 to 6 μm (average 4 μm) in diameter and do not exhibit any branching, and with these characteristics are interpreted as cyanobacterial filaments. Similar filaments, in a similar association, were described by Hudson (1970) from Middle Jurassic algal limestones from Scotland. That interpretation, with which this current study concurs, is that these can be compared with Recent *Schizothrix* filaments (*cf.* Monty, 1976) that nowadays are assigned to the cyanobacteria.

One fragment of an algal thallus, abraded and coated by a micritic crust has been found, in the basal Hard Cap of Worbarrow Bay (Fig. 4F and G). This comprises a thallus of closely spaced filaments with circular to polygonal shapes in transverse section and diameters varying from 35 to 75 μm (average 52 μm). The filaments are divided into cells separated by curved walls. This is similar to

fragments previously identified as *Solenopora* (Pugh, 1968), an ancestral coralline alga also reported from the basal Caps by Brown (1963) and by West (1975). However, the current status of *Solenopora* is that it is now regarded as an Ordovician sponge (Riding, 2004). Previously, Rothpletz (1908) placed *S. jurassica* in the genus *Solenoporella* and this attribution is followed in this study for the Purbeck material (Fig. 4E and F). This alga is a common framework builder in shallow-marine patch reefs in the underlying Portland Limestone (Townson, 1971, 1975) and as it only occurs as fragments it is interpreted as a derived fossil and therefore cannot be used as a palaeoenvironmental indicator (*cf.* Brown, 1963).

Fragments of filaments, and degraded and diagenetically altered filaments, with deci-micron-sized diameters occur throughout the thrombolites of the Caps (for example, Figs 5, 6A and 6B) but these do not have sufficient morphological detail for positive identification, or even assignment to different algal/microbial groups. They are, therefore, referred to just as microbial filaments in this work.

Peloids

Some peloids (see Table 1; Fig. 5) are comparable to types 2 and 3 of Samankassou *et al.* (2005) from the PLG, described as containing relics of fossils (commonly ostracods), or rounded, micritic intraclasts respectively. However, in the Caps these two types occur within a spectrum of peloid types (Table 1). Brown (1961, 1963) described similar peloids from the lower Purbeck beds of Dorset to those described here (Table 1). Brown (1961, 1963) compared the ‘mud grains’ in the pellets with those of the associated algal nodules (thrombolite framework of this paper) and proposed that they were derived from abrasion of these micritic mesoclots, an interpretation with which this study concurs. However, a faecal origin cannot be ruled out for the rounded, undifferentiated peloids, even though this was discounted by Brown (1963) and by Samankassou *et al.* (2005).

Intraclasts

Intraclasts are described in Table 1 and illustrated in Fig. 6. Their textural immaturity and microstructure and close proximity to eroded microbial frameworks all indicate a local origin.

Skeletal fossils

No entire specimens of molluscs or ostracods have been recovered in this study from these generally

massive and well-indurated rocks. However disarticulated valves and fragments are commonly preserved (Table 1; Fig. 7A and B). Arkell (1947) records “freshwater gastropods *Hydrobia* and *Valvata*, with *Cyrena*” from the lowest beds of the PLG at Holworth House. Subsequently, Radley (2002) recorded a molluscan fauna from Portesham Quarry that was interpreted to represent a mixture of marine with low-salinity and freshwater taxa. Similarly, a brackish to ‘near-marine’ environment was interpreted by Coram and Radley (2021).

Previous work on the ostracods from the Hard Cap at Portesham Quarry by Barker *et al.* (1975) identified three palaeoenvironmental groups; marine, euryhaline and oligohaline, from which they concluded that the marine forms were most likely transported and that the remainder indicated brackish-water conditions. Horne (2002) examined entire ostracod valves from the Hard Cap of Freshwater Bay, Portland, containing “probably *Fabanella* sp.” and “probably *Mantelliana purbeckensis*”. The former was regarded by Horne (2002) as ‘athalassic’ (saline, but not connected to the sea) and the latter, a cypridoidean, whose members largely inhabit fresh waters. To conclude, the invertebrate fossils indicate a mixture of marine, low salinity and freshwater habitats in the PLG caps.

EARLY DIAGENETIC STRUCTURES AND TEXTURES

Early diagenetic features of the thrombolites (Table 1; Figs 5 to 12) were formed during or soon after construction of the thrombolite framework near to the sediment-water interface. These are described below in order of their abundance within these rocks. Later-stage processes that have also affected these rocks such as fracturing, pressure solution and blocky calcite cementation are not considered in this paper.

Erosion/dissolution surfaces

The outer surfaces of the mesoclots are commonly irregularly shaped and truncate internal structures (Table 1). Similarly, irregular-shaped erosional cavities occur within the mesoclots (Fig. 7C and D) where primary thrombolite frameworks have been eroded or dissolved. The truncation surface is commonly overlain by internal sediments containing the components described above or overgrown by early cement fringes (see below). Similar erosion surfaces were described by Hudson (1970) from the ‘nodular algal beds’ of the Great Estuarine Group, Scotland, in which subaerial exposure for the dissolution of the microbial framework was favoured. Similarly Arp (1995) interpreted dissolution cavities in microbialites from the Ries crater as vadose in origin as they are associated with

pedogenic facies. Both physical erosion by bottom currents, and/or chemical dissolution were possible erosional processes in the Purbeck thrombolites, acting independently or together. Physical erosion is supported by the abundance of microbialite intraclasts, peloids of erosional origin and the context of moderate-energy to high-energy grain supported facies of the adjacent intermound sediments (Gallois *et al.*, 2018). However, it is difficult to envisage currents powerful enough to erode material from the early-lithified mesoclots within the thrombolites. Dissolution is therefore the favoured mechanism and could have been driven by increased dissolved organic carbon and organic acids from metabolic activity within the mat community itself, leading to decreased pH (*cf.* Monty, 1976; Dupraz *et al.*, 2009), undersaturated lake waters, or to vadose dissolution below the emergent microkarstic surfaces and palaeosols (Fig. 3). Present-day thrombolites commonly have cavities that are considered to result from dissolution (Golubic, 1973; Monty, 1976) or, have been recorded, but not interpreted (for example, Laguna Bacalar, Mexico, Gischler *et al.*, 2008; Shark Bay, Australia, Jahnert & Collins, 2011). Internal dissolution is favoured against vadose dissolution as the cavities are filled with cements and sediments typical of the Purbeck sublacustrine thrombolites as opposed to fabrics commonly described from vadose regimes (e.g. Arp, 1995; James & Jones, 2015).

Fibrous cement fringes

These early cements are described in Table 1 and illustrated in Fig. 8A and B. Similar, cement fringes were described from the Purbeck caps by Brown (1961) and by Kirkham & Tucker (2018) and are also commonly reported in modern analogues such as Holocene thrombolites of Mono Lake, USA (Fig. 8C and D), Quaternary tufas from the UK (Pedley *et al.*, 2014) and in other ancient thrombolite examples. Both Hudson (1970) and Andrews (1986) from the Jurassic; and Riding (1979) and Arp (1995) from the Miocene, describe similar rim cements in algal limestones as ‘micro-tufa’ and ‘laminated sinter’, respectively. These were interpreted as having formed during emergence; the former on the basis of its brecciation and associated gypsum pseudomorphs, and the latter on the basis of pendant morphologies, and reworked extraclasts in adjacent sand-filled channels. None of the above features are found in the examples from the Purbeck thrombolites, where cement fringes grew over an earlier erosional surface and are overlain by internal sediments. They are therefore considered to be early cements precipitated in a sub-aqueous setting. The fibrous fringing cements, along with their thrombolite substrate, are locally reworked into internal cavities in the thrombolites. This is interpreted as resulting from shallow sub-lacustrine erosion and redeposition as other intraclasts are also common within the thrombolites as well as in the intermound packstones (Gallois

et al., 2018). No evidence is seen of microbial remains within these calcite cements, despite their abundance in the main thrombolite fabrics, suggesting there is no *biological control* (*sensu* Dupraz *et al.*, 2009) on their formation.

Microspar

This texture (Table 1; Fig. 9) has aspects of both a depositional and a diagenetic origin. Its laminated appearance with size-sorted intraclasts (Fig. 9A) indicate an initial sedimentary origin, as does the composition, with pockets of silicate minerals between the spar (Fig. 9B, C and E). However, the current texture is of interlocking calcite crystals (Fig. 9B and D) and is clearly diagenetic. Pockets of presumed clay minerals are located between the spar crystals (Fig. 9E). It is proposed that an original fine-grained calcite has recrystallized to a microspar (*sensu* Bathurst, 1971). This interpretation agrees with Andrews (1986) who described similar features preserved in porostromate facies from the Jurassic of Scotland. The origin of the original silt-grade calcite sedimentary particles is less clear but the laminated geopetal fills and abundant preservation of <4 µm micrite in the surrounding mesoclots argues against a micrite precursor for the microspar (*cf.* Bathurst, 1971). However, it does have a strong resemblance to the ‘crystal silt’ of Dunham (1969) that could then have recrystallized to a microspar in line with the process described by Andrews (1986). If silts, then these could have two possible origins in the Caps; either derived from erosion of early cements and filtering of crystals down through the framework cavities in the shallow lacustrine environment, or, as vadose diagenetic products associated with overlying palaeosols. The former interpretation is favoured as the microspar occurs at many different levels within the thrombolites and is not associated with any other features of vadose diagenesis or with the palaeosols.

Quartz spherulites

Chalcedonic spherulites are only found within the thrombolites of the Purbeck Caps (Table 1; Fig. 10A to D) and are seen to replace the thrombolite frameworks, early fringe cements and calcite spherulites (see below) but are not seen reworked into internal sediments of the thrombolites. These aspects indicate *in situ* formation within the thrombolite and some distance from the actively growing, and commonly eroded, thrombolite surface. Intraclasts of thrombolite containing spherulites are observed, but only rarely.

Whilst silicified microbial filaments have not been found, oriented ghosts of the filament framework are locally preserved in the spherulites. No evidence is seen of quartz spherulites

associated with former evaporite minerals as reported by West (1964) for the Caps in general. The facies restriction of these spherulites suggests an early diagenetic control on their formation. Francis (1982) proposed that diatoms could be the source of the silica, but diatoms of this age are rare, and can now be discounted, because their incursion into freshwater took place early in the Cenozoic (Sims *et al.*, 2006). Siliceous, non-marine, sponges [for example, *Spongilla purbeckensis* (Young, 1878; Pronzato *et al.*, 2017)] are a possible source of biogenic silica in the PLG, although no evidence of spicules has been seen in the Caps.

An inorganic source from detrital quartz is possible as grains occur sparsely in the surrounding, intermound facies. Inorganically precipitated silica is reported from the Coorong lakes of Western Australia (Francis, 1984) being driven by high seasonal increases in pH (*ca* 9), for the dissolution of detrital silica (Peterson & Von der Borch, 1965). This silica-rich brine then precipitates as gelatinous opal-cristobalite during the dry season in areas of lower pH such as just below the sediment surface where plant material is decaying. In the Caps an equivalent silicification site could have been the organic-rich mesoclots and might explain the absence of spherulites in the nearby internal and external granular sediments. More recently, Brehm *et al.* (2005) reported experiments where microbial communities in biofilms caused the dissolution of detrital quartz and this process may explain the supply of silica for spherulite formation uniquely within the thrombolites in the Caps. Traces of silica are detected within the mesoclots associated with Type 2 calcareous spherulites (see below) and detrital quartz is occasionally seen in the surrounding intermound sediments. Higher in the PLG silicification is common in a range of facies (West, 2018b) so the original source for the silica is not restricted to the Caps. A further aspect of this problem is that marine Jurassic sponge-thrombolite mounds from Europe and Morocco commonly have dissolved siliceous spicules, however, there are no reports of silica replacement of the adjacent mesoclots (e.g. Leinfelder & Keupp, 1995; Reitner *et al.*, 1995; Della Porta, 2013; Aurell & Bádenas, 2015).

Alternative sources of inorganic silica from clay mineral or feldspar diagenesis are considered unlikely as the rocks have not been buried deep enough (Bray *et al.*, 1998) to release silica. Similarly, there is no evidence of an external source of silica, such as volcanism, in this non-volcanic basin margin and silica is not seen in faults or fractured fabrics.

Calcite spherulites

Four types of calcitic spherulites are recognized within the thrombolites of the Caps, that occur, within cavities, within mesoclots and as reworked intraclasts. They do not appear to be spatially

related to the quartz spherulites (above) except where they are locally replaced by silica, or to the ooids in surrounding packstones and grainstones.

Type 1 spherulites

Spherical crystal aggregates of calcite (Table 1; Fig. 11A and B) are contiguous with the isopachous fringe cements (see above) and in these occurrences apparent spherulites are likely to represent two-dimensional slices through three-dimensional botryoidal protuberances (Fig. 11A). Examples also occur as isolated grains in cavities within the thrombolites alongside other allochems (Fig. 11B) where their continued growth after settling is indicated by fitted textures. Rarely, larger (<800 µm) spherulites are seen developing as syntaxial overgrowths on ostracods.

Brown (1961, 1963) described and illustrated brown, fibrous botryoidal growths and spherulites with calcite-mudstone cores similar to the spherulites described here. The colour, the association with preserved calcareous algae and a comparison with the Pleistocene tufas of Searle Lake, California (Scholl, 1960), were taken by Brown (1961, 1963) as evidence of these having formed in an ‘algal gel’ on the mudstone nuclei. Hudson (1970) also described brown, radial crystal spherulites of a similar size from the Middle Jurassic of Scotland occurring in a pellet limestone. It was noted that the spherulites showed fitted textures and that they occurred alongside, but also partially replacing, micritic pellets. These appear to be similar to Type 1 spherulites. Brown (1961) and Kirkham & Tucker (2018) considered that the fibrous cements nucleated on the top of calcite spherulites. The evidence from the current work is that the cement fringes and the spherulites show growth interference and were therefore forming at the same time. However, it seems clear that apparent spherulites can also form from sections through botryoidal heads, that such heads might be reworked to form individual spherulites, and also that fringe cements may precipitate around micritic clasts (for example, peloids) to form individual spherulites. Both spherulites and cement fringes comprise microporous calcite with minimal Mg and Fe within background values (Figs 6 and 12) and microbial remains have not been seen despite their abundance in the adjacent mesoclots.

Experimental work by Pedley *et al.* (2009) and Mercedes-Martin *et al.* (2016) showed that small spherulites and botryoidal crusts grow in close proximity from artificial alkaline and saline waters supersaturated with CaCO₃ as long as organic acids are present. Alginic acid binds onto the 1014 cleavage planes of calcite crystals thus promoting radial growth and spheroidal morphologies. As the Purbeck fringe cements and spherulites grew on the eroded, presumed dead, substrate of mesoclots and with no preserved microbial remains, then the microbial community could not have

induced calcite precipitation (*sensu* Dupraz *et al.*, 2009). Therefore, an organic matrix or extracellular polysaccharides (EPS) with associated organic acid molecules on the eroded surface of the mesoclots is proposed (*cf.* Mercedes-Martín *et al.*, 2016) that would have *influenced* (*sensu* Dupraz *et al.*, 2009) calcite precipitation of the closely associated fringe cements and Type 1 spherulites.

Type 2 spherulites

The fitted margins to these calcite spherulites (Table 1; Fig. 11C to E) and clusters of spherulites that occur ‘floating’ within the micrite and peloidal wackestones–packstones of thrombolite mesoclots (Fig. 11C) indicate that these spherulites result from recrystallization of mesoclots to form neomorphic spherulites. EDS analysis of the calcite spherulite cortex indicates inclusion of Al and silica from the host muddy sediment.

Type 2 spherulites are similar to replacive spherulites found in thrombolites from Mono Lake (Fig. 8D), Searle Lake (Scholl, 1960) and Great Salt Lake (Chidsey *et al.*, 2015) although there are some differences in their detail. The modern examples are not always spheroidal and can be fans and botryoidal morphologies but are seen to have replaced microbial fabrics and early fringe cements just beneath the actively growing margin of the thrombolite (Fig. 8D), but also growing into adjacent cavities as a cement. Otherwise, replacive calcite spherulites in thrombolite fabrics do not appear to have been previously described. Monty (1976) described the process whereby microspherulites growing within pore spaces in modern microbial mats from Mono Lake, USA, and Shark Bay, Australia, that develop and enlarge to form the mesoclots, thereby involving spherulites in the formation of mesoclots and thrombolites. This study sees no evidence of this progression in the Purbeck thrombolite fabrics and view the spherulites as a neomorphic replacement of mesoclots rather than being involved in the primary thrombolite framework formation. As the spherulites do not show any preserved evidence of organic remains a *microbially-influenced* process (*cf.* Dupraz *et al.*, 2009) of crystal growth in the mesoclots is envisaged for their formation, as for Type 1 spherulites (above).

Type 3 spherulites

These occur in cavities alongside Type 2 spherulites, are slightly larger, and have better ordered radial crystal growth reflected in their extinction crosses in thin section between crossed polars (see Table 1; Fig. 11C and F to H). As they also show growth interference with neighbours they are interpreted as a type of cement that precipitated within cavities in the thrombolites. Clearly Types 2

and 3 are closely associated and similar conditions for precipitation existed within the mesoclots and the nearby cavities. The larger size, and more organized radial arrangement of the calcite crystals of Type 3 suggests that growth in cavities was more favourable, possibly due to greater pore fluid flow, or microbial activity in cavities, or due to free crystal growth as a cement as opposed to replacement of a micritic substrate. As with Type 1 examples, there is no evidence of preserved microbial organisms within the spherulites in thin sections, SEM or reflected UV light, despite their preservation in the surrounding thrombolite fabric.

Type 4 spherulites

Clusters of spherulites are also found locally as intraclasts in packstones and rudstones (Table 1; Fig. 12F and G). Some occurrences are difficult to separate from Type 2 spherulites when present in packstones. However, distinguishing features include sharp outlines with micritic envelopes to the intraclasts (Fig. 12F) and reworked Type 2 spherulite clusters in their original matrix now preserved in packstones and rudstones with a different texture (Fig. 12G), indicating erosion, transport and redeposition as a particular type of spherulitic intraclast.

FIVE TYPES OF MICROBIALITE

From field study, hand specimen (Fig. 13) and thin section (Fig. 14) examination of the microbialite facies of the three levels of the Caps, and throughout the study area, it is apparent that there is considerable diversity in the way they are constructed. The previously described components (Table 1) combine in different ways, to form five distinct types of microbialite; three thrombolites, a stromatolite and a leiolite. These all occur within the ‘Thrombolite subfacies’ of Gallois *et al.* (2018). The different types are not always expressed in the weathered or quarry cut surfaces studied in the field and may only become apparent when viewed in slabbed specimens, or thin sections, where different components can be traced out and their construction interpreted (Figs 15 to 18).

Peloidal thrombolite – PTh

This is the commonest thrombolite type occurring in all of the Caps, and in 46% of the samples examined. It has a distinctly blotchy appearance at the mesoscale with the mesoclots either darker or lighter than the intervening pockets of internal sediment (Figs 13A, 14A and 15). The mesoclots are equant to lobate and may show a preferred elongation along the larger-scale accumulation layering of the thrombolite (for example, Fig. 3D). The darker, irregularly shaped mesoclots are micrite-rich and

peloid-rich constructions and locally have poorly preserved, unidentifiable fragments of microbial filaments. The arrangement of the components within the mesoclots appears chaotic with no internal layering or preferred filament orientation. Locally, mesoclots are lighter in colour and these have clusters of Type 2 calcite spherulites replacing the mesoclots or Type 3 spherulites, infilling cavities (for example, Fig. 11C to G). The mesoclots are surrounded by irregular-shaped framework pores (Fig. 13A) infilled with peloids, micrite matrix and microspar, either overgrown by later blocky spar, or remaining as voids. There are few differences between the components of the mesoclots and the cavity infills so that they are better defined by their morphology and cross-cutting relations rather than their sedimentary components. An earlier generation of smaller and more irregular shaped cavities occur within the mesoclots (Figs 14A and 15). These are interpreted as erosional in origin because of their shape and truncated marginal filaments (Fig. 14A).

The fabric of this rock indicates a construction of mesoclots that accumulate upwards and outwards from the substrate. The variably preserved filaments within the mesoclots indicate a microbial component to the clotted thrombolite fabric (Fig. 1). There are few clues to the processes involved in the formation of the mesoclots themselves apart from poorly preserved microbial filaments, which may originally have aided in trapping, binding and early lithification of the contained peloids, lime mud and skeletal debris. Microbially influenced micrite precipitation is expected but cannot be proven. Internal cavity formation is early and infilled by later fibrous cement and sediment, and may have been driven by oxidation of organic material (Monty, 1976) and/or dissolution from lowered pH waters with organic acids (Dupraz *et al.*, 2009). A similar combination of processes is interpreted in the formation of present-day mamillate and pustular mats in Shark Bay, Australia, by Monty (1976), albeit from colonies of unicells (*Entophysalis*) rather than filamentous forms.

***Cladophorites* thrombolite – CTh**

This thrombolite type is easily identified in the field as the mesoclots have distinctive, irregular through to columnar shapes, and variations in the morphology of these mesoclots pick out large-scale accretion surfaces within the thrombolites (Figs 3B and 13B). Mesoclots are commonly 0.5 to 1.0 cm across and the columns extend upwards and outwards, for up to 4 cm. On the inclined sides of the thrombolite domes, the columns are seen to have a subvertical orientation. The mesoclots are primarily constructed by upwardly and outwardly growing, radiating and branching filaments of *Cladophorites* (Figs 13B, 14B and 15) with dense, dark, micrite walls. This thrombolite fabric can

preserve a large amount of primary growth framework porosity (Fig. 13B). These cavities are filled with an internal sediment comprising lighter-coloured micrite and peloids, together with early fibrous cements, microspar, calcite spherulites, or later spar cements, or they may remain open as pores (Fig. 13B). Locally, this thrombolite is seen to develop small (hundreds of microns across), irregular-shaped cavity systems that truncate the filament framework (Figs 14B and 17). These are filled with different generations of internal sediment of varying composition or by spar cement. The CTh occurs in the Hard and the Skull Caps in 21% of the thin sections studied.

Bosence (1987) labelled this microbialite as a ‘skeletal stromatolite’ (*sensu* Riding, 1977) because of the microscale, concave-down layering seen in the columns (for example, Fig. 15) and the construction from calcified filaments. The current study is more extensive and indicates that the *Cladophorites* filaments occur in many shapes of mesoclots and, as the layering is only locally present, they are more accurately described as thrombolites. Similar, millimetre-scale layering is described by Arp (1995) from their *Cladophorites* framestone microfacies that is interpreted as seasonal.

A pervasive organic framework typifies this thrombolite as the mesoclots are constructed principally by filaments. Their vertical elongation, even on the inclined sides of thrombolite domes suggests a phototrophic response that is consistent with the presumed green algal affinities of *Cladophorites*. The organic framework is interpreted to have *biologically-induced* (*sensu* Dupraz *et al.* 2009) precipitation of calcite on and around the filaments. The filament network trapped peloids, lime mud and less commonly, skeletal debris to form the mesoclot. The small, irregular cavities within the mesoclots with truncated filaments are similar to those described from the PTh (above) and are also interpreted to result from dissolution. Similar, non-marine, filament frameworks and associated grains and cements are described from the Recent by Monty (1976) and Freytet & Verrechia (1998), and from the Cenozoic (Riding, 1979; Arp, 1995; Freytet, 1997). Possibly equivalent, ‘nodular algal beds’ from the Jurassic are also described by Hudson (1970). Similar looking columnar growths to the *Cladophorites* thrombolite are also described that are constructed by the filamentous alga *Cayeuxia nodosa* although the author believed that this did not occur in the Purbeck Group (Hudson, 1970, p. 26).

Concentrically layered thrombolite framework – CLTh

This framework appears in 16% of the studied thin sections coming only from the Skull Cap and the Hard Cap. It has distinctive, but irregular to rounded mesoclots commonly appearing as botryoidal

growths at outcrop and in thin section (Figs 13C, 14C and 16). The mesoclots are built from concentrically arranged layers of micrite. Under SEM and EDS analysis the layers are seen to consist of a microporous low-Mg calcite micrite (Fig. 14D). However, other clots comprise layers of coarser, columnar crystals, amorphous patchy micrite, or some have small areas of poorly preserved filaments. The mesoclots in this framework appear darker brown than the intervening cavities that are either filled with fibrous fringe cement, internal geopetal sediment (peloids, skeletal debris and calcite spherulites), or, late-stage, blocky spar. Some cavities remain unfilled (Figs 14C, 14D and 16). Mesoclot centres may appear paler in colour where more porous, where recrystallized to a neomorphic calcite spar, or, where quartz or calcite spherulites are present (Figs 14C, 14D and 16).

The orientation of the layering and accumulation of the mesoclots indicates an extremely irregular thrombolite framework with an overall upward and outward growth, in common with the other framework types, but also show inward growth into cavities (Fig. 16). With these microscale characteristics and the local preservation of filaments, this fabric is interpreted as microbial, however it is not known if there are similar modern microbial fabrics, and some examples may be inorganic precipitates of layered micrite and columnar calcite.

Peloidal fenestrate stromatolite – PFS

This microbialite occurs in 15% of the thin sections from all three levels of the Caps. It comprises an irregular and porous accumulation of small (10 to 20 μm) peloids forming a spongiostromate . Peloids occur in clusters but may also be stacked normal to the internal lamination (Fig. 14F). The peloidal fabric is permeated with fenestrae (<1 cm across) that are commonly aligned along accretion surfaces (Figs 13D, 14F and 18) and are commonly filled with two generations of pore-filling, calcite cements (Fig. 14F). An initial brown, inclusion-rich isopachous rim of small (<10 μm) followed by a clearer, equant cement (10 to 200 μm across) spar. The layered, fenestrate, peloid-rich fabric is typical for a spongiostromate texture (*sensu* Flügel, 2004), and the fabric resembles the ‘layered thrombolite’, and the ‘peloidal stromatolite’ classes (Fig. 1) established by Schmid (1996). The microbial fabric has similarities with the Stromatolite sub-facies of Gallois *et al.* (2018). However, these occurrences are regarded as distinct and different, as the latter contain micritic filaments and only occur beneath the mounds in the Skull Cap at a lower stratigraphic level. The PFS is probably equivalent to the “laminated and peloidal Stromatolitic layer” figured by Brown (1961, fig. 30) from Mupe Bay.

Dense micritic leiolite – DML

This fabric is only present in the Hard Cap and in just one of the samples studied from Portesham Quarry. It consists of a dense, structureless, micritic crust that overgrows existing thrombolites; either the CTh, or the PTh frameworks. It is not seen forming a primary framework in the microbialites. The crust may have irregular darker and lighter layers and can be up to 1 cm thick (Figs 14E and 15). The fabric lacks filaments, fenestrae, early fibrous fringe cements and calcite spherulites. The dense micrite is accreted onto subvertical to overhanging mesoclots and supports disarticulated and fragmented ostracod valves and other skeletal debris (Fig. 14E). These clasts are oriented parallel with the variably oriented underlying surface of the mesoclots resembling the ‘trapstone’ fabric of thrombolites described by Monty (1976) and the leiolite of Braga *et al.* (1995) (Fig. 1). Such accretion and trapping is interpreted as agglutination by a microbial mat even though no filaments or coccoid forms are seen in thin section or SEM.

LAKE WATER CHEMISTRY – ISOTOPIC EVIDENCE

There has been considerable debate about the chemistry of the original lake waters that deposited the Purbeck limestones and previous interpretations, based on biota and mineralogy, have varied from hypersaline to brackish to freshwater as outlined above and reviewed by Gallois *et al.* (2018). The dominant mineralogy of primary fabrics and early cements in the thrombolites, described in this paper, are considered to be low-Mg calcite (above) but just three out of 63 thin sections of the microbialites have gypsum pseudomorphs, now calcitized. Two of these are secondary replacements (i.e. gypsum moulds are not sediment filled) and the replaced gypsum is within transported intraclasts. Just one example is found with evidence of primary gypsum (dissolved and now a sediment-filled pseudomorph) that comes from the Soft Cap, the highest unit within the Caps. Gallois *et al.* (2018) document the main incoming of sulphate and chlorite evaporites described by West (1975) from beds overlying the Soft Cap. These observations are thought to help explain “the paradoxical association of evaporites with well-developed forest vegetation” (Francis, 1984) because the trees occur in the three palaeosols which occur prior to the onset of syndimentary evaporites. Isotopic ratios ($^{13}\text{C}/^{12}\text{C}$, $^{18}\text{O}/^{16}\text{O}$ and $^{87}\text{Sr}/^{86}\text{Sr}$), presented here, provide some additional evidence of lake water chemistry, independent of faunal and floral occurrences and mineralogy.

$^{13}\text{C}/^{12}\text{C}$ and $^{18}\text{O}/^{16}\text{O}$ stable isotope ratios

Regularly spaced, bulk sampling through the Skull and Hard Caps in Perryfield Quarry (Fig. 2)

provide trends of $\delta^{13}\text{C}$ and $\delta^{18}\text{O}$ (Fig. 19). The profile goes through lithologies typical for the Caps on the Isle of Portland arranged within two coarsening-upward sequences, including thrombolites, separated by palaeosols (Fig. 19). Stratigraphic trends in these isotopes within this profile occur throughout the entire profile and within each sequence. Throughout the entire section the $\delta^{13}\text{C}$ values show an overall, up-section, 2‰ negative shift whilst the $\delta^{18}\text{O}$ values show an overall slight (1‰) stratigraphic shift to more negative values. The $\delta^{13}\text{C}$ shift is interpreted as a freshening-upward change in the lake waters (*cf.* Leng & Marshall, 2004) or a lake level rise (*cf.* Sarg *et al.*, 2013) prior to emergence at the subsequent microkarstic surface and palaeosol. Little can be interpreted from the change in $\delta^{18}\text{O}$ values as these are minor and may be influenced by a number of interlinked, environmental processes in lacustrine systems (Bellanca *et al.*, 1992; Leng & Marshall, 2004). However, the ranges of both $\delta^{13}\text{C}$ and $\delta^{18}\text{O}$ are within the ranges for microbialite textures and early diagenetic calcites from the marginal lagoonal, Mid Jurassic, Duntulm Formation, of Scotland recorded by Andrews (1986) and ratios are considerably lighter in both isotopes compared with contemporaneous marine fossils (Fig. 19; Nunn & Price, 2010). Their low covariance ($R^2 = 0.47$) indicates an open lake system (Talbot, 1990).

Individually, the two sequences (the Skull and the Hard caps) both show an up-section 2‰ negative trend in $\delta^{13}\text{C}$. The thrombolite framework and thrombolite-rich, intraclast rudstone in the Hard Cap do not have distinctive $\delta^{13}\text{C}$ and $\delta^{18}\text{O}$ values in these bulk samples. The $\delta^{18}\text{O}$ values show a slight upward increase in the Skull Cap but little change in the Hard Cap (Fig. 19). These negative stratigraphic trends in $\delta^{13}\text{C}$ are similar to those described from limestones, albeit marine, beneath present-day exposure surfaces from the Caribbean (Alan & Mathews, 1982; Budd & Land, 1990). These modern examples have 2 to 4‰ upward decrease in $\delta^{13}\text{C}$ and about 1‰ upward increase in $\delta^{18}\text{O}$ within metres of the soil. Such negative $\delta^{13}\text{C}$ values are interpreted as due to enrichment by ^{12}C from soil gas and the more positive $\delta^{18}\text{O}$ values from preferential evaporation of ^{16}O within the soil. The similarity in these trends with those below the karstic surfaces and soil horizons in the Purbeck Caps is therefore considered to reflect, early vadose diagenesis. These isotope profiles from what is interpreted as an open, through-flowing lake basin in the PLG contrast with those from below palaeosols from the closed lake system of the Miocene, Madrid Basin, Spain that show a positive $\delta^{18}\text{O}$ shift up to pedogenic horizons and a strong covariance of $\delta^{13}\text{C}$ and $\delta^{18}\text{O}$ (Bellanca *et al.*, 1992).

$^{87}\text{Sr}/^{86}\text{Sr}$ isotope ratios

Strontium isotope ratios have value as tracers in determining the source of calcium carbonate in lacustrine carbonates as they do not reflect fractionation by temperature or evaporation of precipitating waters, or meteorological and vital effects (Benson & Peterman, 1996; Pache *et al.*, 2001; Jagniecki *et al.*, 2021). Potential sources for the extensive precipitation of calcium carbonate within the Purbeck microbialites are drainage off adjacent limestone terrains, episodic connections with penecontemporaneous (late Tithonian) seawater, or fluids sourced from nearby active faults (Fig. 20). Five samples drilled from Hard Cap thrombolite fabrics at Bowers and God Nore quarries have $^{87}\text{Sr}/^{86}\text{Sr}$ ratios with a mean value of 0.707357 (± 0.000030 , 0.707249 to 0.707380) and a slightly more radiogenic value 0.707476 (± 0.000030 , 0.707461 to 0.707491) was obtained from two samples of late, blocky calcite cement (*cf.* Fig. 9A).

The values from the thrombolites are too radiogenic to derive solely from seawater values of the same, late Tithonian, age (Fig. 20; approximately $^{87}\text{Sr}/^{86}\text{Sr}$ 0.70717; Jones *et al.* 1994b; Wierbowski *et al.*, 2017) which is consistent with the absence of marine fossils from the Caps. However, the thrombolite values are within the range recorded for Early Jurassic seawaters as recorded in marine fossils (Jones *et al.*, 1994a). Marine limestones of this age in the west of the basin would have been exposed for erosion during Oxfordian to later rifting (McMahon & Turner, 1998; Underhill & Stoneley, 1998). In addition, Garden (1987) identified a suite of derived siliciclastic grains from this western basin margin within the PLG. Mixing of surface waters with a westerly source together with the less radiogenic Tithonian seawater is also consistent with the data. A more locally-derived origin of Sr from dissolution of uplifted Callovian – Kimmeridgian limestones from footwall areas to the north of the Purbeck–Wight and Abbotsbury faults may have contributed but is unlikely to be the sole source, despite the occasional finds of reworked Kimmeridgian ammonites within the Purbecks (West & Hooper, 1969; Garden, 1987). These marine limestones would have had considerably less radiogenic values (Fig. 20). Another, possible alternative local source for the carbonate would be from basement-derived fluids, rising to the surface along the Purbeck–Wight and Abbotsbury faults, which are known to be active during Purbeck times (Underhill, 2002). However, this is considered to be unlikely for the Purbeck thrombolites because Devonian meta-sediments (including limestones), from the basement are very much more radiogenic with a mean $^{87}\text{Sr}/^{86}\text{Sr}$ of 0.740790 (range 0.712679 to 0.766605) from rocks that outcrop in Cornwall (Fig. 20; Darbyshire & Shepherd, 1994). The marginally more radiogenic late cement values indicate a slightly different source than that of the thrombolites as recorded by other workers for later cements in Jurassic limestones (e.g. Emery *et al.*, 1987).

To conclude, the isotopic data from the thrombolites, and the sequences that they occur within, complement and extend the information on lake water chemistry that comes from the preserved biota and mineralogy. The C and O stable isotope ratios indicate an open lake system that has a slight freshening upward trend through the Skull and the Hard caps. Above the overlying Soft Cap, the preserved evaporite minerals, or their pseudomorphs, indicate a change to hypersaline conditions in the lake. The thrombolite facies do not have a distinctive isotopic signature in these bulk samples but a negative $\delta^{13}\text{C}$ trend beneath emergent soil horizons indicates a strong vadose diagenetic overprint. Analyses of $^{87}\text{Sr}/^{86}\text{Sr}$ indicate that the source waters for the PLG lake were largely derived from erosion of Lower Jurassic marine limestones on the western basin margin but some mixing from Late Jurassic seawater and locally eroded Upper Jurassic limestones cannot be discounted.

OCCURRENCE AND DISTRIBUTION OF MICROBIAL FRAMEWORK TYPES

Out of the five microbialite types, the three thrombolites are the most dominant and make up 83% (68 out of 82 occurrences) of the frameworks as recorded from 63 thin sections (Fig. 21). In order of decreasing abundance, they comprise; PTh (56% or 46/82), CTh (21% or 17/82), CLTh (16% or 13/82), PFS (15% or 12/82) and finally the DML with just two occurrences in one sample (Fig. 21). This order of abundance does not vary significantly between the Skull Cap and Hard Cap microbialites, but the Soft Cap is dominated by the PTh and the PFS (Fig. 21). Within the thrombolites the two most abundant types (PTh and CTh) commonly occur together, rather than having different distributions or stratigraphic occurrences. This raises the question as to whether the two fabrics are in any way related? They both form upwardly and outwardly growing thrombolites but the CTh framework develops a columnar mesoclot in addition to equant and lobate mesoclots that are found in both frameworks. It is known that organic decay occurs in the early stages of accumulation of microbialites (Monty, 1976; Dupraz *et al.*, 2009) and it may have been possible that the filaments of *Cladophorites* thrombolites decayed resulting in the peloidal thrombolite with scattered remains for filaments. Intermediates between the two types have been seen but are not common. However, the former has distinctive orientations of filaments, which, together with the distinctive columnar mesoclots with their concave-down laminae that suggest that these two thrombolite types have different origins. However, they had similar distributions and therefore, presumably, similar environmental requirements.

When the data are viewed spatially throughout this region of the Wessex Basin, there are variations in proportions of the different framework types that can be related to their tectono-sedimentary settings. In the western area in the hangingwall sub-basin to the Ridgway Fault (Fig. 2), the numbers of occurrences are small, but in the Skull and Hard caps the microbialite types are similar (Fig. 21). The Soft Cap is either not exposed or, where present, does not develop microbialites (for example, Portesham Quarry). The eastern area, the hangingwall basin to the Purbeck Fault (Fig. 2), is unique in that it has significant development of the PFS in all three units. In the southern area of Portland, interpreted to have accumulated in the shallow waters associated with a relay ramp (Gallois, 2016), the PTh is most abundant in all three levels, followed by the CTh, the CLTh and then, in the Soft Cap only, the PFS. This differentiation correlates with sedimentological interpretations that indicate shallower facies closer to the Ridgeway Fault in the west and in the present-day area of Portland adjacent to a relay ramp. Eastwards, where the PFS occurs, the outcrops are located further away from the syndepositional Purbeck fault and the deposits are thinner, mound thickness decreases, palaeosols thin out, and deeper-water facies are interpreted (Gallois, 2016, Gallois *et al.*, 2018).

Braga *et al.* (1995) record a range of microbial fabrics preserved in basin margin deposits from the Miocene of SE Spain. Here, in a setting with a physical bathymetric control, they also find stromatolites in the deeper water settings, thrombolites and irregular stromatolites at the shelf break and leiolites and stromatolite domes in the mid shelf.

However, Jahnert & Collins (2012) find the opposite relationship in the present-day microbialites of Shark Bay, with laminated fabrics in shallow waters and colloform and cerebriform (i.e. thrombolitic) fabrics in deeper settings. In this setting the microbialites are more abundant and thicker in shallow settings, as is the case with the microbialites of the Purbeck Caps.

DISCUSSION

Calcareous spherulites

Calcareous spherulites are not reported as common components of Mesozoic or Recent lacustrine microbialites, being absent from the reviews of Gierlowski-Kordesch (2010) and Leinfelder & Schmid (2000). Similar grains to those described in this paper are known from modern shallow-marine reefs and labelled as peloidal cements (Macintyre, 1985). Despite their different occurrences they have similarities in their construction (equant to bladed radial calcite) and precipitation within

bio-constructed cavities. Differences include the Mg-calcite composition, smaller size and origin, only as a cement, in marine reefs.

Although not common within the thrombolites of the Caps, calcite spherulites have been shown to have grown, *in situ*, in a number of different settings; as cements in close association with botryoidal crust cements, as grains growing in adjacent cavities (Type 1), neomorphically within thrombolite mesoclots (Type 2), as cements in adjacent cavities (Type 3) and Type 4 that were reworked as spherulitic intraclasts. None have been found that appear to have formed in association with, or were controlled by, preserved microbial organisms but their location, only within the thrombolites, and commonly, only within mesoclots, is interpreted as an organic influence on calcite precipitation. In the light of experimental work (Mercedes-Martin *et al.*, 2016) this precipitation is probably associated with an organic matrix, or EPS, that would be expected to have been present in each of these three locations of *in situ* spherulite formation. Whether or not the observed microporosity in the calcite cortex is evidence of an organic origin is open to question. Earlier work emphasized that intracrystalline microporosity indicated a microbial influence (Folk & Chafetz, 2000) and flume tank experiments on tufa formation resulted in formation of microporous spar (Pedley *et al.*, 2009). However, more recent work by Pedersen *et al.* (2019) illustrates a high degree of intracrystalline microporosity that results from near-surface diagenesis of present-day, calcite muds from freshwater to brackish-water environments in the Everglades, Florida.

The spherulite occurrences in the thrombolites of the Caps differ significantly from those described from the Barra Velha Formation, Santos Basin (Terra *et al.*, 2010; Wright & Barnett, 2015) and an analogue from the East Kirkton Limestone (Carboniferous, UK) (Mercedes-Martin *et al.*, 2017). In both examples, larger, well-ordered, fibrous calcite spherulites occur in bedded successions apparently not associated with thrombolites. These are associated with stevensite (Mg-rich clay) that is not seen in the Purbeck material. Clearly, the precipitation of calcite spherulites can occur in different forms (sizes and crystal arrangement) in different facies within lacustrine carbonates and this probably relates to varying chemistry of the lake waters and the environment of growth. Mg-rich alkali lakes, in volcanic settings (for example, Barra Velha and East Kirkton limestones) produce large (sand to pebble size), well-ordered spherulites, with associated shrub fabrics and associated stevensite, which are interpreted to grow on the lake floor and not in association with thrombolites. In contrast, in the Purbecks, a Ca-rich alkaline lake with limestone source areas, resulted in smaller (very fine to fine sand size) spherulites that only grew in intimate association with thrombolite cement crusts, as neomorphic recrystallization of mesoclots, and as locally reworked grains.

Therefore, rather than emphasizing similarities between the Purbeck spherulites and those of the pre-salt of the South Atlantic (Kirkham & Tucker, 2019), the current study recognizes significant differences in their structure, occurrence and environment of formation. Chafetz *et al.* (2018) report on the wide range of environments where calcite and aragonite spherulites can form.

Types of thrombolites and mesoclots

Mesoclots (Kennard & James, 1986) were originally described by Aitken (1967, as ‘clots’) as the diagnostic feature of thrombolites “characterized by a macroscopic clotted structure”. Shapiro (2000), Shapiro & Awramik (2006) and Riding (2011) recognize that Aitken’s use of the term clot was for both the mesoscale, clotted internal structure, but also for the larger (macroscale) branching form of thrombolites, as these also appear as clots when viewed in rock sections. No attempt has been made to rename these two scales of thrombolite structure by previous authors, and there is no need for new terminology here, as there is no hierarchy of different types of mesoclot. The Purbeck mesoclots (Fig. 13), whilst varying in size (from millimetres to centimetres), only occur at approximately one mesoscale and different thrombolite types are defined by the distinctive microstructures of the mesoclots.

In this paper, an attempt is made through petrographic investigation, to understand the constructional elements of mesoclots and how they originate. Three distinct forms of mesoclots have been found which are used to define different thrombolite types, or frameworks; one with irregular to spherical to columnar mesoclots with a distinct filamentous microbial framework (*Cladophorites* Thrombolite – CTh), and two with rarely preserved filaments but with very different forms of mesoclot; a Peloidal Thrombolite (PTh) is the commonest type found with irregular-shaped mesoclots constructed of peloidal micrite that is locally recrystallized into calcite spherulites, and a thrombolite with very distinctive rounded mesoclots with concentric micrite layers is seen in the Concentrically Layered Thrombolite or CLTh. The major difference in construction is that the *Cladophorites* mesoclots are considered to have *biologically-induced* form of mineralization (*sensu* Dupraz *et al.*, 2009) as a well preserved, presumed algal framework of filaments with externally calcified micrite walls. This type therefore may be classified as a ‘Calcified microbe thrombolite’ of Riding (2011) in that the mesoclots are, in part, constructed by calcified microfossils. The remaining two types (PTh and CLTh) have mesoclots with no clear evidence of biological control but an interpreted *biologically-influenced* mineralization (*sensu* Dupraz *et al.*, 2009) from presumed organic matrix or EPS. The CLTh appears to be a new fabric and is unusual in that at the mesoscale it is

clearly a clotted fabric, but at the microscale it may be finely (tens of microns) laminated, and with little evidence of microbial organisms. Are these stromatolites? As the terms stromatolite and thrombolite are macroscale and mesoscale terms (Aitken, 1967; Kennard & James, 1986) the latter term is preferred, but it must be recognized that use of these terms (Fig. 1) is scale dependent. With this proviso, the microbialites of the Purbeck Caps fit well within the end members of the classification of microbialites developed in the 1990s (Fig. 1) with few intermediate forms, despite the diversity of microbialites represented in these rocks. A more detailed understanding of the formation of the mesoclots might come from bio-lipids (if preserved) and C and O stable isotope analyses from very carefully targeted sampling but is beyond the scope of this paper.

Multiphase thrombolite construction

From the above descriptions and discussion it is clear that these non-marine thrombolites are complex carbonate rocks resulting from a range of different biotic, sedimentological and diagenetic processes. Whilst for convenience of description, the many components of the thrombolites were divided into depositional and diagenetic features (text above and Table 1), some of these, such as microspar and spherulites, cut across this artificial classification and a continuum of processes exist from the initial microbial framework construction through to its recrystallization and replacement in the early diagenetic environment.

In an attempt to further understand the role of these different processes, this study recognizes a sequence of seven phases and products of thrombolite construction from overgrowing and cross-cutting relations that are commonly, but not everywhere, observed in all three levels of the Caps (Fig. 22). These phases of accumulation are repeated within any one thrombolite dome but no attempt has been made to study this repetition as correlatable surfaces are near-impossible to trace within the complex mesostructure of a thrombolite.

Phase 1

Four different microbial frameworks are recognized that build the microbialites. They are intimately associated and overgrow each other and may be overgrown by a leiolite crust (DML). Observations indicate that the mesoclots form the primary framework to the thrombolites in the same way that corals or coralline algae form the primary framework of modern reefs (Ginsburg & Schroeder, 1973; Bosence, 1984). This primary framework construction is subsequently altered by many erosional and depositional processes. This may mean that the original framework is preserved as small relics, or a network, of a presumed more continuous structure now replaced by cavities, internal sediment and

early cements (*cf.* Fig. 17; with Bosence, 1985, fig. 3).

Phase 2

Cavities are a distinctive feature of the thrombolites and the stromatolite of the Caps. Some are filled but others remain open, which makes some of these microbialites extremely porous structures (Figs 3B to D, 14B). Cavities may be internal within the mesoclots (Figs 15D and 21), or growth-framework pores between mesoclots (Figs 14B and 16) or macrostructural features between thrombolite domes. Cavities within mesoclots are the most challenging to interpret but are considered to result from dissolution by waters of lower pH within the original mat community (see above). However, the external surfaces to thrombolites have also been eroded at this stage so it is possible that this represents a stage of lowered dissolved carbonate or pH or temperature within the lake waters. Seasonal variation in the intensity of calcification of freshwater tufas is well documented (Andrews & Brasier, 2005) and Gischler *et al.* (2008) record a correlation between reduced dissolved carbonate levels and thrombolite occurrence in the modern Laguna Bacalar, Mexico. It is therefore envisaged that lake waters could have been periodically undersaturated with respect to calcite leading to dissolution or reduction in intensity of calcification of the external surface of mesoclots in addition to the dissolution within mesoclots.

Phase 3

A phase of fibrous calcite cement growth forms an isopachous coating to the main thrombolite frameworks and their cavities in association with Type 1 calcite spherulites (below; Fig. 22). These cements have never been observed to intergrow with microbialite fabrics but are commonly seen to encrust eroded surfaces to the frameworks. However, at the macroscale, phases of framework growth may alternate with cement fringes but the three dimensional structure of the microbialites is too complex to map these relations. Therefore, the conditions for microbialite growth are thought to be different to those for cement crusts and associated spherulites because the cements have no evidence of preserved microbial remains. A commonly observed sequence is that original mesoclots formed the framework that was then eroded. This erosional surface was then encrusted with fringe cements and their associated Type 1 spherulites (below; Fig. 22). The mesoclots were formed from a combination of biologically induced and influenced carbonate precipitation, however following erosion, the microbial substrate may have contained EPS that is known to be an active catalyst in calcium carbonate precipitation (Rogerson *et al.*, 2008; Pedley, 2014) that could drive the precipitation of the cement fringe and associated spherulites.

Phase 4

The cement fringe phase preceded but then was intimately involved in subsequent, Type 1 calcite spherulite growth. Botryoidal and spherulitic growths developed *in situ* from fringe cements and adjacent cavities have petrographically identical, but reworked spherulites as grains. These have continued to grow alongside other spherulites with compromise boundaries. In addition, Type 2 spherulites replace thrombolite fabrics, through neomorphic recrystallization, and the associated Type 3 forms grew, also with interference boundaries, in adjacent cavities. It is not possible to place Types 1 and 2 spherulites in a growth sequence but Types 2 and 3 occur together and appear to be synchronous. Type 4 spherulites were the last to form as they were derived from the reworking of Types 1 and 3. The intimate relation between Type 1 and the fringe cements indicate similar conditions of biological influence, through organic matrices such as EPS for calcite precipitation and similar drivers are considered to exist in the surrounding mesoclot matrix for Types 2 and 3.

Phase 5

Alongside the reworked calcite spherulites of Phase 4 other internal sedimentary grains were deposited; peloids, intraclasts (with or without fringe cements), calcareous invertebrates (molluscs and ostracods), microspar (after crystal silt?) and a micritic matrix. This diverse grain assemblage indicates continuity with intermound environments external to the microbialites and moderate hydraulic energy. Cavity fills are multigenerational (Figs 17 and 22) with the more internal, smaller cavities with more spherulites and microspar and the larger, presumed more external cavities, with intraclasts and skeletal grains. Peloids are universally common.

Phase 6

Chalcedonic quartz spherulites replaced frameworks, fibrous fringe cements and calcite spherulites and occur within a few hundred microns of the thrombolite surface. However, they are never found reworked into cavities, as were calcite spherulites, so they are regarded as a relatively later stage in the diagenesis of the thrombolites. The quartz spherulites are not seen to preferentially replace the calcite spherulites, they replace and cut across the earlier mesoclots and diagenetic phases. The origin of the silica for the spherulites remains enigmatic but an organic origin from sponge spicules or an inorganic origin, from detrital quartz, are both considered possibilities.

Phase 7

A final diagenetic phase that is commonly present is a coarse, blocky, low-Mg calcite spar cement. This has a slightly more radiogenic $^{87}\text{Sr}/^{86}\text{Sr}$ ratio than the thrombolite framework. Despite the C and O isotope trends reflecting cementation within the vadose zone no pendant or meniscus cements have been observed and this coarse spar is regarded as a later stage phreatic phase of cementation.

The only comparable analysis of the multistage origin of such microbialites is from Miocene lacustrine microbial bioherms from the Ries crater in southern Germany (Riding, 1979; Arp, 1995, Pache *et al.*, 2001). These authors differ in some of their interpretations and a more complex diagenetic history is presented for the Ries than is seen in the PLG involving pedogenic modification, aragonite to calcite transformation, dissolution, and dolomitization driven by different phreatic and meteoric waters and their mixing. The Purbeck examples also show significant early dissolution but are mineralogically less complex and the majority of the phases described are all interpreted to have formed in the shallow, lacustrine environment, albeit, the phases being cyclical, and repeated within thrombolite domes. This indicates a high frequency fluctuation in the chemistry of the lake waters from those supersaturated with respect to calcite to undersaturated waters. No evidence of aragonite precursors are seen in the mesoclots, the calcite cements or neomorphic recrystallization. Whilst this is not fully understood it is in line with many (but not all) natural or experimental Ca-rich freshwater microbialites (e.g. Guo & Riding, 1984; Pedley, 2014; Pedersen *et al.*, 2019). Subsequent formation of later stage, clear equant spar and fracturing in the Purbeck Caps is considered to have occurred during Cretaceous burial and subsequent Cenozoic inversion (but has not been investigated). Thrombolites are hereby shown to be complex rock fabrics with a multi-phase construction and early diagenetic alteration that is repeated in a cyclic fashion to generate thrombolite domes and mounds.

CONCLUSIONS

This paper focuses on the question of how thrombolites form and this is answered for non-marine examples through detailed petrographic studies that reveal a complex and cyclically changing micro-environment that favours, at different times; microbial framework formation, dissolution, biologically induced cement and spherulite formation and internal sedimentation. Although thrombolites are complex rocks, detailed analysis and mapping out of their different components leads to a greater understanding of the different processes involved in their construction. The main conclusions of this work are:

- Within rocks previously described as ‘tufas’, ‘burrs’, ‘stromatolites’ and ‘thrombolites’ three different thrombolite types are found to occur together with a laminated stromatolite and a rare crust-forming leiolite.
- The most abundant thrombolites comprise mesoclots of peloidal micrite with remnants of microbial filaments. Less commonly, a more distinct thrombolite framework is formed as

equant to columnar mesoclots with a framework of branching filaments of *Cladophorites*, a presumed filamentous green alga.

- A new form of thrombolite is found with rounded mesoclots with an internal laminated micrite structure that is described with only rarely preserved microbial remains.
- In addition to growth framework cavities, pores occur within mesoclots and their external surfaces are also eroded. This is considered to be the product of chemical dissolution by organic acids from microbial activity within the mesoclots acting alongside, or independently, to frequent fluctuations in lake chemistry leading to undersaturated waters.
- Early fibrous calcite cement rims with botryoidal and spherulitic growths are common on the eroded, and presumed dead, cavity wall and mesoclot surfaces. These cements were likely to have been driven by a microbial influence on carbonate precipitation through the presence of organic matrices.
- More regular-formed radial calcite spherulites are also present that neomorphically recrystallize the mesoclots and also grow as cements within adjacent cavities. Finally, the clusters of spherulites may get eroded out of the mesoclots to form spherulitic intraclasts. These specific occurrences, together with the size and structure of the spherulites indicate that they differ in many respects to the spherulites described from the Cretaceous pre-salt of Brazil.
- Infill of cavities was complex and involved a number of different depositional components but dominated by near ubiquitous peloids that are considered from their size, shape and internal structure to form from reworking abrasion and size-sorting of micritic material within the thrombolites. Microspar is also a common component of cavities and its occurrence and microstructure suggests a derivation from early cements within the thrombolite frameworks. Intraclasts of the different mesoclot frameworks are common and together with their abundance in surrounding intermound sediments provide evidence that supports the interpretation of surrounding facies by Gallois *et al.* (2018) of moderate-energy to high-energy hydraulic conditions during growth of the microbialite mound.
- Spherulites of chalcedonic quartz commonly replace thrombolite mesoclots and early calcite cements but are not reworked as individual grains. There is no obvious source for the silica but siliceous sponges are a possibility, as is dissolution of detrital quartz.

- The Purbeck thrombolitic mounds are considered to have formed in alkali, lime-rich waters and Sr isotope analyses suggest that the likely source area was dissolution of earlier Jurassic limestones exposed on the western margin of the basin.
- The associated skeletal fossils (ostracods, bivalves and gastropods), mineralogy (low-Mg calcite), near absence of evaporite minerals and negative stable isotope ratios of O and Ca are consistent in indicating a through-flowing, brackish-water lake. This contrasts with previous interpretations of a hypersaline environment based largely on mis-identifications of the fossil algae and their palaeoenvironmental significance.
- The thrombolite facies do not show distinctive O and calcite stable isotope ratios from bulk samples but periodic emergence is interpreted to explain up-section, negative ^{13}C excursions below microkarsts and palaeosols.
- These brackish-water thrombolites were subjected to high-frequency fluctuations in lake waters from oversaturated to undersaturated that led to alternate phases of biotically induced precipitation of calcite (mesoclots), biotically influenced precipitation (calcite cements and spherulites) and dissolution that resulted in dissolved mesoclot surfaces and internal cavities.
- The three thrombolite types were all involved in mound construction, occur in all mound-bearing levels in the Purbeck Limestone Group and in shallow-water marginal lacustrine sites throughout the study area.
- Thrombolites are all found in shallow-water mound-building sites near fault-controlled, sub-basin margins and on a relay ramp, whilst the stromatolite occurs in deeper lacustrine areas.

ACKNOWLEDGEMENTS

Special thanks are to Robert Riding (University of Tennessee, USA) for his expertise and the time spent elucidating microbial morphology and taxonomy that informs our section on Microbial Filaments. Similarly we thank Jim Marshall (University of Liverpool, UK) for lengthy discussions on lacustrine stable isotope records and Mathew Thirlwall for overseeing Strontium isotope analysis. This research is an extension of a grant by BP Exploration Operating Company Limited and Baker Hughes Limited on “Modelling Mesozoic Non-Marine Microbialites” and this support is gratefully acknowledged. We also appreciate the assistance provided by quarry managers on the Isle of Portland, Mark Godden (Albion Stone) and Andrew Jackson (Portland Stone Firms), who

have willingly granted us access to working and sampling in their quarries. Expert technical work by Neil Holloway (thin sections), Sharon Gibbons (SEM preparation and operation) and Kevin D'Souza (specimen photography) at RHUL is acknowledged with thanks. EDS analyses were carried out with excellent technical support from Gareth Roberts at CGG, Llandudno, Wales, and Matthew Bilton at the University Liverpool. Finally we thank André Strasser, two anonymous referees, and Editors Peir Pufahl and Jim Hendry for their careful reviews and constructive criticisms of this paper.

REFERENCES

- Aitken, J. D. (1967) Classification and environmental significance of cryptalgal limestones and dolomites, with illustrations from the Cambrian and Ordovician of southwestern Alberta. *J. Sed. Petrol.* **37**, 1163–1178.
- Allen, J.R. and Mathews, R.K. (1982) Isotopic signatures associated with early meteoric diagenesis. *Sedimentology*, **29**, 797-817.
- Andrews, J.E. (1986) Microfacies and geochemistry of Middle Jurassic algal limestones from Scotland. *Sedimentology*, **33**, 499-520.
- Andrews, J.E. and Brasier, A.T. (2005) Seasonal records of climate change in annually laminated tufas: short review and future prospects. *J. Quat. Sci.* **20**, 411-421.
- Arkell, W.J. (1947) The Geology of the Country Around Weymouth, Swanage, Corfe & Lulworth. His Majesty's Stationery Office, London, 386 pp.
- Arp, G. (1995) Lacustrine bioherms, spring mounds, and marginal carbonates of the Ries-impact-crater (Miocene, southern Germany). *Facies*, **33**, 35-90.
- Aurell, M. and Bádenas, B. (2015) Facies architecture of a microbial-siliceous, sponge-dominated carbonate platform: the Bajocian of Moscardón (Middle Jurassic, Spain). In: *Microbial Carbonates in Space and Time: Implications for Global Exploration and Production* (Eds D.W.J. Bosence, K. Gibbons, D.P. Le Heron, W.A. Morgan, T. Pritchard and B.A. Vining), Geol. Soc. London Spec. Publ. 418, London, 155-174.
- Barker, D., Brown, C.E., Bugg, S.C. and Costin, J. (1975) Ostracods, land plants, and *Charales* from the basal Purbeck Beds of Portesham Quarry, Dorset. *Palaeontology*, **18**, 419-436.
- Bathurst, R.G.C. (1971) Carbonate Sediments and their Diagenesis. Elsevier. Amsterdam. 620 pp.
- Bellanca, A, Calvo, J.P., Censi, P., Neri, R. and M. Pozo (1992) Recognition of lake-level changes in Miocene lacustrine units, Madrid Basin, Spain. Evidence from facies analysis, isotope geochemistry and clay mineralogy. *Sed. Geol.* **76**, 135-153.

Benson, L. and Peterman, Z. (1995) Carbonate deposition, Pyramid Lake subbasin, Nevada: 3. The use of ^{87}Sr values in carbonate deposits (tufas) to determine the hydrologic state of paleolake systems. *Palaeogeogr. Palaeoclimatol. Palaeoecol.* **119**, 201–213.

Bosence, D.W.J. (1984) Construction and preservation of two Recent algal reefs, St Croix, Caribbean. *Palaeontology*, **27**, 549-574.

Bosence, D.W.J. (1985) Preservation of coralline algal reef frameworks. 5th International Symposium on Coral Reefs, Tahiti, **6**: 623-628.

Bosence, D.W.J. (1987) Mesozoic platform carbonates and benthic calcareous algae of the Severn and Wessex basins. In: *Excursions Guide Handbook* (Ed. R. Riding), IVth International Symposium on Fossil Algae. Cardiff.

Bosence, D.W.J., Collier, J.S., Fleckner, S. Gallois, A. and I.M. Watkinson (2018) Discriminating between the origins of remotely sensed circular structures: carbonate mounds, diapirs or periclinal folds? Purbeck Limestone Group, Weymouth Bay, UK. *J. Geol. Soc. London*, **175**, 742-756.

Braga, J. C., Martín, J. M. and Riding, R. (1995) Controls on microbial dome fabric development along a carbonate-siliciclastic shelf-basin transect, Miocene, S.E. Spain. *Palaios*, **10**, 347–361.

Bray, R.J., Duddy, I.R. and P.F. Green (1998) Multiple heating episodes in the Wessex Basin: implications for geological evolution and hydrocarbon generation. In: Underhill, J.R. (Ed.) *Development, Evolution and Petroleum geology of the Wessex Basin*, Geol. Soc. London Spec. Publ. 133. 199-213.

Brehm, U., Gorbushina A. and Mottershead, D. (2015) The role of microorganisms and biofilms in the breakdown and dissolution of quartz and glass. *Palaeogeogr. Palaeoclimatol. Palaeoecol.* **219**. 117–129.

Brown, P.R. (1961) Petrology of the Lower and Middle Purbeck Beds of Dorset. PhD Thesis. Liverpool University (Unpublished), 209 pp.

Brown, P.R. (1963) Algal limestones and associated sediments of the basal Purbeck of Dorset. *Geol. Mag.* **100**, 565–573.

Budd, D.A. and Land, L.L. (1990) Geochemical imprint of meteoric diagenesis in Holocene ooid sands, Schooner Cays, Bahamas: correlation of calcite cement geochemistry with extant groundwaters. *J. Sediment. Petrol.* **60**, 361-378.

Cayeux, L. (1935) *Les Roches Sedimentaires de France; Roches Carbonatées*. Masson, Paris. 463 pp.

Chafetz, P.H., Barth, J., Cook, M., Guo, X. and Zhou, J. (2018) Origins of carbonate spherulites: implications for Brazilian Aptian pre-salt reservoir. *Sediment. Geol.* **365**, 21-33.

Chidsey, T.C., Vanden Berg, M.D. and Eby, D.E. (2015) Petrography and characterisation of microbial carbonates and associated facies from modern Great Salt Lake and Uinta Basin's Eocene Green River Formation, in Utah, USA. In: *Microbial Carbonates in Space and Time: Implications for Global Exploration and Production* (Eds D.W.J. Bosence, K. Gibbons, D.P. Le Heron, W.A. Morgan, T. Pritchard and B.A. Vining), Geol. Soc. London Spec. Publ. 418, London, 261-286.

Coram, R.A. and Radley, J.D. (2021) Revisiting climate change and palaeoenvironments in the Purbeck Limestone Group (Tithonian-Berriasian) of Durlston Bay, southern UK. *Proc. Geol. Assoc.* doi.org/10.1016/j.pgeola.2021.03.001

Darbyshire, D.P.F. and Shepherd, T.J. (1994) Nd and Sr isotope constraints on the origin of the Cornubian batholith, SW England. *J. Geol. Soc. London.* **151**, 795-802.

Della Porta, G., Merino-Tomé, O., Kentner, J.A.M. and Verwer, K. (2013) Lower Jurassic microbial and skeletal carbonate factories and platform geometry (Djebel Bou Dahar, High Atlas, Morocco). In: *Deposits, Architecture and Controls on Carbonate Margin, Slope and Basinal Settings* (Eds K. Verwer, T.E. Playton and P.M. Harris), *SEPM. Spec. Publ.* 105, 237-263.

Della Porta, G. (2015) Carbonate build-ups in lacustrine, hydrothermal and fluvial settings: comparing depositional geometry, fabric types and geochemical signature. In: *Microbial Carbonates in Space and Time: Implications for Global Exploration and Production* (Eds D.W.J. Bosence, K. Gibbons, D.P. Le Heron, W.A. Morgan, T. Pritchard and B.A. Vining), Geol. Soc. London Spec. Publ.

418, London, 17-68.

Dunham, R.J. (1969) Early vadose silt in Townsend mound (reef), New Mexico. In: *Depositional Environments in Carbonate Rocks* (Ed. G.M. Friedman), *SEPM. Spec. Publ.* 14, 139-181.

Dupraz, C., Reid, R.P., Braissant, O., Decho, A.W., Norman, R.S. and Visscher, P.T. (2009) Processes of carbonate precipitation in modern microbial mats. *Earth-Science Rev.* **96**, 141–162.

Dupraz, C. and Strasser, A. (1999) Microbialites and micro-encrusters in shallow coral bioherms (Middle to Late Oxfordian, Swiss Jura mountains). *Facies*, **4**, 101–129.

Emery, D., Dickson, J.A.D. and Smalley, P.C. (1987) The strontium isotope composition and origin of burial cement in the Lincolnshire Limestone (Bajocian) of central Lincolnshire, England. *Sedimentology*, **34**, 795-806.

Ensom, P. (2002) The Purbeck Limestone Group of Dorset, southern England: Guide to lithostratigraphic terms. In: *Life and Environments in Purbeck Times* (Eds A.R. Milner and D.J. Batten), *Palaeont. Ass. Spec. Pap. in Palaeontology*, 168, 7-11.

Flügel, E. (2004) *Microfacies of Carbonate Rocks: analysis, interpretation and application*. Springer, Berlin, 976 pp.

Folk, R.L. and Chafetz, H.S. (2000) Bacterially induced microscale and nanoscale carbonate precipitates. In: *Microbial Sediments* (Eds R.E. Riding and S.M. Awramik), Springer, Berlin, pp. 40-49.

Francis, J.E. (1982) The Fossil Forest of the basal Purbeck Formation (Upper Jurassic) of Dorset, southern England. Palaeobotanical and palaeoenvironmental investigations. Unpublished PhD thesis, University of Southampton. 317 pp.

Francis, J.E. (1984) The seasonal environment of the Purbeck (Upper Jurassic) fossil forests. *Palaeogeogr. Palaeoclimatol. Palaeoecol.* **48**, 285–307.

Freytet, P. (1997) Non-marine Permian to Holocene algae from France and adjacent countries (Part 1). *Ann. Paléontol.* **83**, 289-332.

Freytet, P. and Verrechia, E.P. (1998) Freshwater organisms that build stromatolites: a synopsis of biocrystallization by prokaryotic and eukaryotic algae. *Sedimentology* **45**, 535-563.

Gallois, A. (2016) Late Jurassic lacustrine carbonates; a multi-scale analysis of the Mupe Member (Purbeck Limestone Group) of the Wessex Basin, UK. Unpublished PhD thesis, Royal Holloway University of London. 496 pp.

Gallois, A., Bosence, D. and P. Burgess (2018) Brackish to hypersaline facies and facies transitions in lacustrine carbonates: Purbeck Limestone Group, Upper Jurassic-Lower Cretaceous, Wessex Basin, Dorset, U.K. *Facies*, **64**, 1–39.

Garden, I.R. (1987) The provenance of Upper Jurassic and Lower Cretaceous coarse-grained detritus in Southern Britain and Normandy. PhD thesis, University of Southampton. 410 pp. plus Appendices.

Gierlowski-Kordesch, E.H. (2010) Lacustrine carbonates. In: *Carbonates in Continental Settings. Facies, Environments and Processes*, (Eds A.M. Alonso-Zarza and T.H. Tanner), *Dev. Sedimentol.* 61. Elsevier, Amsterdam, pp. 1–101.

Ginsburg, R.N. and Schroeder, J.H. (1973) Growth and submarine fossilization of algal cup reefs, Bermuda. *Sedimentology*, **20**, 575-614.

Gischler, E., Gibson, M.A. and Oschmann, W. (2008) Giant Holocene fresh-water microbialites, Laguna Bacalar, Quintana Roo, Mexico. *Sedimentology*, **55**, 1293-1309.

Golubic, S. (1973) The relationship between blue-green algae and carbonate deposits. In: *The Biology of Blue-Green Algae* (Eds N.G. Carr and B.A. Whitton), Blackwell, Oxford, pp 434-472.

Guo, L. and Riding, R.R. (1994) origin and diagenesis of Quaternary travertine shrub fabrics, Rapolino Terme, central Italy. *Sedimentology*, **41**, 499-520.

Horne, D.J. (2002) Ostracod biostratigraphy and palaeoecology of the Purbeck Limestone Group of Dorset, southern England. In: *Life and Environments in Purbeck Times* (Eds Milner, A R. and D.J. Batten), *Palaeont. Ass. Spec. Pap. in Palaeontology*, 168, 53-70.

Hudson, J.D. (1970) Algal limestones with pseudomorphs after gypsum from the Middle

Jurassic of Scotland. *Lethaia*, **3**, 11–40.

Jagniecki, E.A., Lowenstein, T.K., Demicco, R.V., Baddouh, M., Carroll, A.R., Beard, B.L. and C.M. Johnson (2021) Spring Origin of Eocene Carbonate Mounds in the Green River Formation, Northern Bridger Basin, Wyoming. *Sedimentology*, <https://doi.org/10.1111/sed.12852>

Jahnert, R.J. and Collins, L.B. (2011) Significance of subtidal microbial deposits in Shark Bay, Australia. *Mar. Geol.* **286**, 106-111.

Jahnert, R.J. and Collins, L.B. (2012) Characteristics, distribution and morphogenesis of subtidal microbial systems in Shark Bay, Australia. *Mar. Geol.* **303-6**, 115-136.

James, N.P. and Jones, B. (2016) *Origin of Carbonate Sedimentary Rocks*. Wiley. 446 pp.

Jones, C.E., Jenkyns, H.C., Coe, A.L. and Hesselbo, S.P. (1994a) Strontium isotopic variations in Jurassic and Cretaceous seawater. *Geochim. Cosmochim. Acta*, **58**, 1285-1301.

Jones, C.E., Jenkyns, H.C., Coe, A.L. and Hesselbo, S.P. (1994b) Strontium isotopic variations in Jurassic and Cretaceous seawater. *Geochim. Cosmochim. Acta*, **58**, 3061-3074.

Kalkowski, E. (1908) Oolith und Stromatolith im norddeutschen Buntsandstein. *Z. Deut. Geol. Ges.* **60**, 68-125.

Kennard, J.M. and James, N.P. (1986) Thrombolites and stromatolites; two distinct types of microbial structures. *Palaios*, **1**, 492–503.

Kirkham, A. and Tucker, M.E. (2018) Thrombolites, spherulites and fibrous crusts (Holkerian, Purbeckian, Aptian): Context, fabrics and origins. *Sed. Geol.* **374**, 69-84.

Leinfelder, R.R. and Keupp, H. (1995) Upper Jurassic mud mounds: Allochthonous sedimentation versus autochthonous carbonate production. In: *Mud mounds: A polygenetic spectrum of fine-grained carbonate buildups* (Eds J. Reitner and F. Neuweiler). *Facies*, **32**, 17-26.

Leinfelder, R.R. and Schmid, D.U. (2000) Mesozoic reefal thrombolites and other microbolites. In: *Microbial Sediments* (Eds R.R. Riding and S.M. Awramik), Springer, Berlin, pp. 289-294.

Leng M.J. and Marshall, J.D. (2004) Palaeoclimate interpretation of stable isotope data from lake sediment archives. *Q. Sci. Rev.* **23**, 811–831.

Macintyre, I. (1985) Submarine cements- the peloidal question. In: *Carbonate Cements* (Eds N. Schneidermann and P.M. Harris), SEPM Spec. Publ. 36. 109-116.

McMahon, N.A. and Turner, J.D. (1998) Erosion, subsidence and sedimentation response to the Early Cretaceous uplift of the Wessex Basin and adjacent offshore areas. In: (Ed. J.R. Underhill) *Development, Evolution and Petroleum geology of the Wessex Basin*, Geol. Soc. London Spec. Publ. 133. 215-240.

Mercedes-Martín, R., Rogerson, M., Brasier, A.T., Vonhof, H.B., Prior, T.J., Fellows, S.M., Reijmer, J.J.G., Billing, I. and Pedley, H.M. (2016) Growing spherulitic grains in saline, hyper-alkaline lakes: experimental evaluation of the effects of Mg-clays and organic acids. *Sed. Geol.* **335**, 93–102.

Mercedes-Martín, R., Brasier, A.T., Reijmer, J.J.G., Rogerson, M., Vonhof, H.B. and Pedley, H.M. (2017) A depositional model for spherulitic carbonates associated with alkaline, volcanic lakes. *Mar. Petrol. Geol.* **86**, 168–191.

Monty, C.L.V. (1976) The origin and development of cryptalgal fabrics. In: *Stromatolites* (Ed. M.R. Walter), *Dev. Sedimentol.* 20, Elsevier, Amsterdam, pp. 193–249.

Nunn, E.V. and Price, G.D. (2010) Late Jurassic (Kimmeridgian–Tithonian) stable isotopes ($\delta^{18}\text{O}$, $\delta^{13}\text{C}$) and Mg/Ca ratios: New palaeoclimate data from Helmsdale, northeast Scotland. *Palaeogeogr. Palaeoclimatol. Palaeoecol.* **292**, 325–335.

Pache, M., Reitner, J. and Arp, G. (2001) geochemical evidence for the formation of a large Miocene “travertine” mound at a sublacustrine spring in a soda lake (Wallerstein Castle Rock, Nördlinger Ries, Germany). *Facies*, **45**, 211-230.

Pedersen, C.L., Klaus, J.S., Swart, P.K. and McNeill, D.F. (2019) Deposition and early diagenesis of microbial mud in the Florida Everglades. *Sedimentology* **66**, 1989-2010.

Pedley, H.M. (2014) The morphology and function of thrombolitic calcite precipitating biofilms: A universal model derived from freshwater mesocosm experiments. *Sedimentology*, **61**, 22-

Pedley, H.M., Rogerson, M. and Middleton, R. (2009) The growth and morphology of freshwater calcite precipitates from *in vitro* mesocosm flume experiments; the case for biomediation. *Sedimentology*, **56**, 512-527.

Peterson, M.N.A. and Von der Borch, C.C. (1965) Chert: modern inorganic deposition in a carbonate-precipitating locality. *Science*, **149**, 1501-1503.

Pia, J. (1927) Thallophyta. In: *Handbuch der Paläobotanik* (Ed. M. Hirmer) 1, pp 1-136.

Pronzato, R., Pisera, A. and Manconi, R. (2017) Fossil freshwater sponges: Taxonomy, geographic distribution, and critical review. *Acta Palaeontol. Pol.* **62**, 467-495.

Pugh, M.E. (1968) Algae from the Lower Purbeck of Dorset. *Proc. Geol. Ass.* **79**, 513–523.

Radley, J.D. (2002) Distribution and palaeoenvironmental significance of molluscs in the Late Jurassic–Early Cretaceous Purbeck Formation of Dorset, southern England: a review. In: *Life and Environments in Purbeck Times* (Eds A.R. Milner and D.J. Batten), *Palaeont. Ass. Spec. Pap. in Palaeontology*, 168, 41-51.

Reiss, O.M. (1921) Erläuterungen zu dem Blatte Donnersberg der Geognostischen Karte von Bayern. Geol. Landesuntersuchung, Munich.

Reitner, J., Neuweiler, F. and Gautret, P. (1995) Modern and fossil automicrites: Implications for mud mound genesis. In: *Mud mounds: A polygenetic spectrum of fine-grained carbonate buildups* (Eds J. Reitner and F. Neuweiler). *Facies*, 32, 4-17.

Riding, R. (1977) Skeletal stromatolites. In: *Fossil Algae; recent results and developments* (Ed. E. Flügel) Springer-Verlag, 57-60.

Riding, R.R. (1979) Origin and diagenesis of lacustrine algal bioherms at the margin of the Ries crater, Upper Miocene, southern Germany. *Sedimentology*, **26**, 645-680.

Riding, R.R. (2000) Microbial carbonates: the geological record of calcified bacterial-algal mats and biofilms. *Sedimentology*, **47** (Suppl. 1), 179–214.

Riding, R.R. (2004), *Solenopora* is a chaetetid sponge, not an alga. *Palaeontology*, 44, 107-122.

Riding, R.R. (2011) Microbiolites, stromatolites and thrombolites. In: *Encyclopedia of Geobiology* (Eds J. Reitner and V. Thiel). Springer, Heidelberg. Pp. 635-654

Riding, 2004 S O L E N O P O R A I S A C H A E T E T I D
S P O N G E ,
N O T A N A L G A
by R O B E R T R I D I N G
S O L E N O P O R A I S A C H A E T E T I D S P O N G E ,
N O T A N A L G A
by R O B E R T R I D I N G
S O L E N O P O R A I S A C H A E T E T I D S P O N G E ,
N O T A N A L

Riding, R.R. (2011) Microbialites, stromatolites, and thrombolites. In: *Encyclopedia of Geobiology* (Eds Reitner, J. and V. Thiel) *Encyclopedia of Earth Science Series*, Springer, Heidelberg, pp. 635-654. Riding, R.R., Braga, J. C. and J.M. Martín (1991) Oolite stromatolites and thrombolites, Miocene, Spain: analogues of Recent giant Bahamian examples. *Sed. Geol.* **71**, 121–127.

Rogerson, M., Pedley, H.M., Wadhawan, J.D. and Middleton, R. (2008) New insights into biological influence on the geochemistry of freshwater carbonate deposits. *Geochim. Cosmochim. Acta.* **72**, 4976-4987.

Rothpletz, A. (1908) Ueber Algen und Hydrozoen im Silur von Gotland und Oesel. *Kungliga Sven. Vetenskapsakademiens Handl.* **43** (s.) 1-25.

Samankassou, E., Tresch, J. and Strasser, A. (2005) Origin of peloids in Early Cretaceous deposits, Dorset, South England. *Facies*, **51**, 264-273.

Sarg, J.F., Tänavsuu-Milkeviciene, S.K. and Humphrey, J.D. (2013) Lithofacies, stable isotopic composition, and stratigraphic evolution of microbial and associated carbonates, Green River Formation (Eocene), Piceance Basin, Colorado. *AAPG Bull.* **97**, 1937-1966.

Schmid, D.U. (1996) Marine mikrobolithe und mikroinkrustiereraus dem Oberjura. *Profil*, **9**, Stuttgart, 101-251.

- Scholl, D.W. (1960) Pleistocene algal pinnacles at Searles Lake, California. *J. Sed. Petrol.* **30**, 414-431.
- Shapiro, R.S. (2000) A comment on the systematic confusion of thrombolites. *Palaios*, **15**, 166-169.
- Shapiro, R.S. and Awramik, S.M. (2006) *Favosamaceria cooperi* new group and form: A widely dispersed, time-restricted thrombolite. *J. Paleont.* **80**, 411-422.
- Sims, P.A., Man, D.G. and Medlin, L.K. (2006) Evolution of the diatoms: insights from fossil, biological and molecular data. *Phycologia*, **45**, 361-402.
- Smith, G.M. (1955). *Cryptogamic Botany; Algae and Fungi*, Volume 1. 2nd Ed. McGraw-Hill, New York. 546 pp.
- Talbot, M.R. (1990) A review of the palaeohydrological interpretation of carbon and oxygen isotopic ratios in primary lacustrine carbonates. *Chem. Geol. Isot. Geosci. Sect.* **80**, 261–279.
- Terra, G.J.S., Spadini, A.R., França, A.B., Sombra, C.L., Zambonato, E.E., Juschaks, L.C.D.S., Arienti, L.M., Erthal, M.M., Blauth, M., Franco, P.P., Matsuda, N.S., da Silva, N.G.C., Junior, P.A.M., D'Avila, R.S.F., de Souza, R.S., Tonietto, S.N., dos Anjos, S.M.C., Campinho, V.S. and Winter, W.R. (2010) Classificação de rochas carbonáticas aplicável às bacias sedimentares brasileiras. *Bull. Geosci. Petrobras, Rio de Janeiro* **18**, 9–29.
- Townson, W.G. (1971) *Facies Analysis of the Portland Beds*. Unpublished PhD thesis, University of Oxford. 575 pp.
- Townson, W.G. (1975) Lithostratigraphy and deposition of the type Portlandian. *J. Geol. Soci. London*, **131**, 619-638.
- Underhill, J.R. (2002) Evidence for structural controls on the deposition of the Late Jurassic-Early Cretaceous Purbeck Limestone Group, Dorset, southern England. In: *Life and Environments in Purbeck Times* (Eds A R. Milner and D.J. Batten), *Palaeont. Ass. Spec. Pap. in Palaeontology*, 168, 21-40.

Underhill, J.R. and Stoneley, R. (1998) Introduction to the development, evolution and petroleum geology of the Wessex Basin. In: (Ed. J.R. Underhill) *Development, Evolution and Petroleum Geology of the Wessex Basin*, Geol. Soc. London Spec. Publ. 133. 1-18.

Walter, M.R., and Heys, G.R. (1985) Links between the rise of the Metazoa and the decline of stromatolites. *Precambrian Res.* **29**, 149-174.

West, I.M. (1964) Evaporite diagenesis in the Lower Purbeck Beds of Dorset. *Proc. Yorks. Geol. Soc.* **34**, 315-330.

West, I.M. (1975) Evaporites and associated sediments of the basal Purbeck Formation (Upper Jurassic) of Dorset. *Proc. Geol. Ass.* **86**, 205-225.

West, I.M. (2013) Purbeck Formation- Facies and Palaeoenvironments. Version 2. Internet webpage: <http://www.southampton.ac.uk/~imw/purbfac.htm>. Version: 19th December 2013 (Accessed 10th July 2020).

West, I.M. (2017) Dinosaur footprints in Jurassic-Cretaceous boundary beds on the Isle of Portland: Geology of the Wessex Coast (Jurassic Coast – World Heritage Site). Internet field Guide: <http://www.southampton.ac.uk/~imw/portdino.htm>. Version: 18th June 2017 (Accessed 10th July 2020).

West, I.M. (2018a) The Fossil Forest – Part 2- Trees, Lulworth Cove and Isle of Portland; Geology of the Wessex Coast (Jurassic Coast – World Heritage Site). Internet field Guide: <http://www.southampton.ac.uk/~imw/Fossil-Forest-Purbeck-Trees.htm>. Version: 14th June 2018 (Accessed 10th July 2020).

West, I.M. (2018b) Durlston Bay – Middle Purbeck Group, Geology of the Wessex Coast of Southern England. <https://wessexcoastgeology.soton.ac.uk/Durlston-Bay-Middle-Purbeck.htm>. Version 12th July 2018 (Accessed 26th May, 2021).

West, I.M. and Hooper, M.J. (1969) Detrital Portland chert and limestone in the Upper Purbeck Beds at Friar Wadden, Dorset. *Geol. Mag.* **106**, 277-280.

Westhead, R.K. and Mather, A.E. (1996) An updated lithostratigraphy for the Purbeck Limestone Group in the Dorset type-area. *Proc. Geol. Ass.* **107**, 117–128.

Wierzbowski, H., Anczkiewicz, R., Pawlak, J., Rogov, M.A. and Kuznetsov, A. B. (2017) Revised Middle-Upper Jurassic strontium isotope stratigraphy. *Chem. Geol.* **466**, 239-255.

Wright, P. and Barnett, A.J. (2015) An abiotic model for the development of textures in some South Atlantic early Cretaceous lacustrine carbonates. In: *Microbial Carbonates in Space and Time: Implications for Global Exploration and Production* (Eds D.W.J. Bosence, K. Gibbons, D.P. Le Heron, W.A. Morgan, T. Pritchard and B.A. Vining), Geol. Soc. London Spec. Publ. 418, London, 209–220.

Yabe, H. and Toyama, S. (1928) On some rock forming algae from the younger Mesozoic of Japan. *Sci. Rep. Tohoku Univ. Sendai. 2nd series (Geology)*, **12**, 141-152.

Young, J.T. (1878) On the occurrence of a freshwater sponge in the Purbeck Limestone. *Geol. Mag.* **5**: 220–221. \

FIGURE CAPTIONS

Fig. 1. Terms used to describe the range of meso-scale (millimetre to centimetre) textures and structures found within microbialites and followed in this paper. Modified from Schmid (1996), Dupraz & Strasser (1999) and Leinfelder & Schmid (2000).

Fig. 2. Location, onshore and offshore geology of study area modified after Gallois *et al.* (2018). Offshore geology is superimposed on sonar image of seafloor (Bosence *et al.*, 2018). Location of logged and sampled sections in text. The following abbreviations are used in the text and figure headings: Portesham Quarry – PQ; Poxwell Quarry – POQ; West Lulworth Cove – WLC; Fossil Forest – FF; Mupe Bay – MB; Worbarrow Tout – WT; Hell’s Bottom – HB; Swanworth Quarry – SQ; Fishermens Ledge – FL; Tout Quarry – TC; King Barrow Quarries – KB; South West Bowers – SWB; Coombefield Quarry – CQ; God Nore – GN; Lawnshed Quarry – LQ; Portland Bill – PB.

Fig. 3. **(A)** Disused quarry face illustrating stratigraphic units (white text) and facies (yellow text) on margin of a 26 m wide microbial mound, God Nore, Isle of Portland (LDB – Lower Dirt Bed, GDB – Great Dirt Bed). Circular and elongate holes in Hard Cap are moulds after trees. **(B)** and **(C)** Examples of thrombolite facies (from Hard Cap, God Nore) with irregular layering (bottom left to top right) parallel to outer accumulation surface of thrombolite. Columnar mesoclots – in **(B)** – with columns normal to accumulation surfaces and irregular mesoclots – in **(C)** – both with abundant framework porosity (‘F’), some with visible cement fringes and some filled with internal sediment (‘S’). **(D)** Thin section micrograph (plain polarized light – PPL) from thrombolite facies illustrating irregularly layered, porous, peloidal column (mesoclot) that grew to upper right. Thrombolite contains burrows (black arrows) (Gallois *et al.*, 2018), irregular cavities (white arrow) multigenerational brown fibrous rim cement (‘B’), framework pores (‘F’), variably filled with laminated geopetal internal sediment of peloids, crystal silt and intraclasts (yellow arrow). Hard Cap, Freshwater Bay, Isle of Portland. **(E)** Stratigraphic column for part of the Upper Jurassic of south Dorset including units discussed in this paper (after Westhead & Mather, 1996; Ensom, 2002; West, 2013, 2017).

Fig. 4. (A) Branching framework of *Cladophorites*. Transverse section of filaments (lower left) and vertical section (right). Note irregular cavities within framework, Skull Cap, (HB 6), Hell's Bottom. (B) Detail of (A) with vertical section through filament of *Cladophorites* to illustrate lateral branching. Note peloidal micrite between filaments. (C) *Cladophorites incrustans* (after Freytet 1997, Pl. II fig. e, in this text same form is referred to as *C. incrustata* Reiss). (D) Sketch of present day *Cladophora glomerata* illustrating filaments and mix of lateral and dichotomous branching (after Smith, 1955, fig. 27). (E) Eroded fragment of *Solenoporella* illustrating closely appressed polygonal filaments and (F) detail of specimen in (E) showing curved cell walls within filaments, Skull Cap (WT 1B). (G) Micron-scale filaments of presumed cyanobacteria entwined within larger (tens of microns) filaments of *Cladophorites*, Skull Cap (WT 1B). WT – Worbarrow Tout. All images are thin sections viewed in plain polarized light (PPL).

Fig. 5. (A) Peloidal packstone with moderate sphericity and sub-rounded to rounded peloids with early rim cement, Hard Cap (PQ 6). (B) Peloids within microbialite framework, Skull Cap (HB 6). (C) Peloids of varied shapes and roundness with ostracods and fish otolith (centre) in grainstone, Hard Cap (WT 3) (D) Scanning electron micrograph of polished and etched surface of peloids (P) illustrating dense micritic structure, with low-Mg calcite composition [inset, top right energy dispersive X-ray (EDS) analysis], with and fringe of bladed spar (BS) surrounded by late-stage, coarse, low-Mg calcite spar (inset, bottom left) cement (CS), Skull Cap (WT 1B). HB – Hell's Bottom, PQ – Portesham Quarry, WT – Worbarrow Tout.

Fig. 6. (A) Intraclasts comprising different microbialite components: spherulitic (Sp) microbialite (PM-C framework and CLM-C framework types). Intraclasts overlain by peloidal, skeletal packstone, Skull Cap (CQ 2). (B) Intraclast of microbialite framework, overgrown with brown, fibrous radial spar fringe cement. Ostracod (top upper left). (C) and (D) Scanning electron microscopy (SEM) and elemental mapping of area outlined in yellow square in (B). Lower right fibrous fringe cement (Ca) of low-Mg calcite (inset in D) passing left and upward into neomorphic microspar (N) irregular interlocking calcite crystals. Note small pockets of silica, Mg and Fe (in

D) suggesting clay minerals between fringing cement and microspar. Ostracod valve (O) top left. Hard Cap (GN 6). CQ – Coombefield Quarry, GN – God Nore.

Fig. 7. **(A)** Articulated and disarticulated, thin and thick valved ostracods; valves oriented parallel with bedding in peloidal and micritic matrix, Skull Cap (PQ 3). **(B)** Gastropod (left) and probable bivalve shells (below) with peloids (P) all within cavity to thrombolite framework (Tf). Quartz spherulite (Q) replacement of micritic matrix, Hard Cap (WLC 3). **(C)** and **(D)** Erosional surfaces (yellow dashed lines) within thrombolite (C) and forming external surface (D) to thrombolite mesoclots. **(C)** Two irregular-shaped internal pores (P) lined with brown rim cement and partially filled with sediment. Eroded portion of *in situ* framework (Tf – lower left) with irregular outline and truncated filamentous (white arrows) framework. Cavities filled with peloidal and intraclastic sediment, Skull Cap (SQ 7). **(D)** Outer surface of thrombolite framework (Concentrically Layered Thrombolite – CLTh f) showing erosional truncation of layering prior to infill with peloidal (P), intraclastic (IC) sediment, Hard Cap (GN 6). GN – God Nore Quarry, PQ – Portesham Quarry, SQ – Swanworth Quarry, WLC – West Lulworth Cove.

Fig. 8. **(A)** Thin section (plain polarized light – PPL) of brown fibrous fringe cement (FC) lining cavity within thrombolite (Tf). Light patches (Q) are chalcedony replacement of thrombolite framework and fringe cement, Hard Cap (GN6). **(B)** Scanning electron microscopy (SEM) magnification of area shown by white arrow in **(A)** showing fibrous and microporous nature of fibrous cement (FC) passing into former cavity (to left) with later, more equant calcite spar cement (LS). **(C)** Broken surface of modern tufa column indicating thrombolite framework (Tf) with mesoclots coated with early fibrous fringe cement (FC), Mono Lake, California. **(D)** Thin section (PPL) of mesoclot in **(C)** showing peloidal thrombolite framework (Tf) overgrown coated by later brown, radial fibrous cement fringes (FC). Both framework and cement fringe are replaced by calcite spherulites and botryoidal growths (white arrows) and spherulites may also grow within cavities (upper right in blue dyed resin) as cements. GN – God Nore Quarry.

Fig 9. **(A)** Cavity within thrombolite with brown fringing cement (FC), lower infill of inclined laminae of calcite crystals and intraclasts and then final fill of low-Mg calcite spar cement. Location of energy dispersive X-ray (EDS) analyses in **(C)** to **(F)** shown in **(A)** and **(B)**.

Laminated fill (**B**) and (**C**) comprises equant interlocking crystals of calcite – analysis in (**D**) – with pockets of aluminium silicate minerals (E) interpreted as clay minerals, features indicating a neomorphic fabric, or microspar. Hard Cap (GN 6). GN – God Nore Quarry.

Fig. 10. (**A**) Chalcedony spherulites replacing thrombolite framework and early fringe cement. Outer surface of thrombolite mesoclots preserved in upper third of the image. Spherulites increase in abundance to centre of mesoclot, Hard Cap (TQ 7); plain polarized light – PPL. (**B**) Similar view as (**A**) but in cross-polarized light (XPL) illustrating extinction crosses in spherulites and their increase in abundance away from the outer surface of the thrombolite (lower right), Hard Cap (TQ 7). (**C**) and (**D**) Detail of chalcedony spherulites showing extinction crosses (in XPL) and in (**D**) with gypsum plate showing second order extinction in north-west and south-east quadrants (Gallois, 2016). TQ – Tout Quarry.

Fig. 11. Thin section images and energy dispersive X-ray (EDS) analyses of calcite spherulites. (**A**) Brown fibrous fringe cement lining cavity in thrombolite framework (Tf) with petrographically identical spherical radiating forms some of which may be sections through mamillate growths and others as discrete Type 1 spherulites. Note interference growth between fibrous crystals (white arrow), Hard Cap (GN 6). (**B**) Reworked Type 1 spherulites, with dark micritic nuclei nucleus and cortices cortex of brown fibrous calcite surrounded by microspar (*cf.* Fig. 9A), Hard Cap (GN 6). (**C**) Peloidal and micritic thrombolite framework (Tf) with Type 2 (replacive) spherulites. Spherulites occur individually, in loose aggregates or larger clusters showing growth interference with adjacent clusters (centre). Also adjacent are Type 3 spherulites growing in cavity (centre right), Soft Cap (KB 7). Location of (**D**) and (**E**) are shown. EDS analyses of (**D**) calcitic composition of spherulite cortex and (**E**) margin of cortex of Type 2 spherulite with minor aluminium and silica peaks, from muddy matrix to packstone of thrombolite. (**F**) and (**G**) PPL and XP views of Type 3 spherulites showing growth interference with neighbours within cavity (pale blue resin fill) within thrombolite. Note cloudy centres and clear rims. Lower right shows example of passage from Type 3 to smaller, replacive Type 2 spherulites within peloidal matrix. XPL view in (**G**) illustrating clear extinction crosses in calcitic cortex – EDS analysis shown in (**H**). Soft Cap (KB 7). GN – God Nore Quarry, KB – King Barrow Quarry.

Fig. 12. (A) and (B) Scanning electron microscopy (SEM) micrographs of Type 1 spherulites from polished and etched surfaces. Overview (A) and detail (B) of spherulites with radiating, microporous, fibrous spar (FC) passing radially outward to bladed (BC) and later, equant spar cement (LS). Skull Cap (WT 1B). Location of energy dispersive X-ray (EDS) analyses are shown in (A). (C) to (E) EDS analyses of nucleus, cortex and spar cement, respectively, indicating calcite composition with very minor Mg and Si peaks – analyses located in (A). (F) Intraclasts of clusters of Type 4 spherulites (arrows) with micrite rim in peloidal packstone, Soft Cap (KB 7). (G) Intraclast of cluster of Type 4 spherulites (arrows) with associated dark coloured peloidal packstone reworked into lighter coloured intraclastic packstone, Soft Cap (KB 7). KB – Kings Barrow Quarry, WT – Worbarrow Tout.

Fig. 13. Mesoscale views of microbialites and their components within Purbeck Caps (m – mesoclot, is – internal sediment, c – framework cavity). (A) Cut and ground surface to show irregular shaped mesoclots (cream with brown rims) in grey peloidal matrix in Peloidal Thrombolite (PTh). Mesoclots elongate along accumulation surfaces in thrombolite, Soft Cap (KB 7). (B) Cut and ground surface of *Cladophorites* Thrombolite (CTh) with irregular-shaped and digitate-shaped mesoclots set in peloidal matrix (lower half) and with original (framework) porosity (upper half), Hard Cap (CQ 6). (C) Weathered surface of rounded mesoclots of Concentrically Layered Thrombolite (CLTh), Hard Cap (BQ 8). (D) Cut and ground surface of Peloidal Fenestrate Stromatolite (PFS) with bedding-parallel, irregular layering and fenestrae, Skull Cap (FF 4), Fossil Forest, Lulworth. BQ – Broadcroft Quarry, CQ – Coombefield Quarry, KB – Kings Barrow Quarry.

Fig. 14. Photomicrographs [(A), (B), (E) and (F) in plain polarized light (PPL); (C) in crossed polars (XP)] of five main framework types of microbialites in the Purbeck Caps. (A) PTh framework with peloids (P) and partial preservation of filaments (F). Three erosional cavities (C) have irregular margins that truncate filaments (white arrow) within mesoclot and are filled with internal sediment, peloids and spar cement, Hard Cap (PQ6). (B) Branching radiating algal filaments of *Cladophorites* within the CTh with cavities, some filled with microspar (M) and

peloids (P) and others with clear calcite spar (S). Erosional cavities with truncated filaments on margins, Skull Cap (HB6). (C) Layered, micritic texture of CLTh with replacement of mesoclot by chalcedony (centre, Ch) and patchy, recrystallization to neomorphic calcite spar (NS) and by calcitic spherulites (Sp) in lower left, Hard Cap (WLC 3). (D) Scanning electron microscopy (SEM) view of mesoclots in (C) illustrating layered, microclotted structure (LM-C), chalcedonic quartz spherulite (Ch), and late-stage calcite spar cement (S). Energy dispersive X-ray (EDS) analyses of: '1' silica replacement of low-Mg calcite in '2' layered fabric in mesoclot and '3' late cavity-filling spar (S). Pore space (P). Hard Cap (WLC 3). (E) Dense Micritic Leiolite (DML) (centre and right) overgrowing mesoclot of CTh with filaments (F) (lower left). Yellow dashed line marks contact between two fabrics. Aligned ostracod valve fragments (white arrows) and peloids within crust. Thin section located in Fig. 15 (yellow outline), Hard Cap (PQ6). (F) Layered, micro-clotted (spongiostromate) texture in Peloidal Fenestrate Stromatolite (PFS) with loose micro-clotted peloidal texture, vertical stacking of peloids (arrows), bedding-parallel fenestrae, and two generations of cement in cavities ('1' and '2'), Skull Cap (WT1B). HB – Hell's Bottom, PQ – Portesham Quarry, WLC – West Lulworth Cove, WT – Worbarrow Tout.

Fig. 15. Thin section micrograph (left) and tracing (right) of succession of thrombolite frameworks in Hard Cap (PQ6). Initial columnar mesoclot of CTh overgrown by crust of DML. A peloidal, intraclastic packstone internal sediment fill overlies this crust and infills cavity (bottom right). Subsequently the PTh overgrows the two previous microbialites and accumulates to upper left. Note the accumulation direction of the thrombolite is to upper left. Boxes in the left image indicate location of photomicrographs 13A (yellow) and 13E (black). Energy dispersive X-ray (EDS) analyses of micrite in (A) between filaments of *Cladophorites*, and (B) within the leiolite crust, indicates low-Mg calcite. PQ – Portesham Quarry.

Fig. 16. Thin section micrograph (left) and tracing (right) of primary framework of CLTh with large growth-framework pores. Note construction of mesoclots with concentric accretion surfaces and preservation of mesoclot morphology in margins to cavity (top centre). Central areas of mesoclots commonly replaced by clusters of chalcedony spherulites, Hard Cap (WLC3) (black box in left image shows location of Fig. 13C and D). WLC – West Lulworth Cove.

Fig 17. Micrograph (left) and tracing (right) illustrating CTh in lower two-thirds of slide cut by truncation surface overlain by angular clasts of thrombolite with internal sediments and fibrous cements. Abundant cavities in CTh interpreted as secondary as they truncate the filament framework. The framework is only preserved as a relict network in a thrombolite comprising principally of internal sediment. The cavities are filled with three stages of internal sediments differentiated by their infilling components. Some (top right centre), with high-angle geopetal structures indicating syndepositional rotation/collapse of thrombolite framework, Hard Cap (GN6), GN – God Nore.

Fig. 18. Micrograph (left) and tracing (right) illustrating intergrowth of thrombolite frameworks with eroded mound debris. The lower third of the section largely comprises a cm-sized fragment of the layered, PFS with a fitted texture, suggesting *in situ* fragmentation soon after deposition. This occurs within a rudstone of thrombolite fragments that is overgrown by a CTh with large irregular, spar filled cavities. Following erosion, the upper surface of the thrombolite is irregular and eroded and overlain by a peloidal intraclastic packstone, Skull Cap (WT1B). WT – Worbarrow Tout.

Fig. 19. Lithological log through the Skull and Hard caps of Perryfield Quarry, Isle of Portland, showing two coarsening and shallowing-upward cycles capped by micro-karstic surfaces and palaeosols. Black dots to left of lithological column indicate drilled samples into fresh quarry face for isotope analysis and arrows indicate location of thin sections. $\delta^{13}\text{C}$ and $\delta^{18}\text{O}$ cross-plots are shown in the inset together with Tithonian seawater values from Nunn & Price (2010). For discussion and interpretation see text.

Fig. 20. $^{87}\text{Sr}/^{86}\text{Sr}$ ratios for thrombolites and their cements from the Hard Cap, Isle of Portland of late Tithonian age plotted alongside $^{87}\text{Sr}/^{86}\text{Sr}$ seawater curve for the Jurassic and Early Cretaceous (Wierbowski *et al.*, 2017). Also plotted are $^{87}\text{Sr}/^{86}\text{Sr}$ ratios from Devonian basement rocks from Cornwall (Darbyshire & Shepherd, 1994) but note changes in scales for these considerably older and more radiogenic rocks. For discussion and interpretation see text.

Fig. 21. Abundance of microbialite types plotted with respect to the three stratigraphic levels of the lower Purbecks (SkC – Skull Cap, HC – Hard Cap, SoC – Soft Cap) from eastern and western palaeogeographic areas and the Isle of Portland to the south. Occurrences (numbers) of microbial types as counted from 63 thin sections. For full names of location initials see Fig. 2.

Fig. 22. Summary sketch showing the seven phases involved in the construction and early diagenesis of thrombolites in the lower Purbeck Limestone Group from framework construction ('1') through to replacement by chalcedony spherulites ('6'). 5a, 5b, 5c and 5d represent stages of internal sedimentation including growth framework cavity-fills through to intermound packstones.

Table 1. Description and brief interpretation of depositional and diagenetic components of microbialites from the lower Purbeck Limestone Group. For discussion and interpretations see text.

Appendix S1. Supplementary information.

| Microbialite components | Morphology | Microstructure and composition | Occurrence | Interpretation |
|---|--|---|---|---|
| <i>Depositional</i> | | | | |
| <ul style="list-style-type: none"> • Peloids | Very fine to medium sand-sized (50–200 μm but locally 300 μm) rounded, micritic grains. Similar in different occurrences. Vary from elliptical to subspherical to irregular shapes and are sub-angular to well-rounded (Fig. 5) | Low-Mg calcite micrite. Three end-members; undifferentiated micrite, micrite with denser micrite patches, micrite with fossil debris (Fig. 5). Commonly coated with radiating bladed spar cement (Fig. 5D), locally with fitted texture | Commonest grain type within microbialites, as internal sediment and also in intermound Intraclastic peloidal packstone – grainstone facies (Gallois <i>et al.</i> , 2018) | Derived by reworking, abrading and size-sorting of intraclasts of micritic sediments from microbialite frameworks and faecal pellets (<i>cf.</i> Brown, 1961; Arp, 1995) |
| <ul style="list-style-type: none"> • Intraclasts | Subangular to rounded clasts with micritic internal structure, commonly with preserved microbial filaments and peloids (Fig. 6) | Similar to microstructure of microbialites. Commonly coated with rim cements of elongate, 10–20 μm , bladed calcite spar (Fig. 6B) | Second commonest grain type within microbialites, as internal sediment and in intermound sediments | Textural immaturity and microstructure indicates derivation from reworking of microbialite frameworks |
| <ul style="list-style-type: none"> • Skeletals <ul style="list-style-type: none"> · Molluscs | Bivalve and gastropod shells and their debris (Fig. 7B) | Shells replaced by calcite spar as a cement or neomorphic recrystallization. Presumed original | Within microbialite cavities as internal sediment and as | Biota indicates mixed marine, low salinity and freshwater taxa (Radley, |

| | | aragonite composition | intermound grains | 2002) |
|-------------|---|---|--|---|
| · Ostracods | Articulated and disarticulated valves and valve fragments (Fig. 7A) | In matrix-free situations are commonly overgrown with fibrous syntaxial calcite spar on both internal (Fig. 6B) and external surfaces | Throughout microbialites and as concentrations in <0.5 cm thick layers of valves and their fragments (Fig. 7A), commonly oriented along bedding, or as trapstone fabrics | Assemblages indicate brackish-water lake (Barker <i>et al.</i> , 1975) and saline to freshwater (Horne, 2002) |





| <i>Early Diagenetic</i> | | | | |
|---|---|---|--|---|
| • Erosion/dissolution surfaces and cavities | Irregular surfaces truncating microbialite frameworks and generating irregular shaped internal cavities (Fig. 7C and D) | Surfaces truncate external surfaces and internal structures of thrombolites. Surfaces either coated with fibrous cement or infilled with internal sediments | Found in all types of thrombolite | Surface removal and cavity formation by dissolution and/or physical erosion (see text) |
| • Fibrous cement fringes | 100–300 μm thick isopachous fringes (Figs 3C, 7A, 8A) on exterior of thrombolites. Commonly on eroded surface | Brown, bladed to fibrous microporous crystals (Fig. 8A and B). In SEM fibrous crystals of low-Mg calcite spar grade outwards to bladed and equant crystals that lack micropores (Fig. 6C and D). Occur in close association with Type 1 calcite spherulites (below) | Coatings to mesoclots overlain by internal sediment, late stage spar or as cavity lining. Commonly the framework is eroded prior to growth of fringe | Early stage, sub-aqueous lacustrine cements growing on microbialite substrates |
| • Microspar | Up to 50 μm across, irregular and equidimensional spar. Size-differentiated laminae with micritic intraclasts suspended in microspar | Spar with irregular boundaries and common triple junctions. Pockets of silica, magnesium and aluminium detected between low-Mg calcite spar (Fig. 9) | Commonly occurs as geopetal infill to primary and secondary cavities in and around mesoclots | Occurrence, laminae, floating intraclasts and composition indicate a original depositional texture. Morphology and size indicates neomorphic recrystallization as microspar |

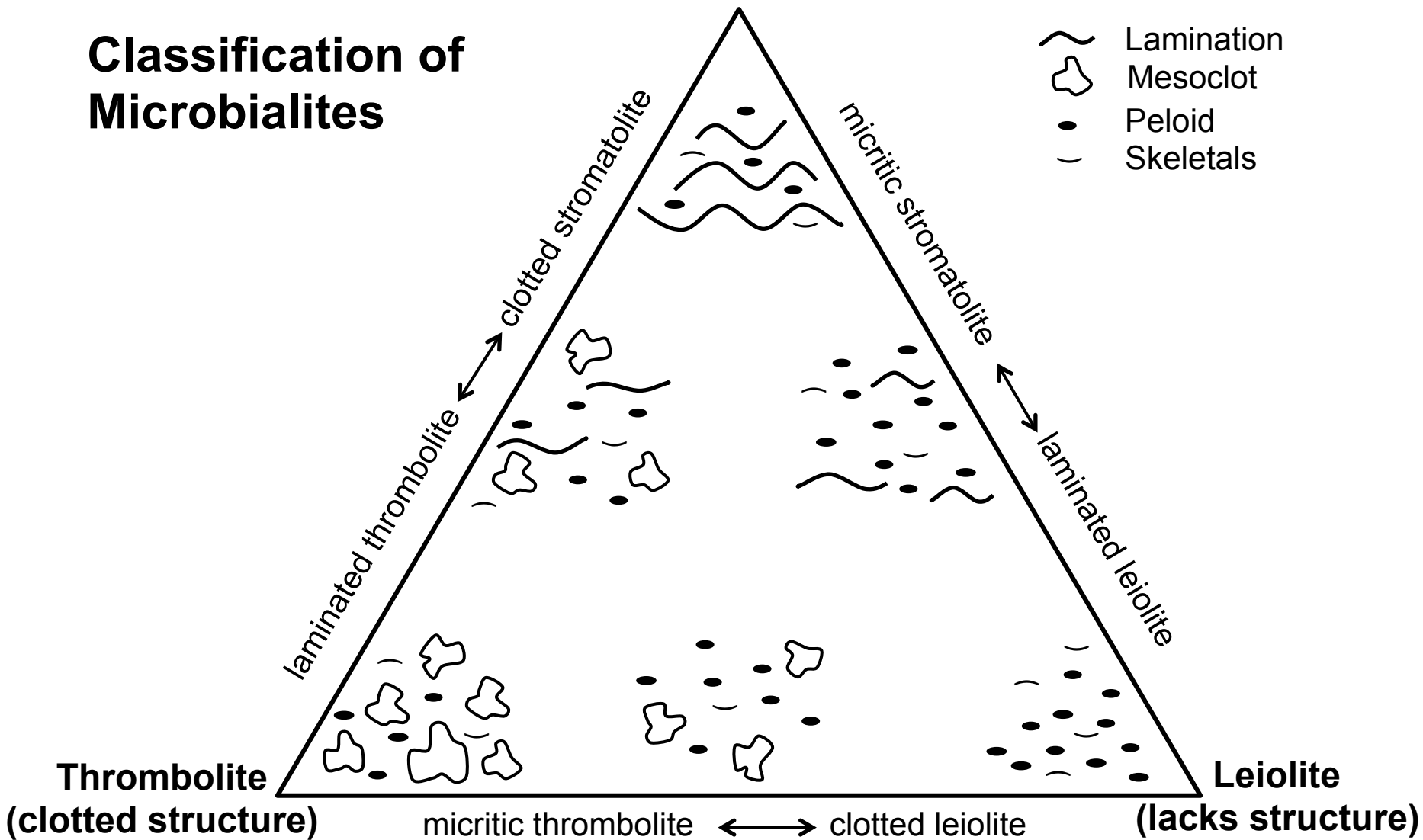
| | | | | |
|-----------------------|--|--|---|---|
| • Quartz spherulites | Spherulites are 50–100 μm across and commonly display extinction cross (Fig. 10) | Quartz is a length-slow chalcedony (Fig. 10) replacing micritic mesoclots and rarely calcite spherulites | Common to abundant in thrombolite mesoclots. Increase in abundance toward mesoclot centre | Silicification of organic-rich thrombolites from Si-rich pore waters from dissolution of sponges or detrital silica (see text) |
| • Calcite spherulites | Sub-spherical, growths constructed of radially arranged calcite crystals. Occurring as four types | Spherical crystal aggregates with dark micritic nucleus and radiating fibrous to bladed calcite crystals | Minor component of thrombolites as cements in cavities or recrystallizing mesoclots. Not found in surrounding intermound facies | Early, subaqueous, lacustrine precipitates as cements and as neomorphic recrystallization |
| • Type 1 | 100–200 μm diameter spherulites composed of radially arranged calcite crystals. Also continuous with growths of the fibrous fringe cements (above) as botryoidal protuberances (Fig. 11A) | Fibrous to bladed to brick-shaped, brown, radially arranged calcite spar (Fig. 11A and B). Under SEM a micritic cores are coated with radiating, microporous, fibrous to bladed calcite crystals (Fig. 12A to E) | Occur in intimate proximity to fibrous cement fringes to cavities and as reworked grains in cavities with microspar, etc (Fig. 11A and B) | Early stage, sub-aqueous lacustrine cements growing as protuberances on fibrous cement fringes, isolated spherulites and as reworked grains |
| • Type 2 | Isolated, or clustered spherulites within mesoclots (Fig. 11C). 20–60 μm (mean 40 μm) in diameter. Fitted textures between adjacent clusters | Cloudy to clear, fibrous radiating fabric with some prominent crystal boundaries giving appearance of equant crystals (Fig. 11C). Extinction crosses present but not common. | Occur within mesoclots to thrombolites | Fitted textures of adjacent clusters set in micritic mesoclots indicate neomorphic recrystallization of mesoclot to spherulite |

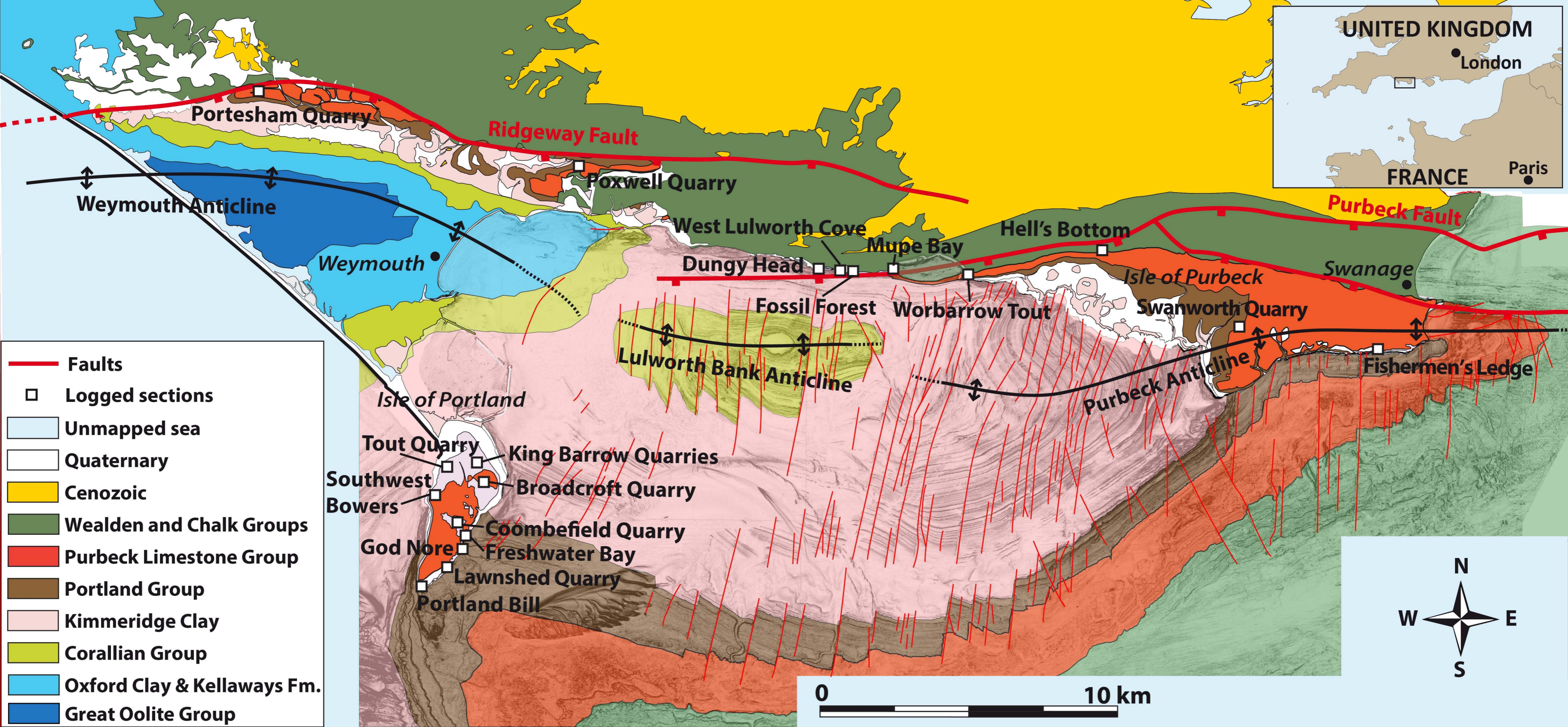
| | | | | |
|----------|---|---|--|--|
| | | Clear crystals, low-Mg calcite and cloudy with some aluminium and silica (Fig. 11C and D) | | |
| • Type 3 | 60–90 μm (mean 78 μm) diameter spherulites. Isolated or clustered | Cloudy centred with clearer rim. Fibrous radiating fabric of low magnesium calcite with extinction crosses (Fig. 11F to H). Fitted fabrics common | Within cavities in thrombolites (Fig. 11F) and transition into Type 2 (Fig. 11C) | Fitted texture of adjacent spherulites in cavities indicate precipitation from pore waters in thrombolite cavities |
| • Type 4 | Irregular shaped, sand-sized clasts comprising spherulites and matrix set in mesoclots and internal sediment (Fig. 12F and G) | Spherulites in clasts similar to Type 2 (above). Clasts have sharp outlines and, locally, micritic envelopes | As clasts within intraclastic packstones infilling cavities in thrombolites | Shape and outline of spherulitic clast and occurrence indicate origin from erosion and redeposition |

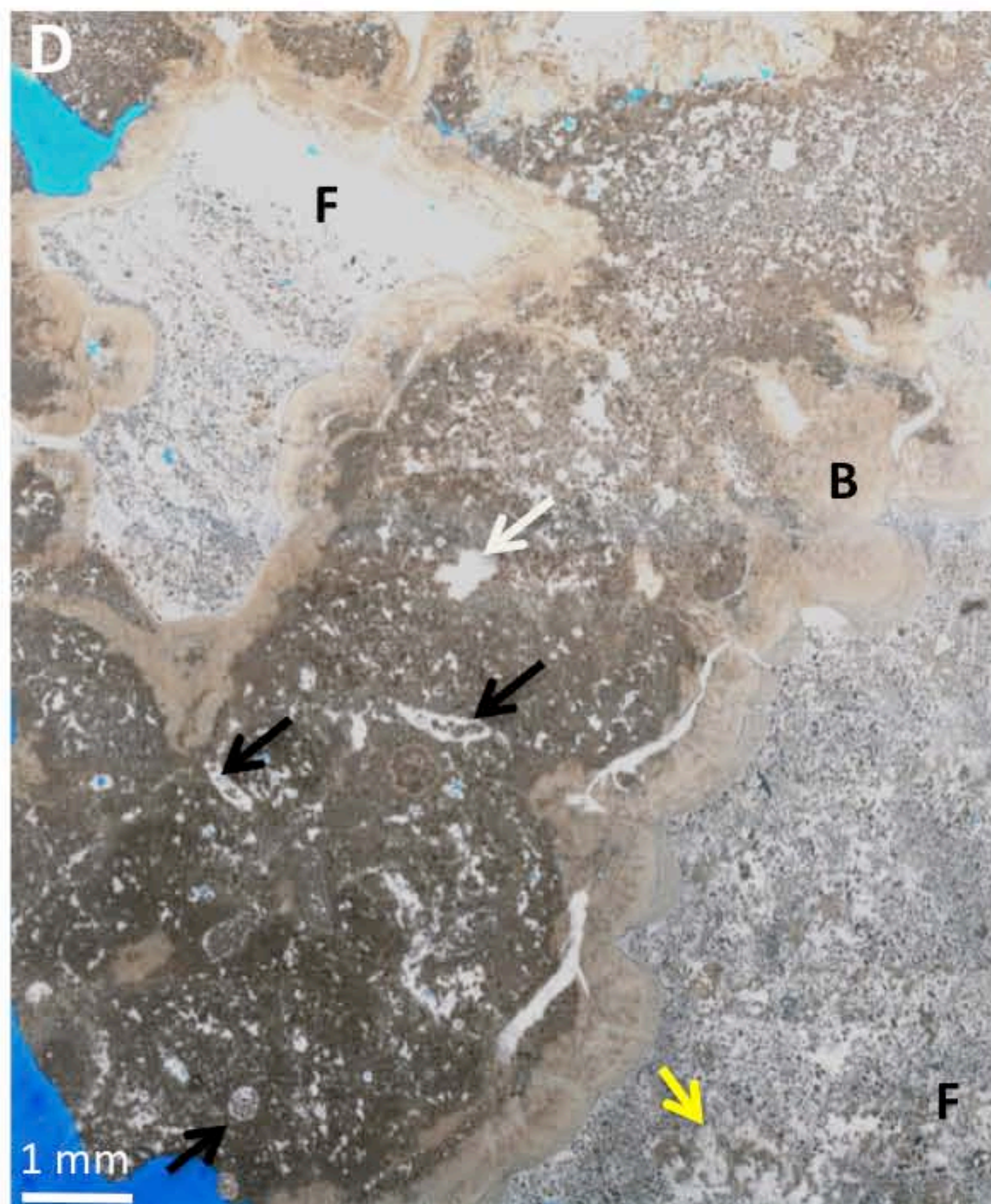
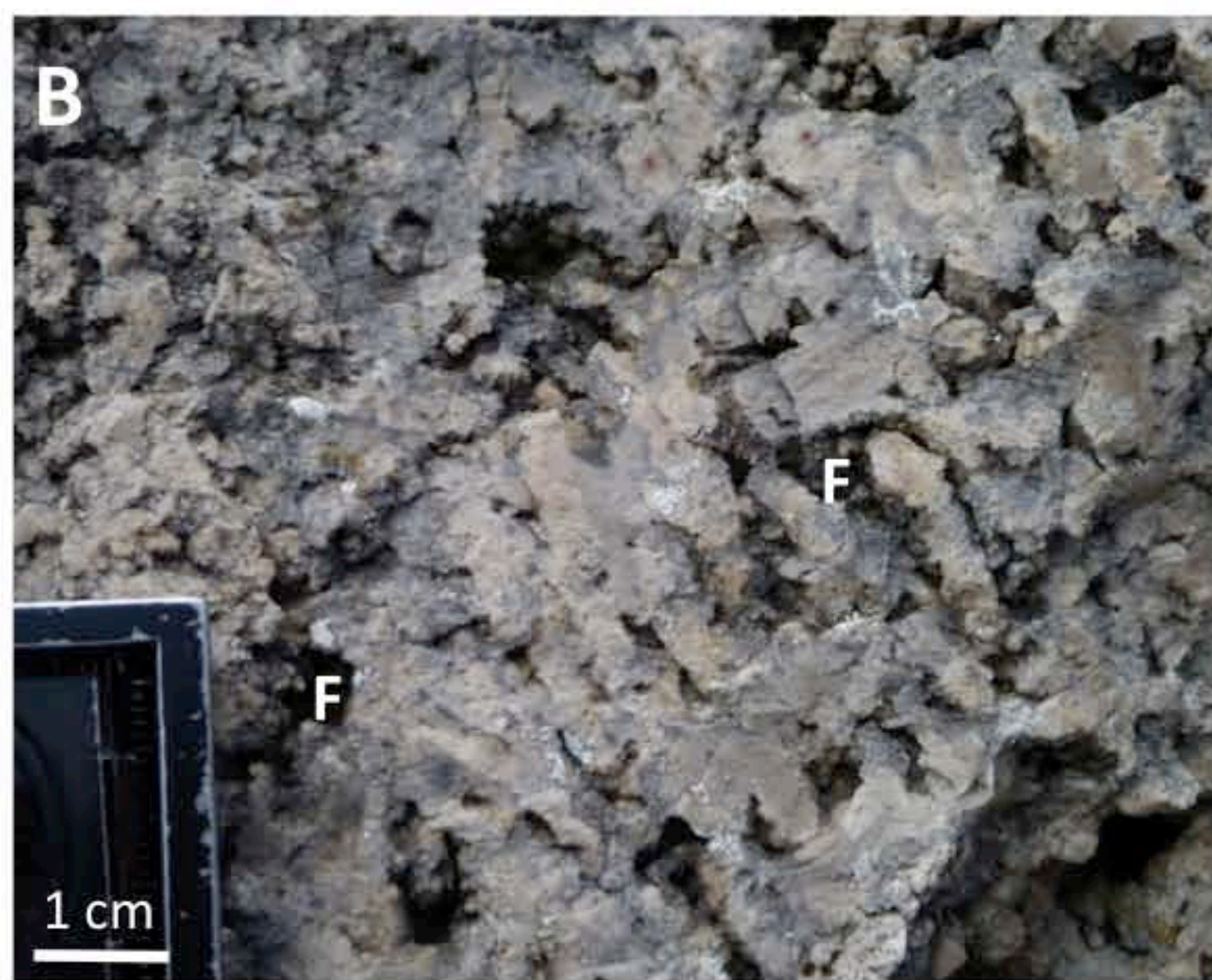
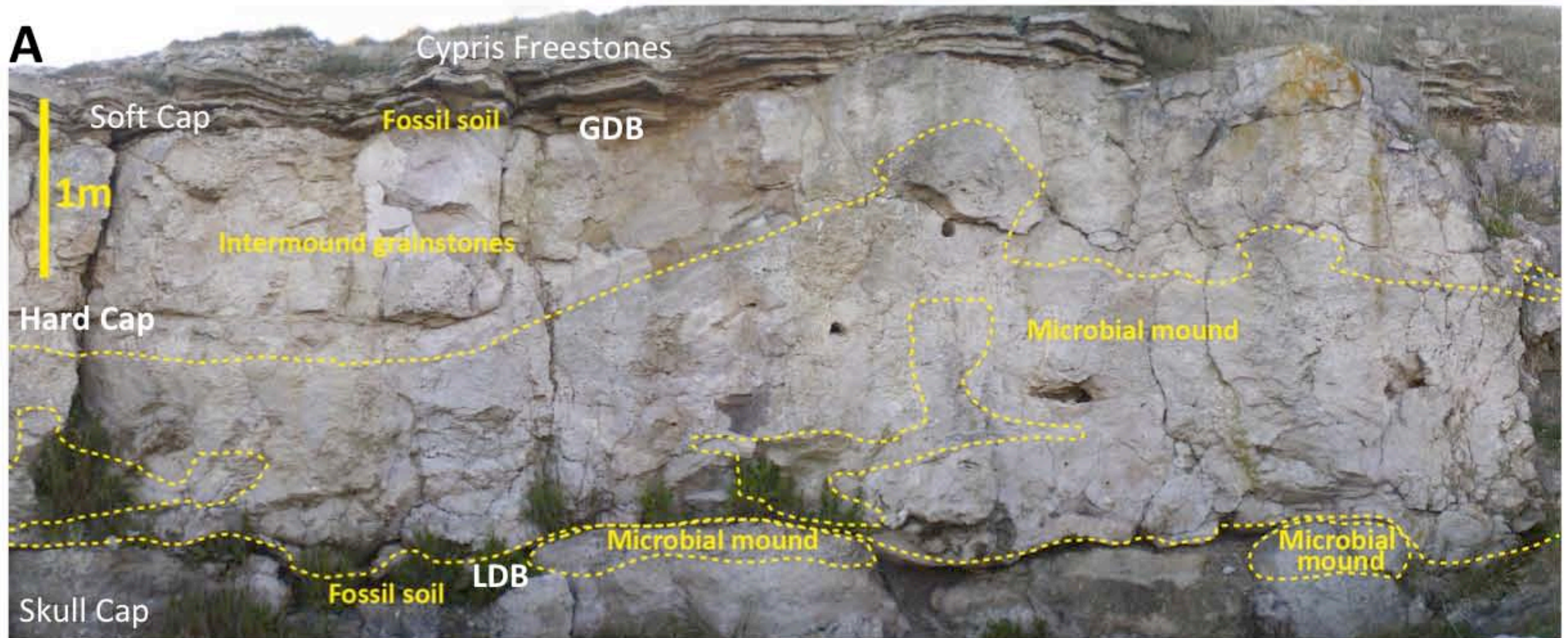
Classification of Microbialites

Stromatolite
(laminated structure)

-  Lamination
-  Mesoclot
-  Peloid
-  Skeletals

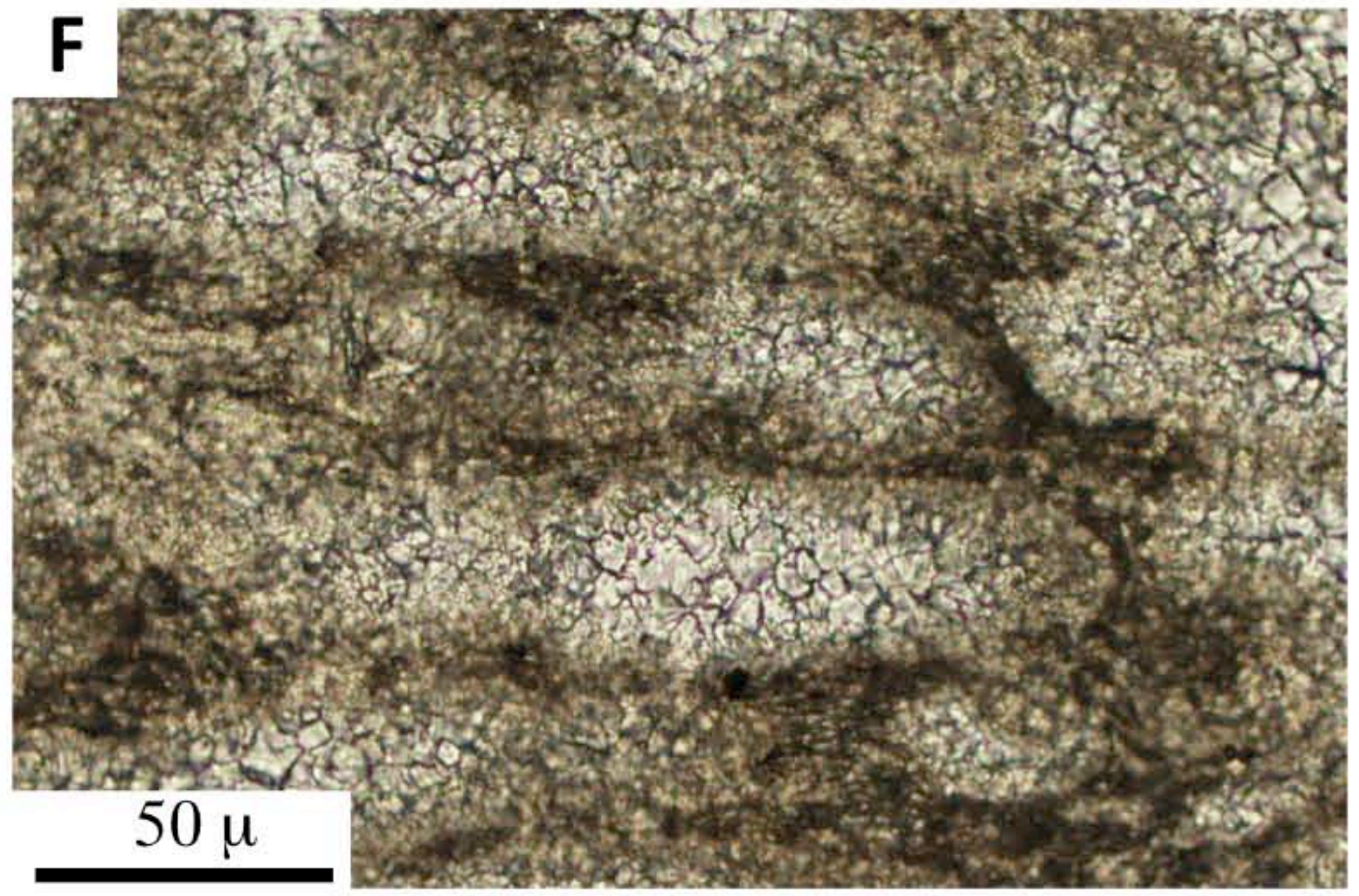
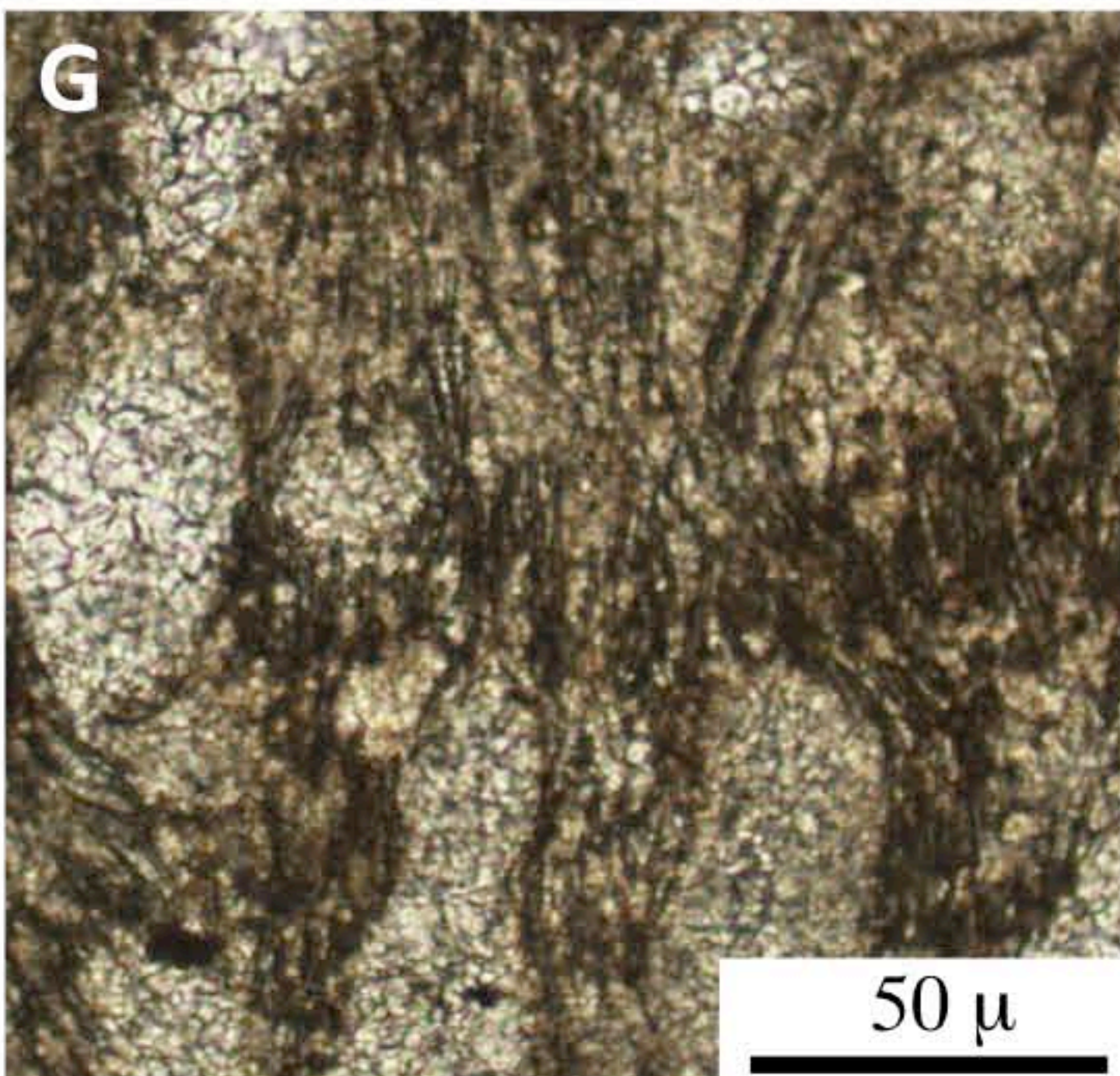
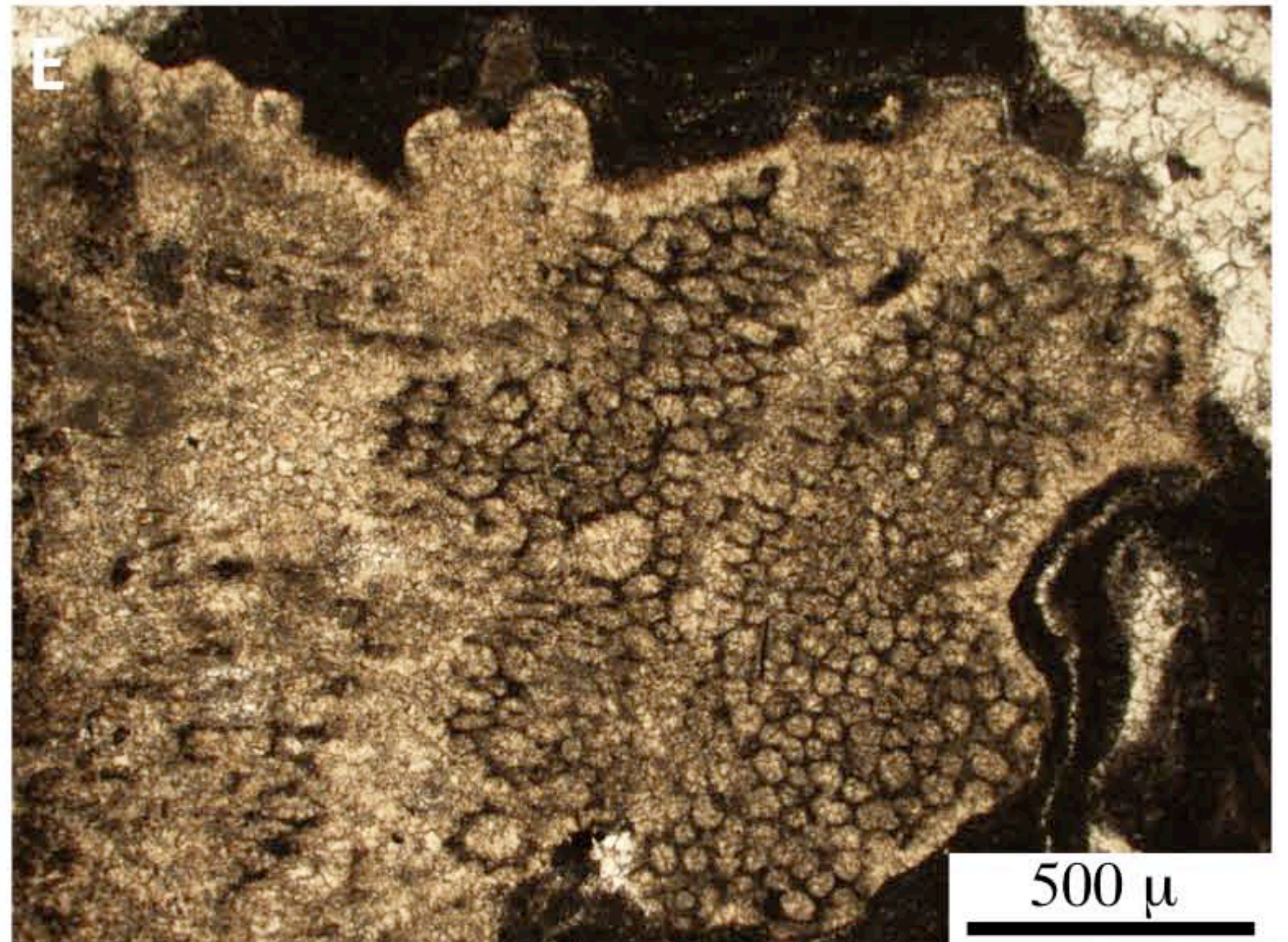
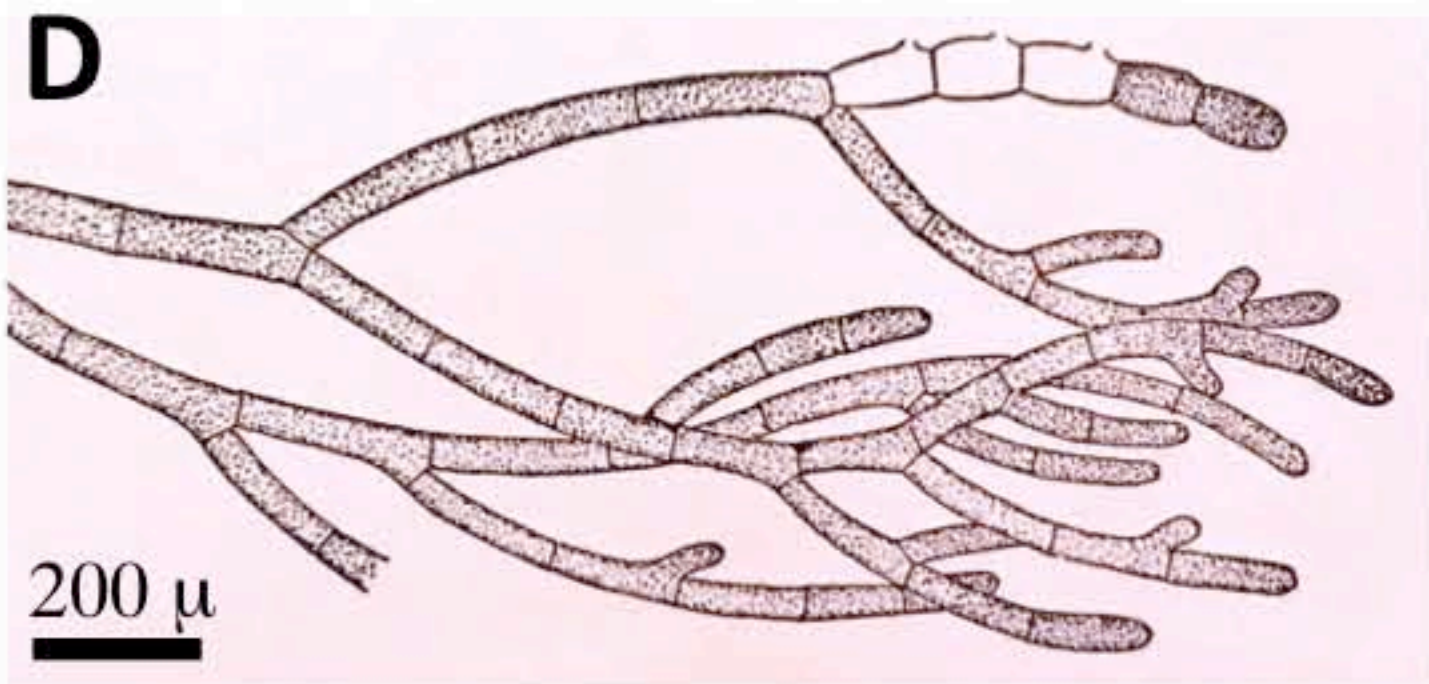
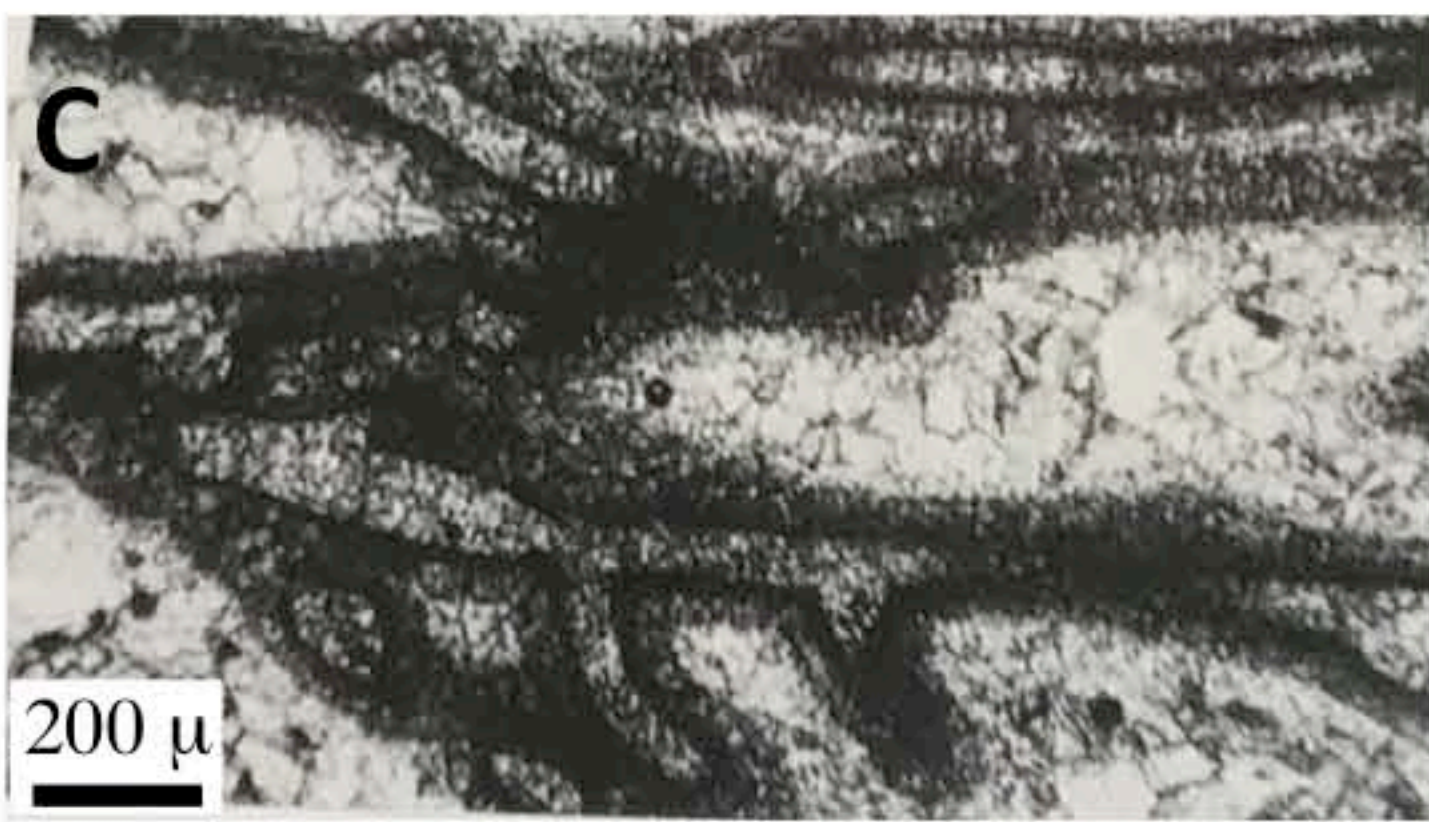
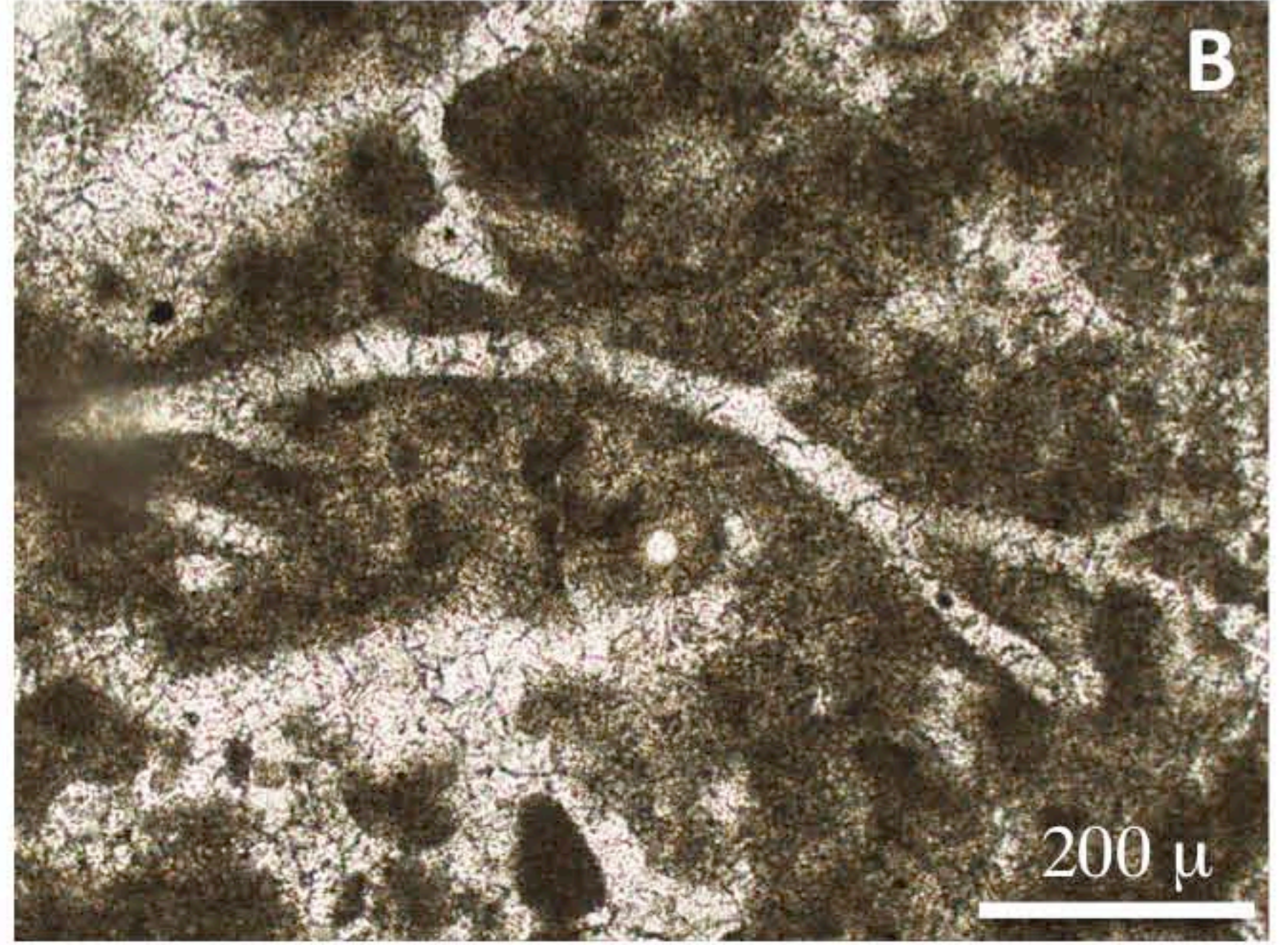
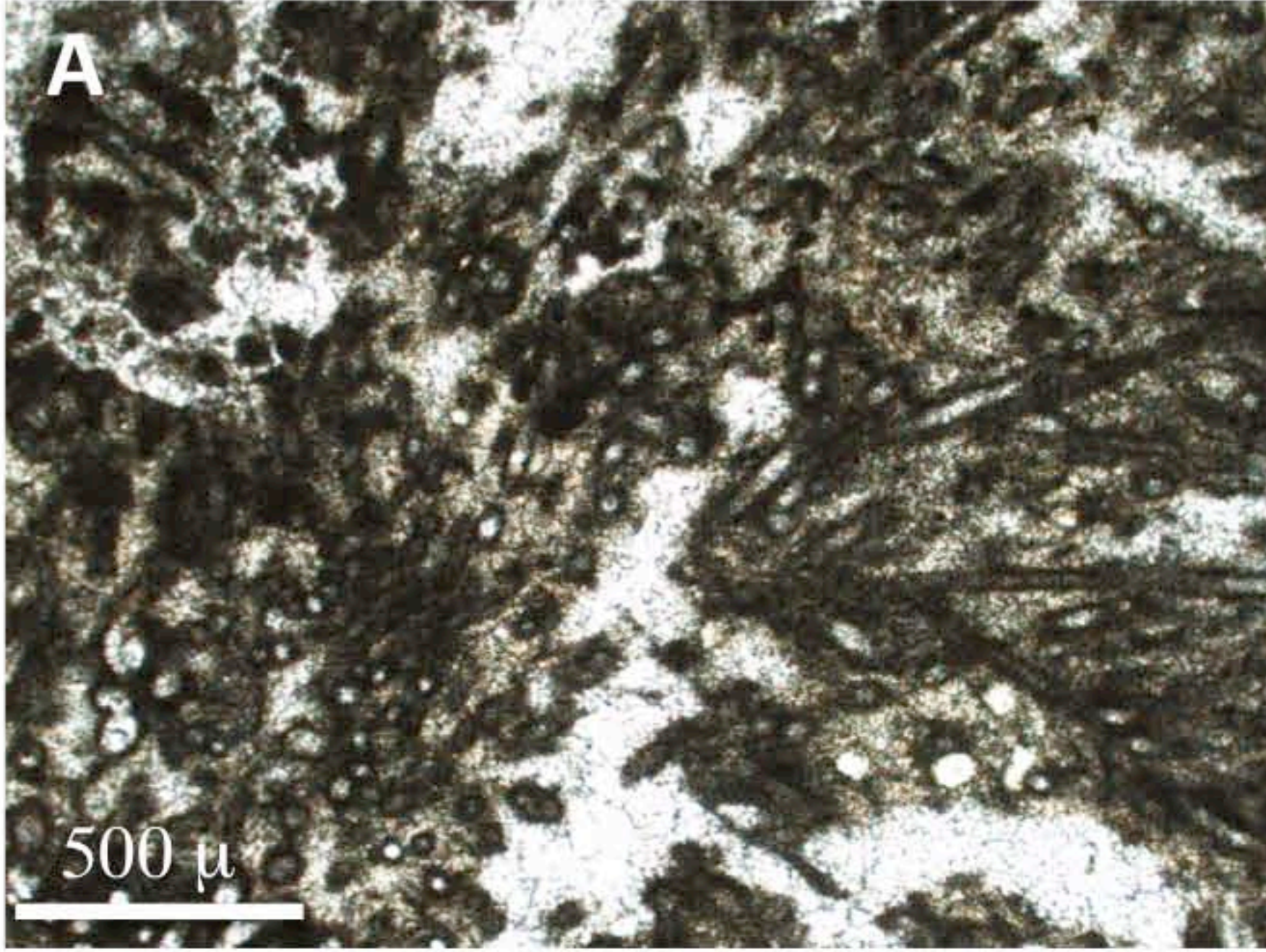


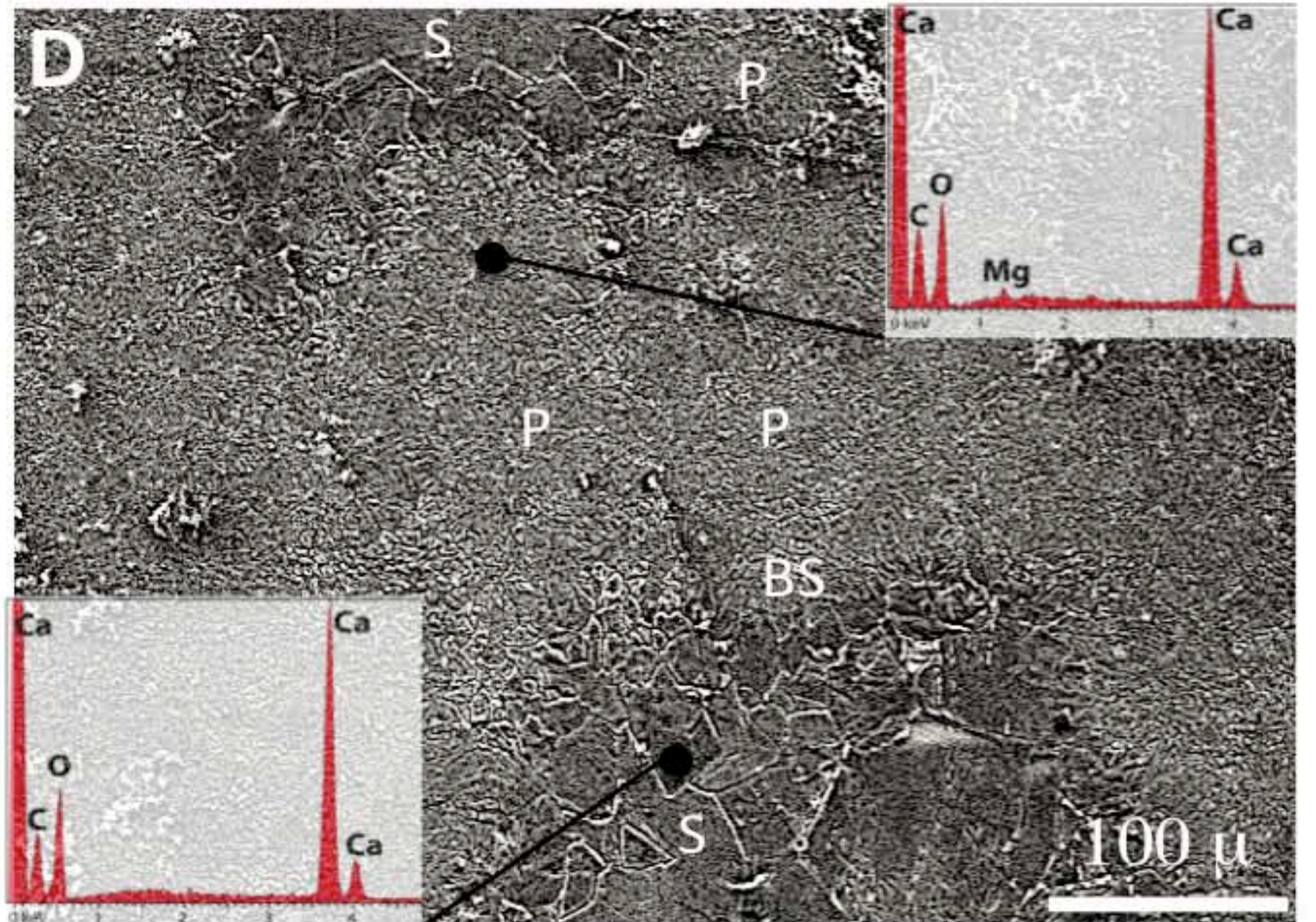
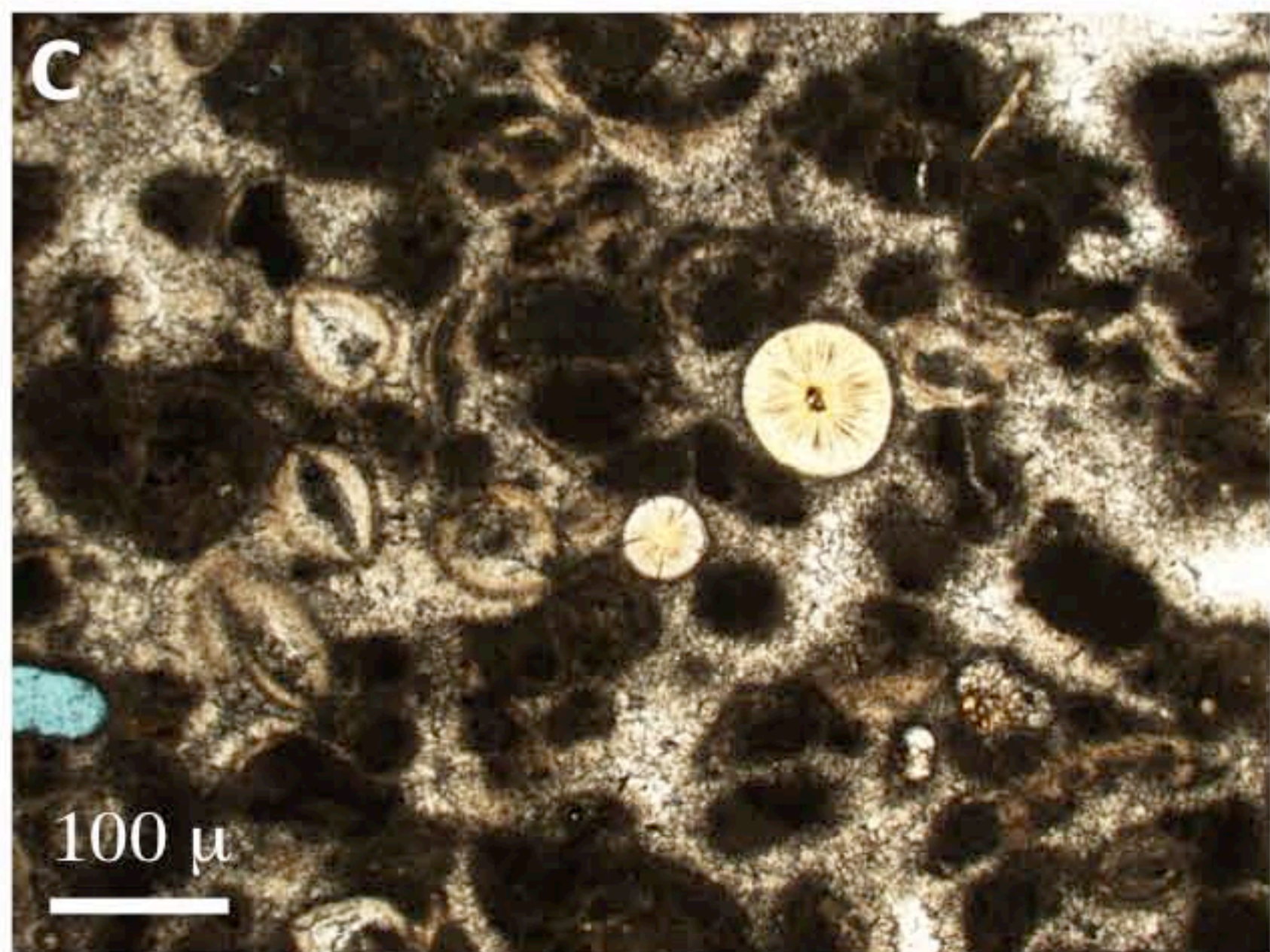
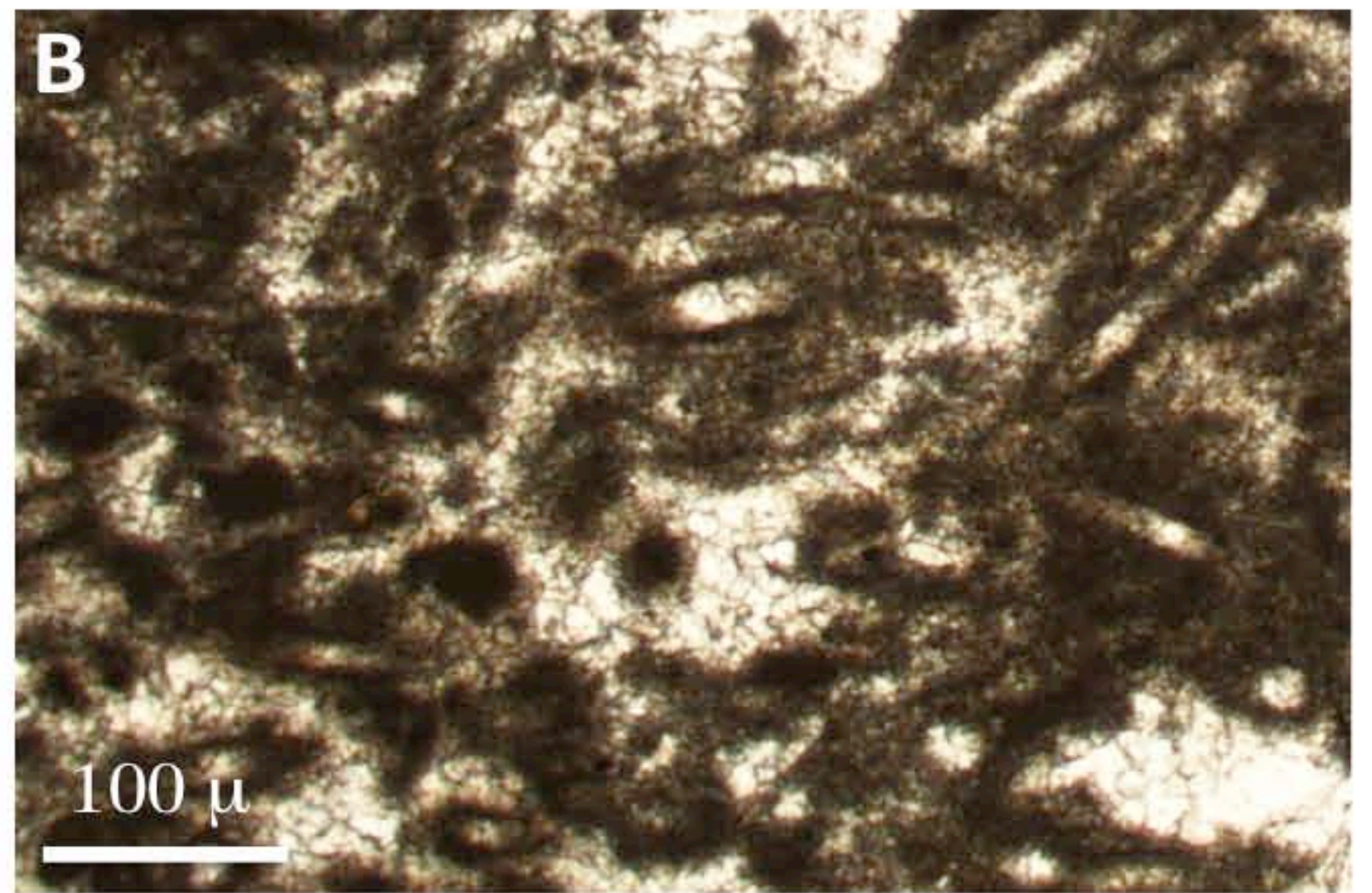
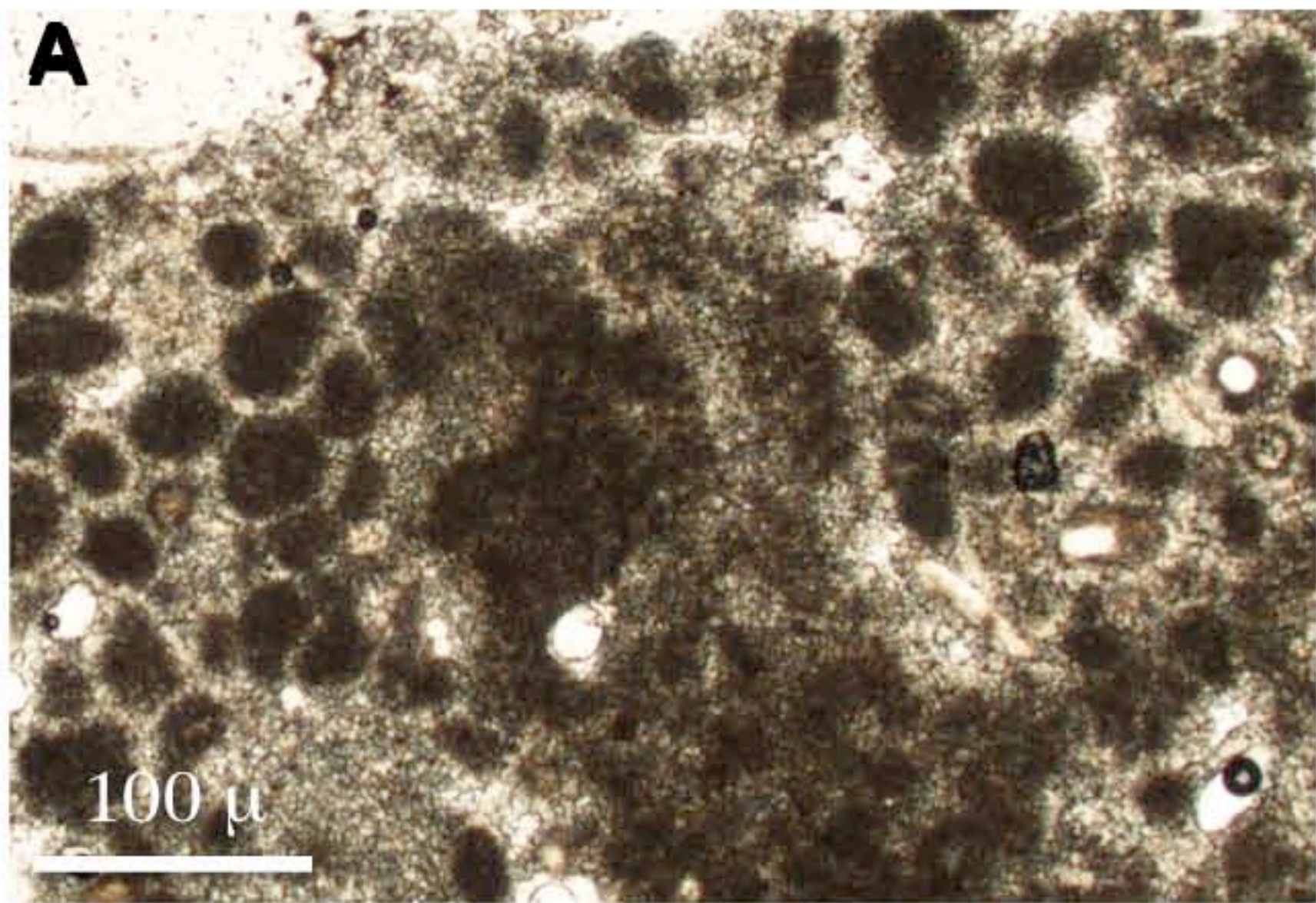


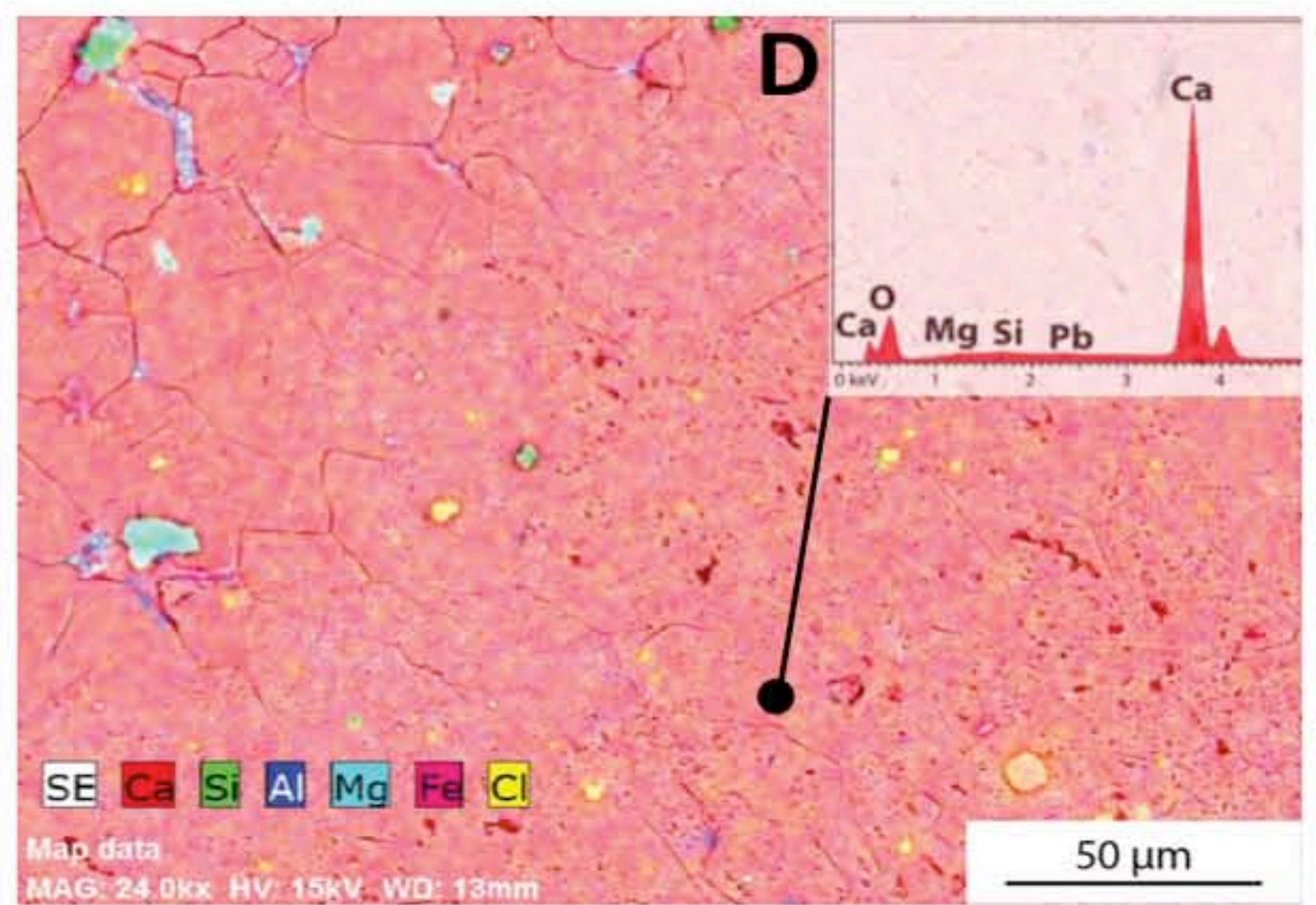
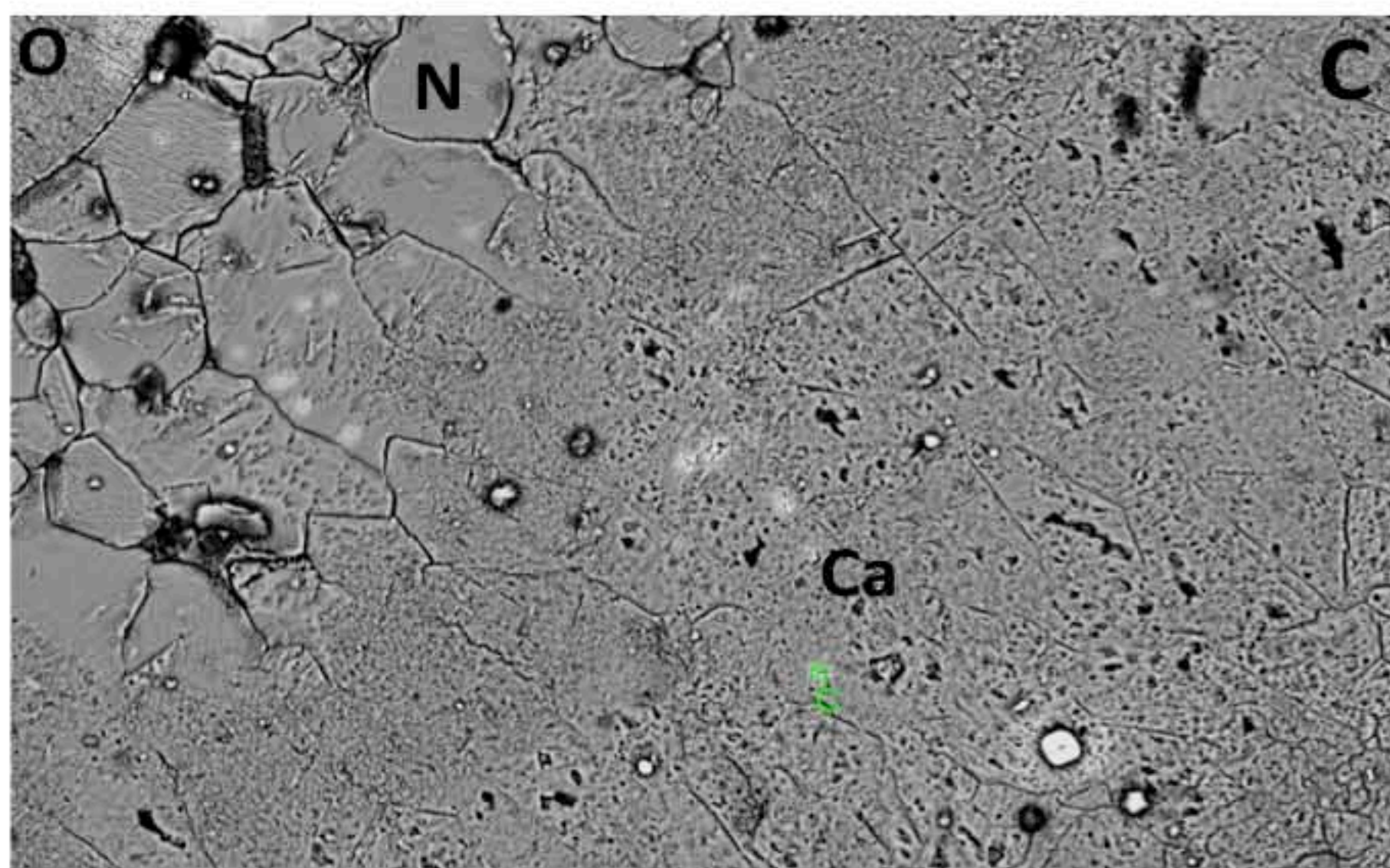
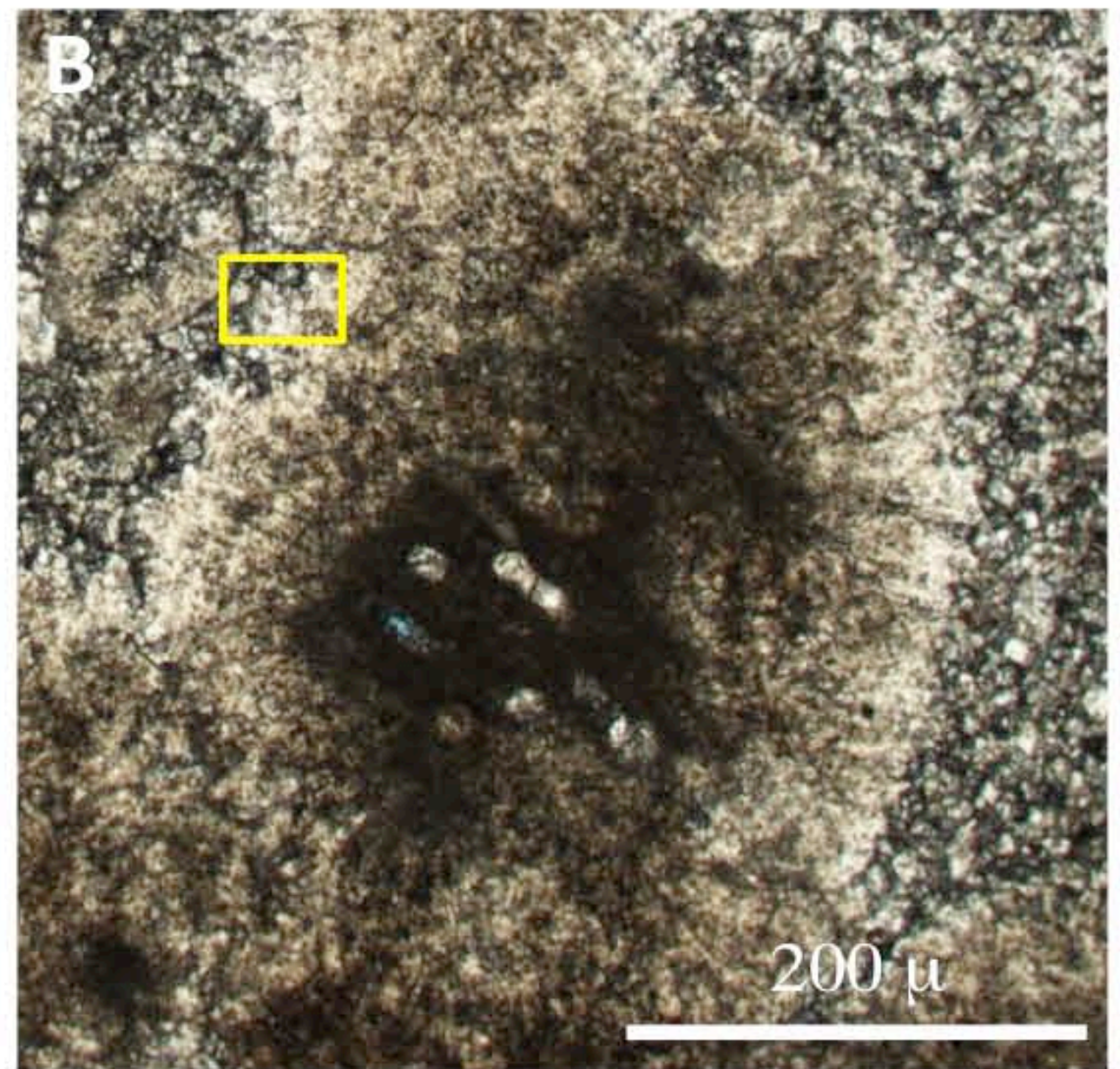
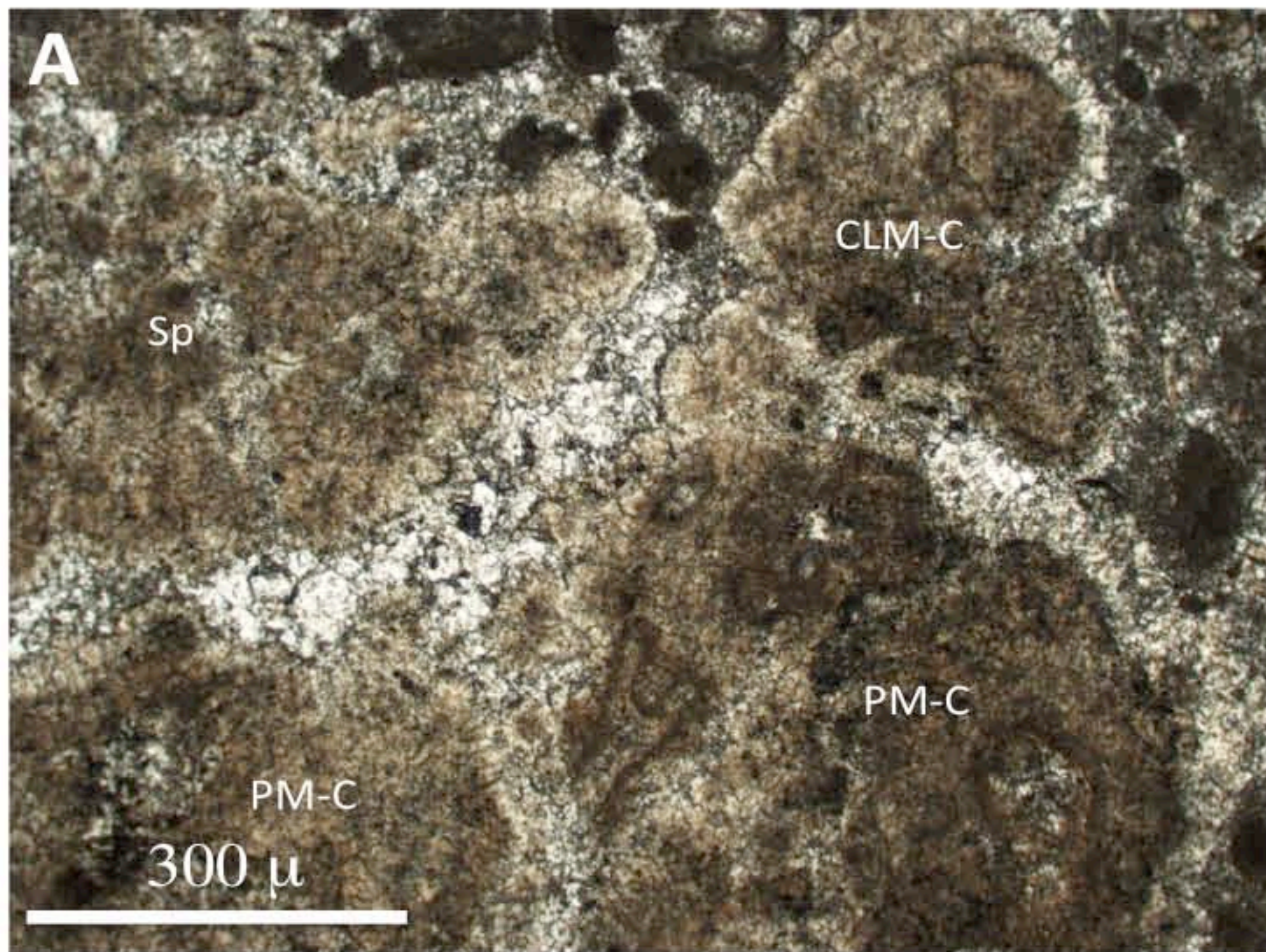


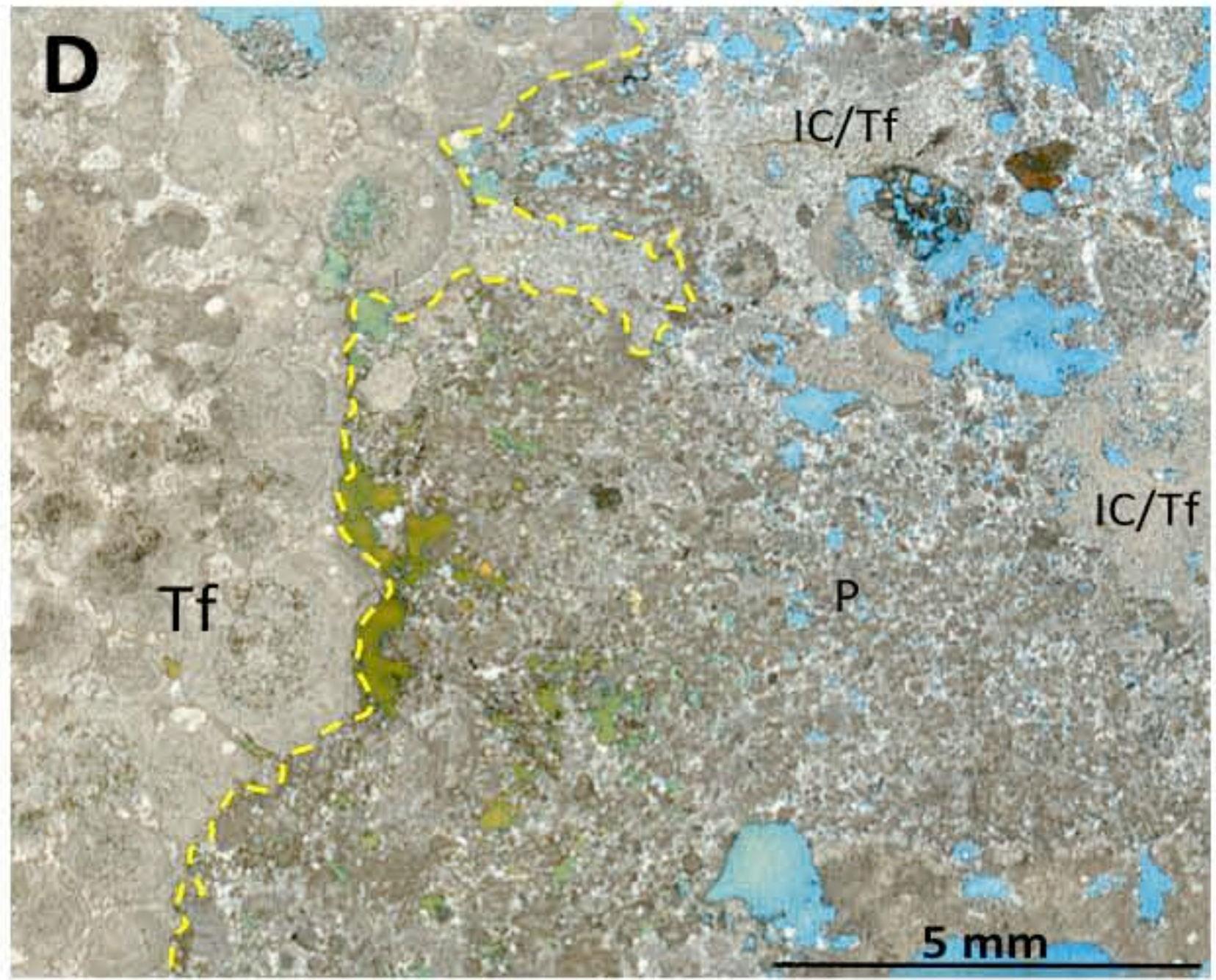
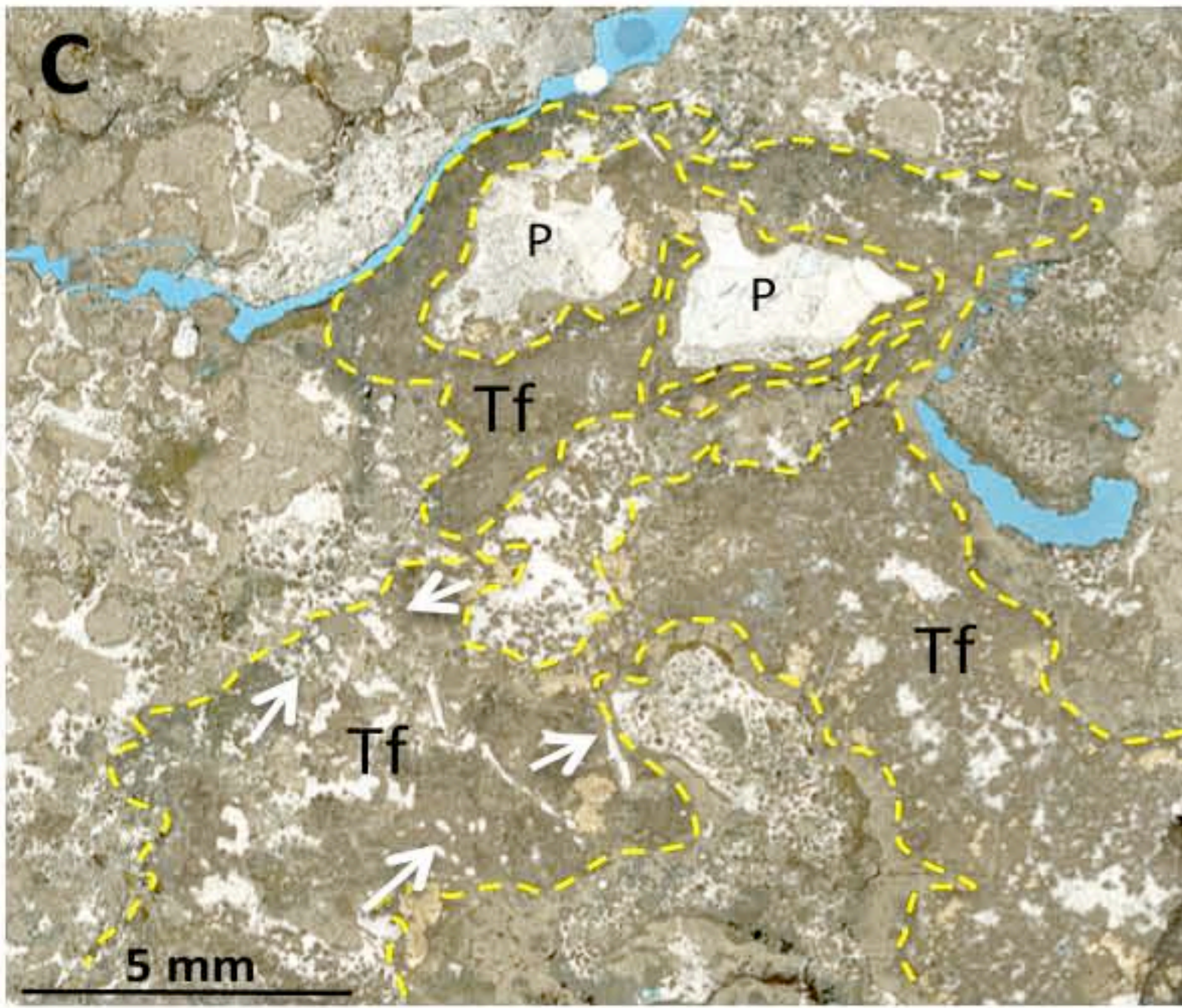
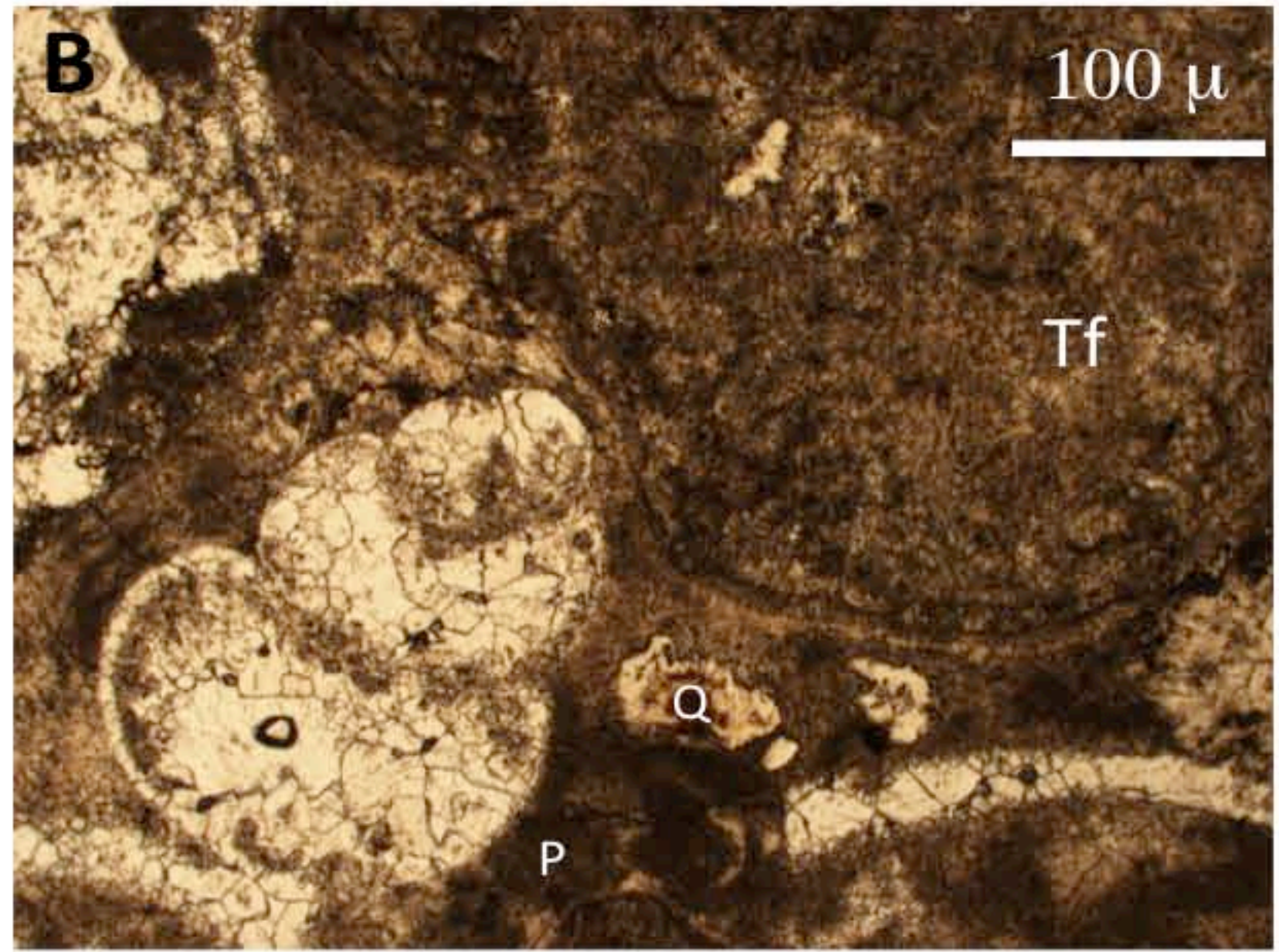
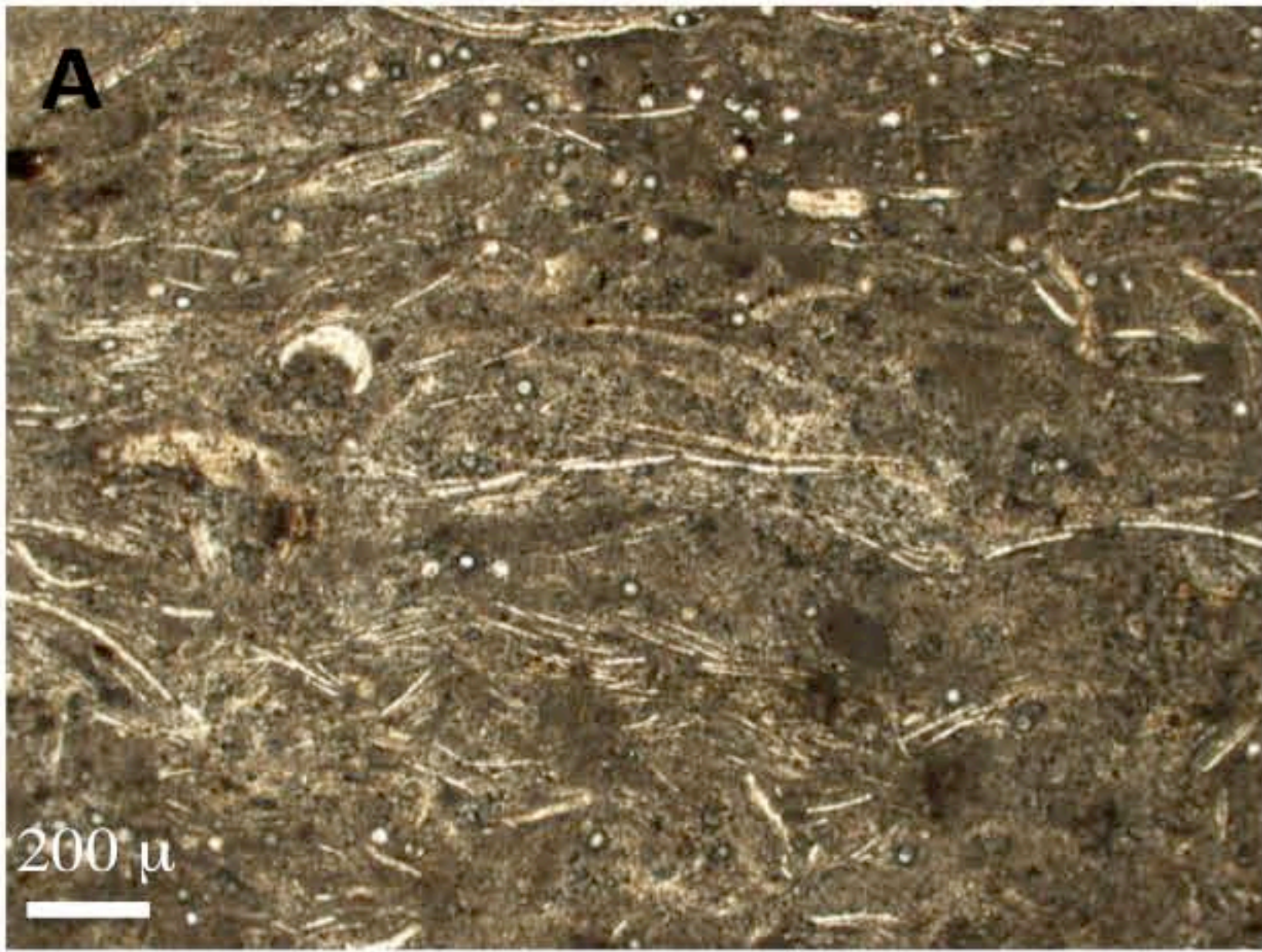
E

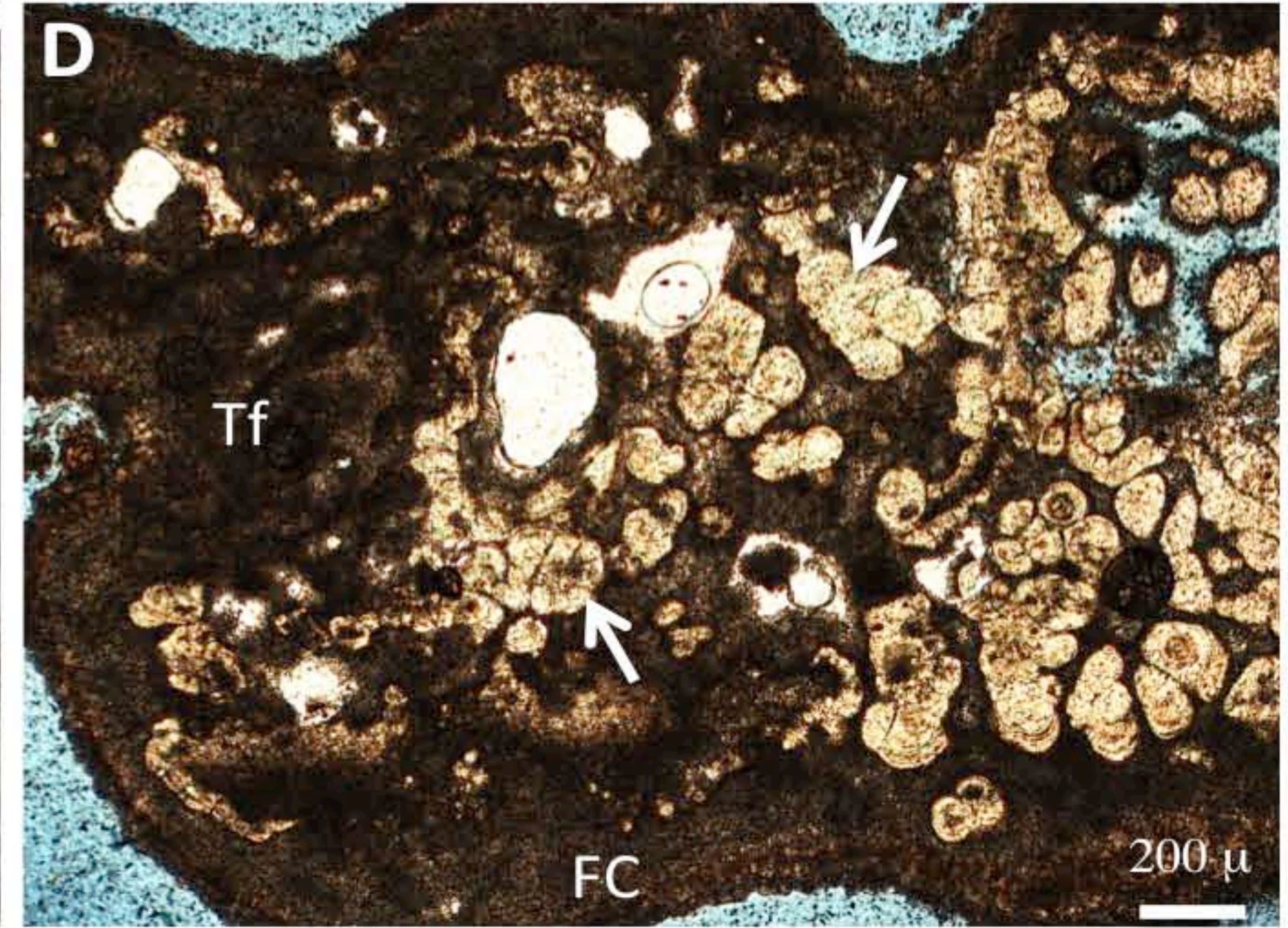
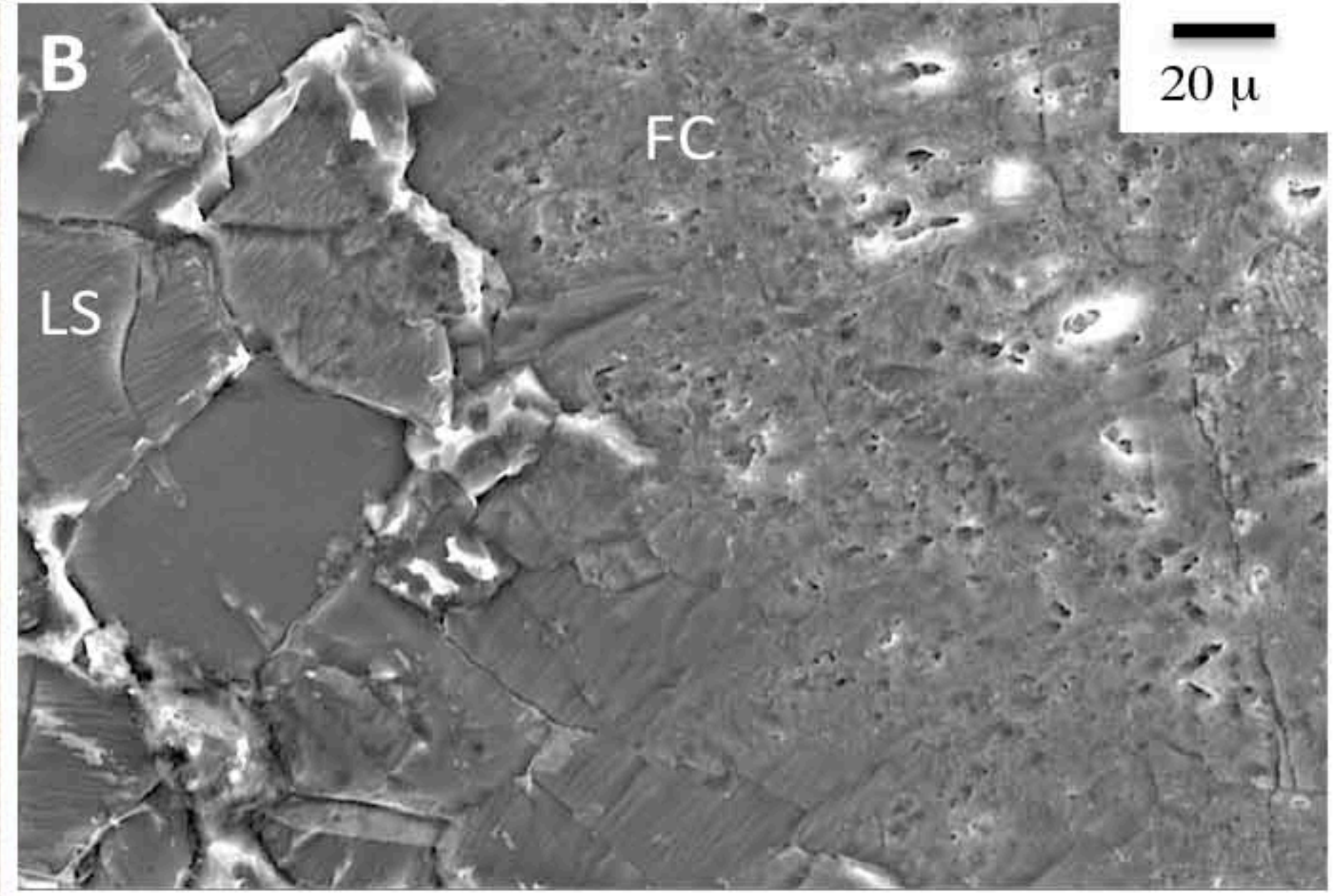
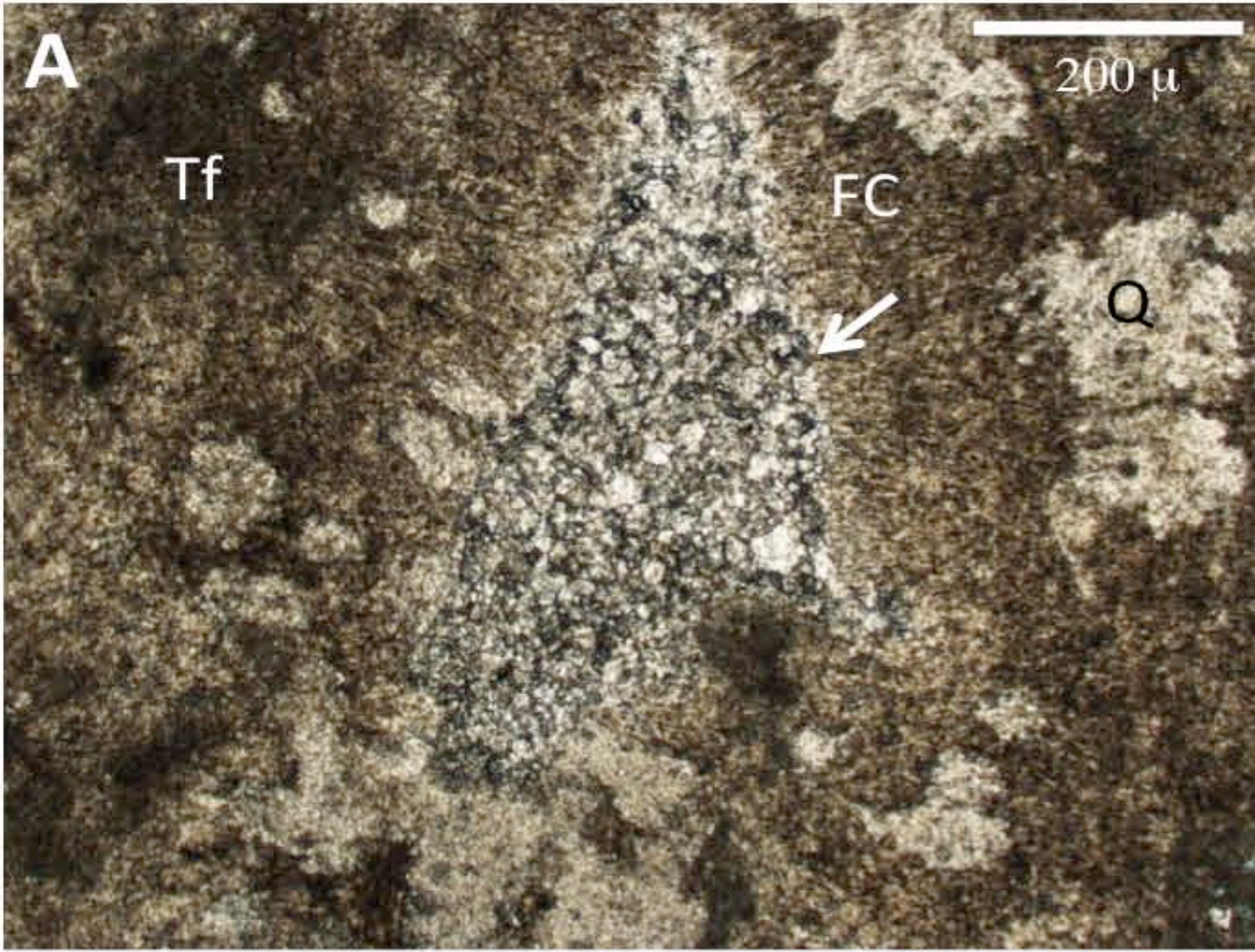
| Groups | Formations | Bed Names |
|---|--|------------------------|
| Purbeck Limestone Group (<i>lower part</i>) | Lulworth Formation (<i>lower part</i>) | Cypris Freestones |
| | | Soft Cap (0-2.8m) |
| | | Great Dirt Bed (<0.6m) |
| | | Hard Cap (0.4-5.3m) |
| | | Lower Dirt Bed (<0.3m) |
| | | Skull Cap (<1.3m) |
| Portland Group | Portland Stone Formation | Basal Dirt Bed (<0.1m) |
| | | Transition Bed (<0.7m) |

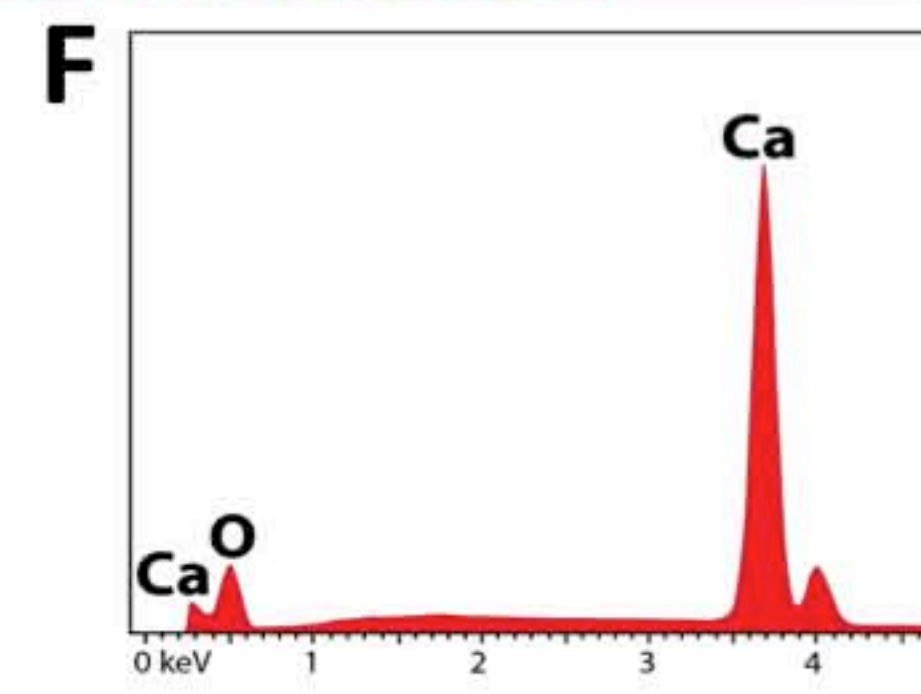
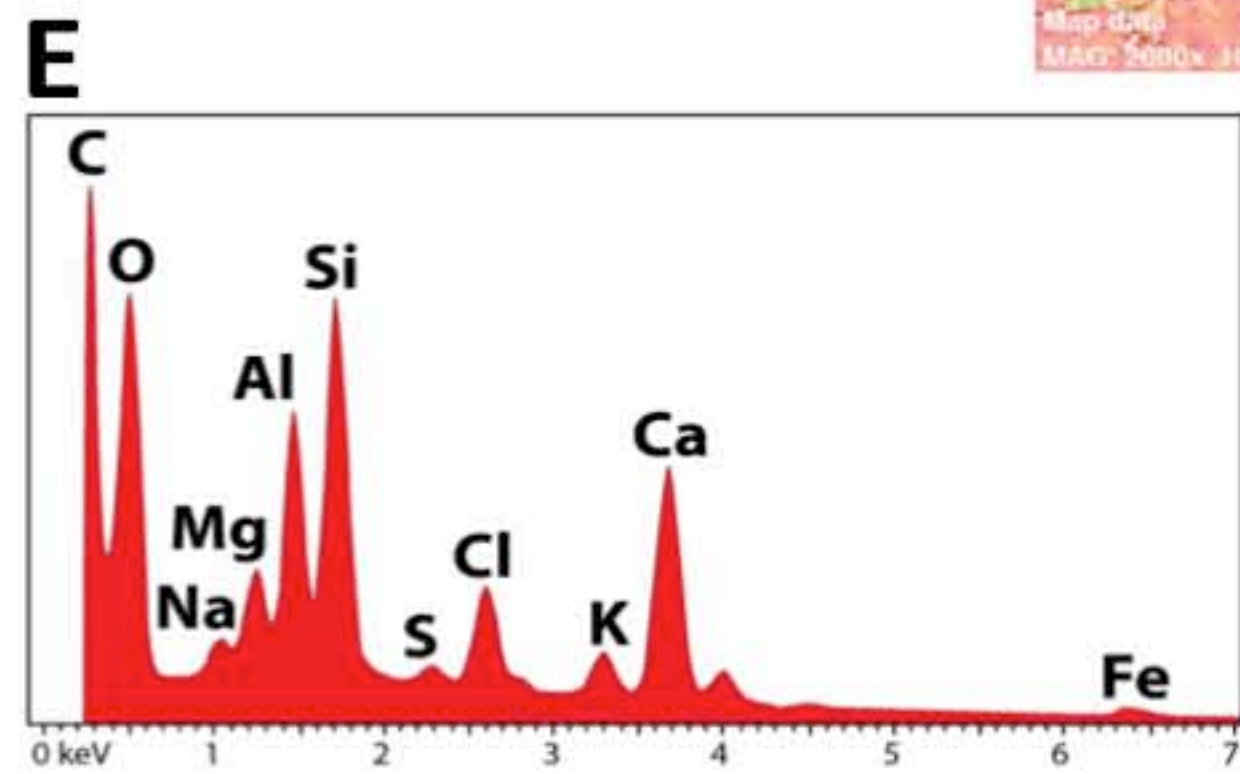
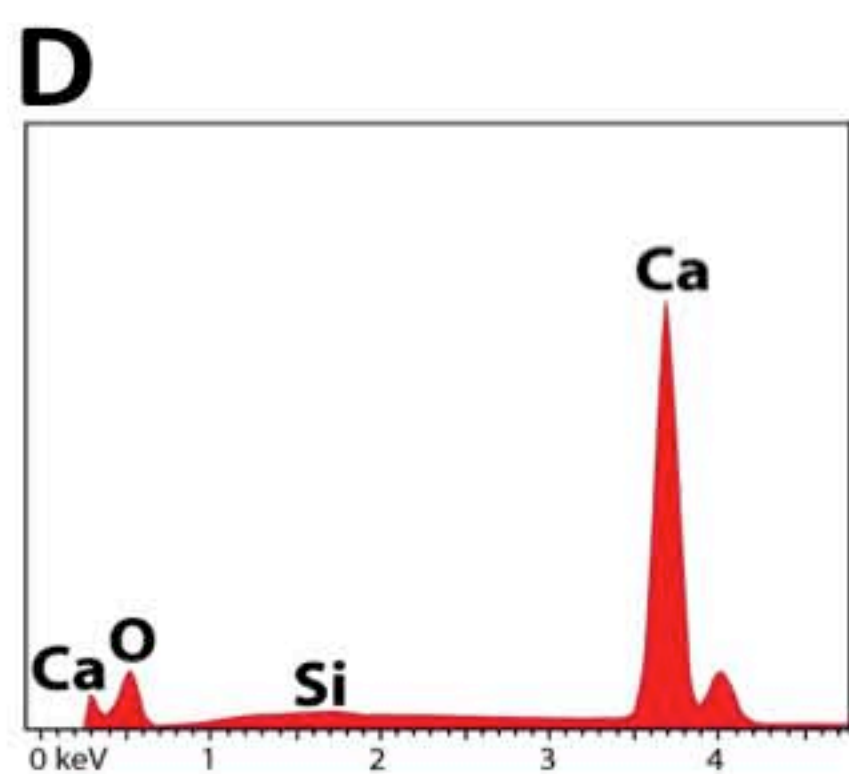
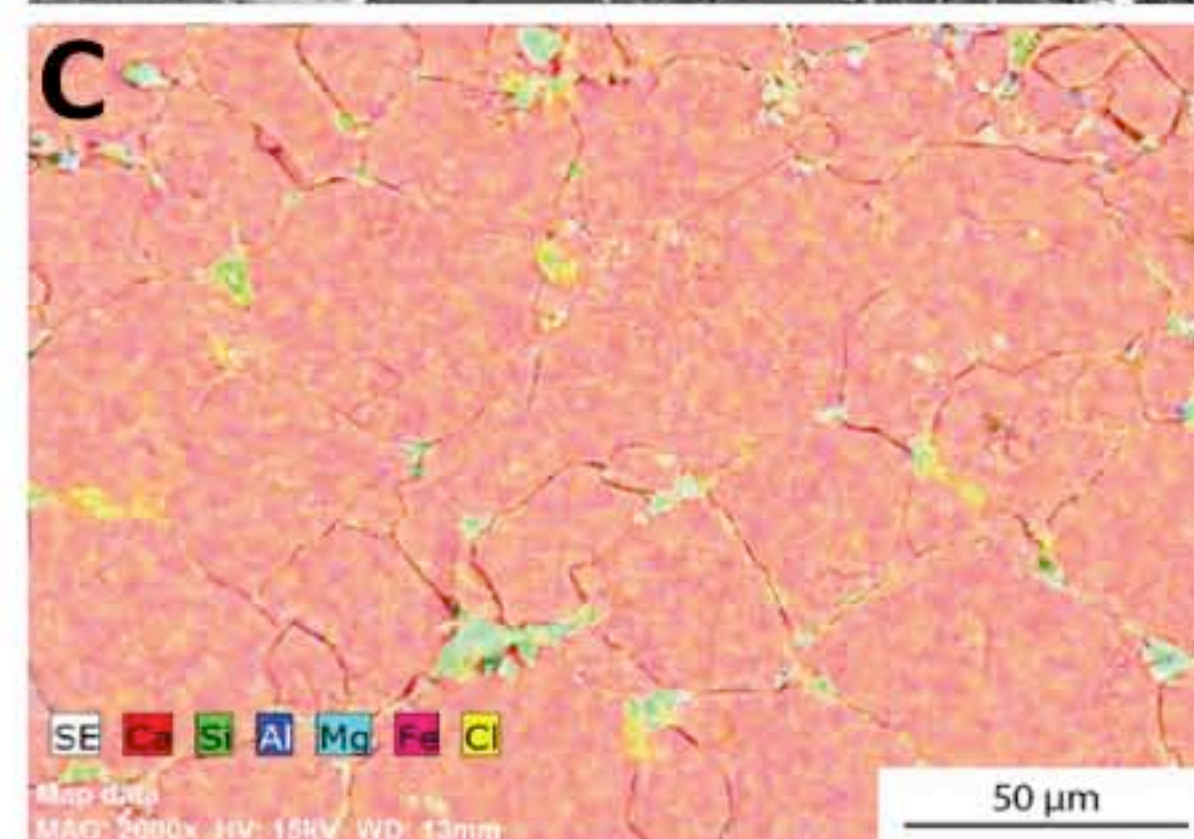
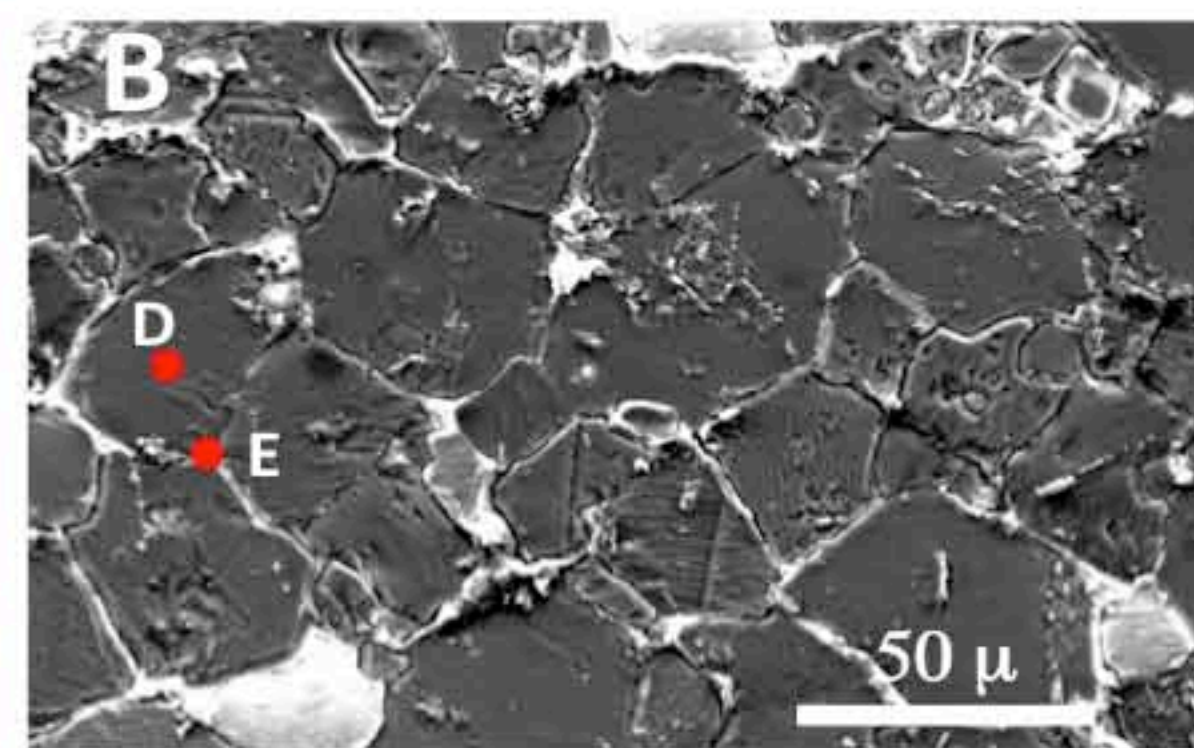
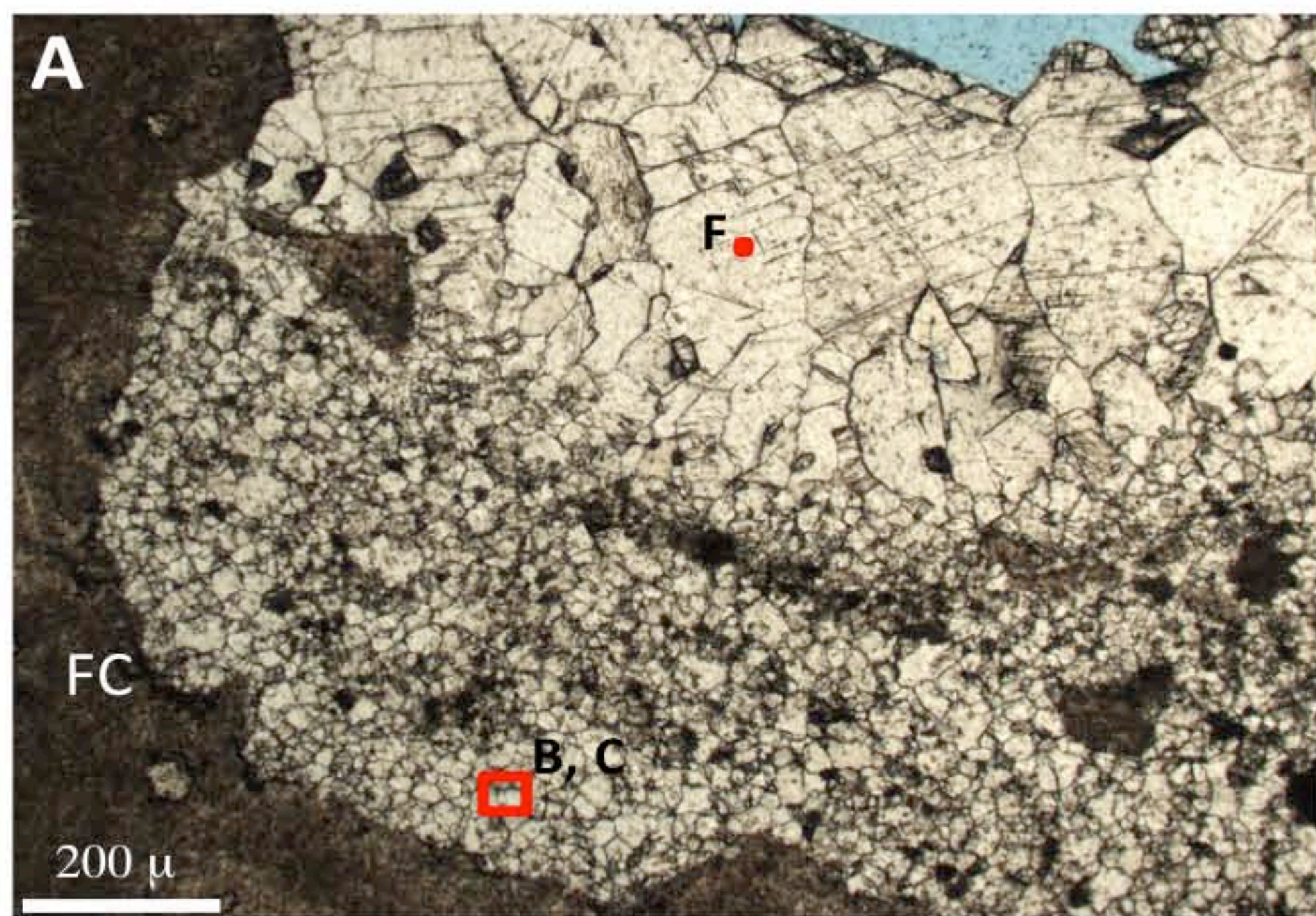


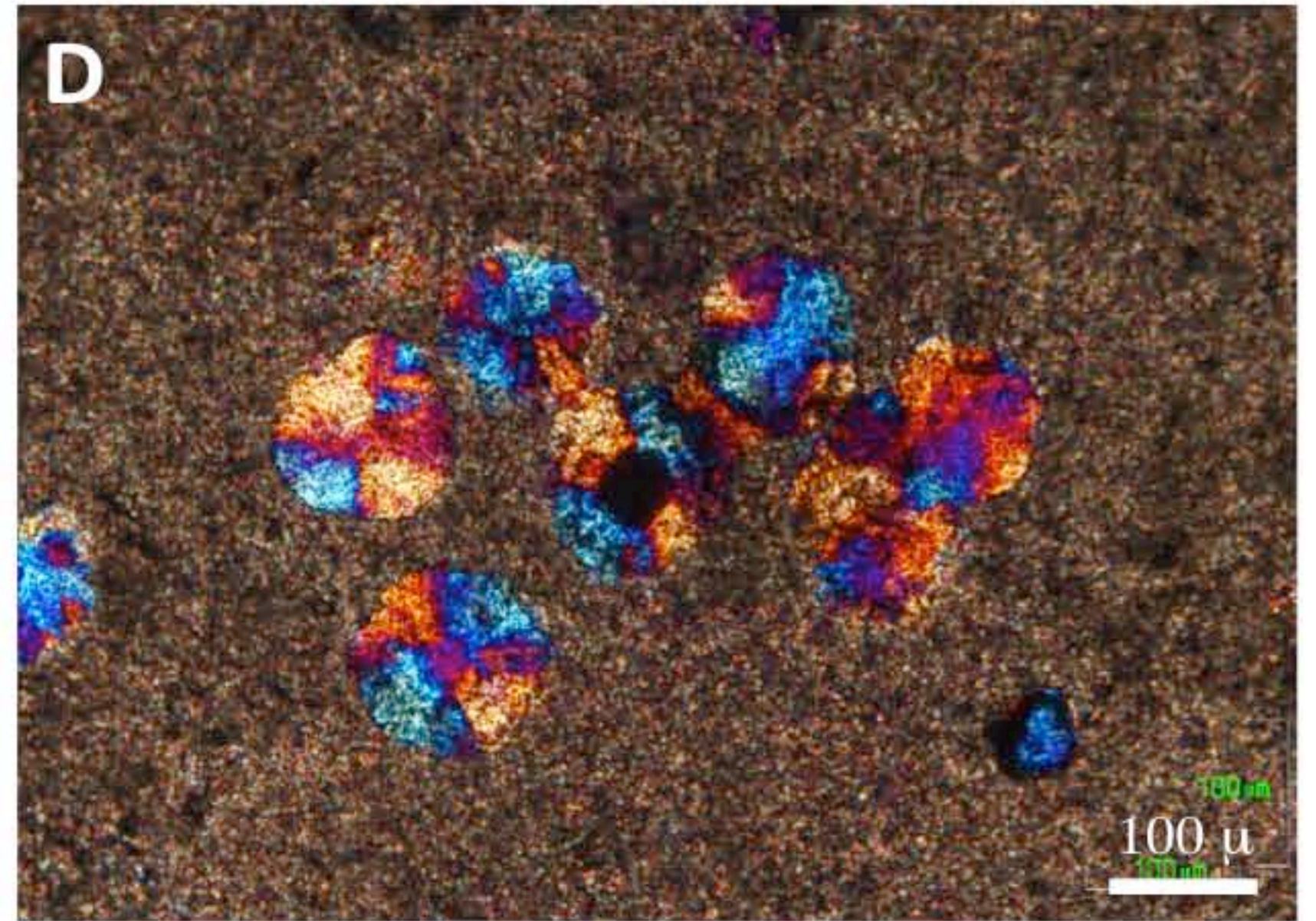
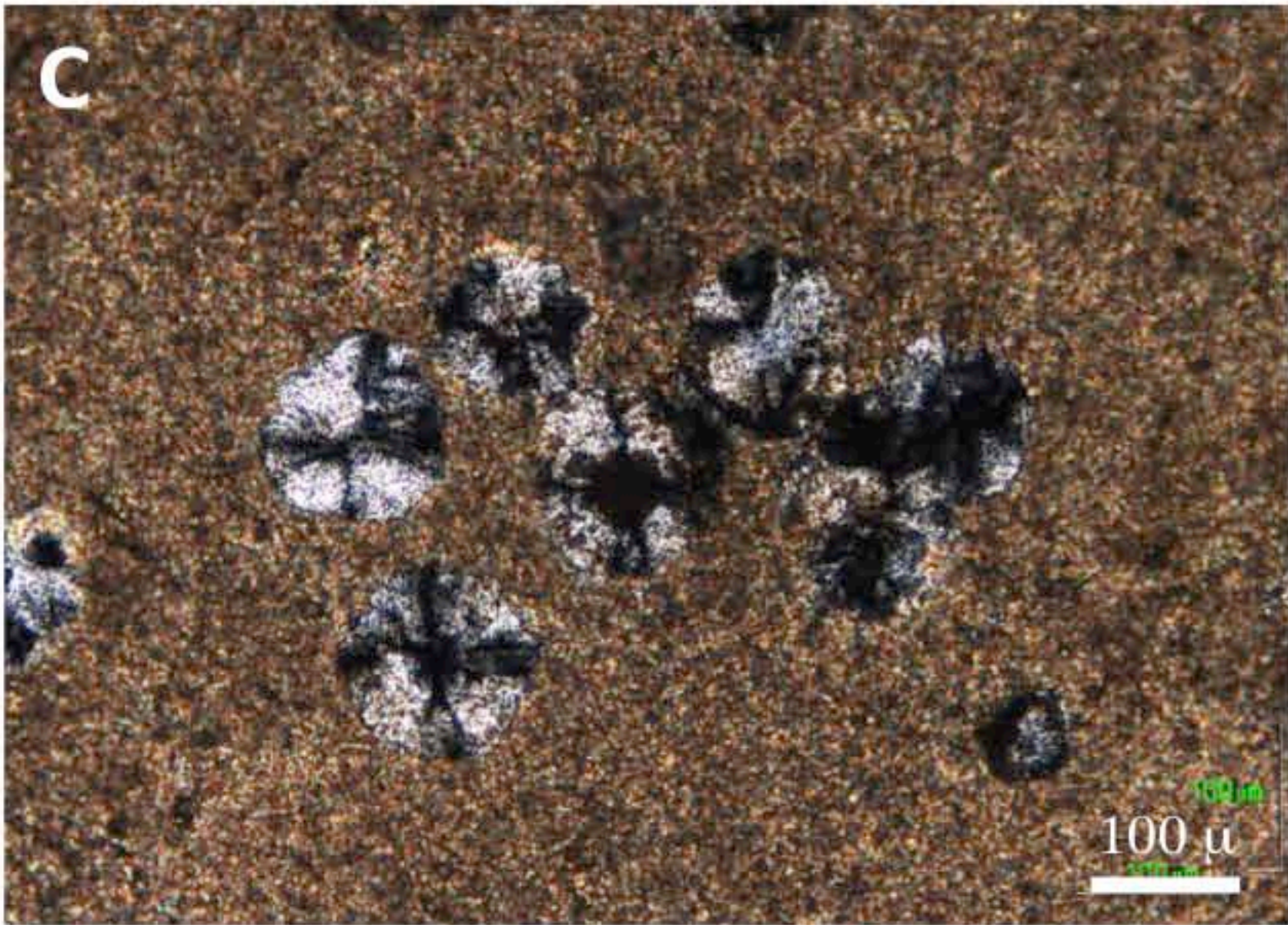
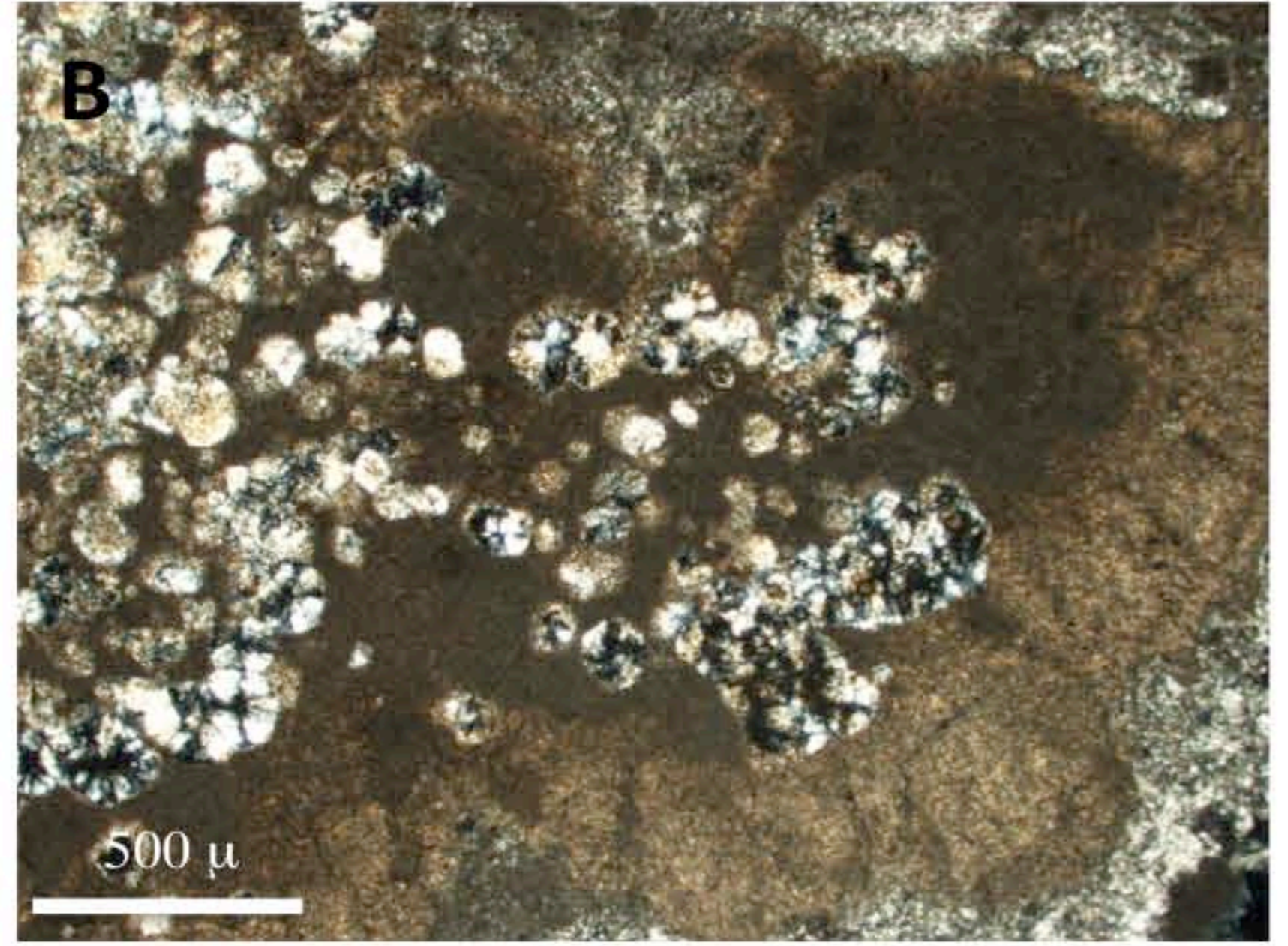
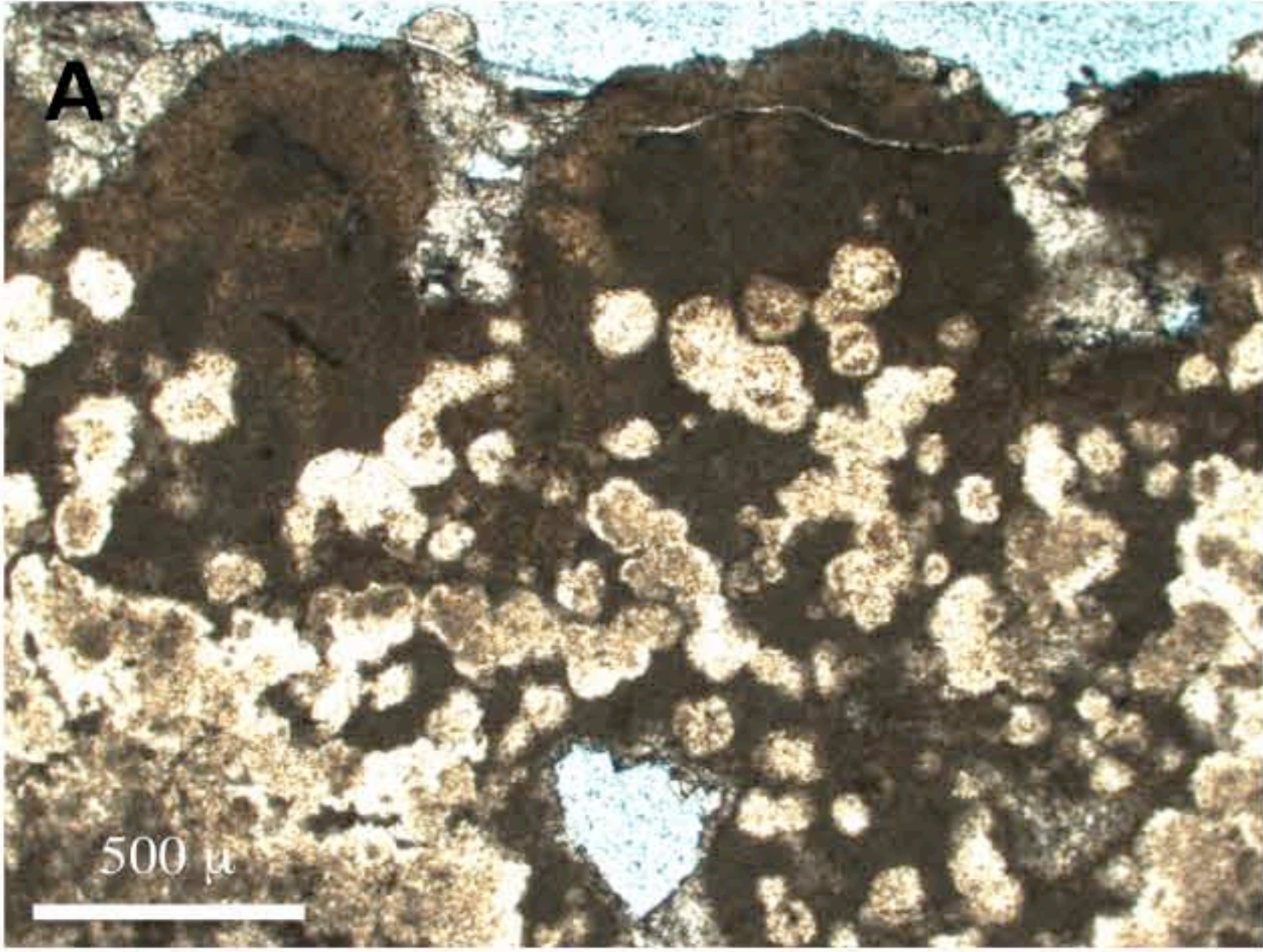


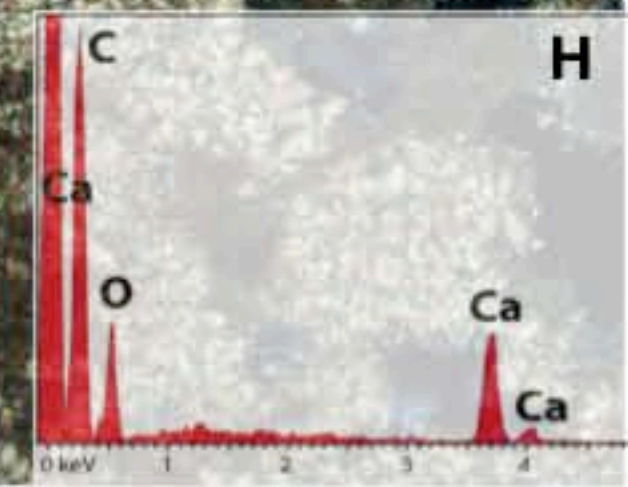
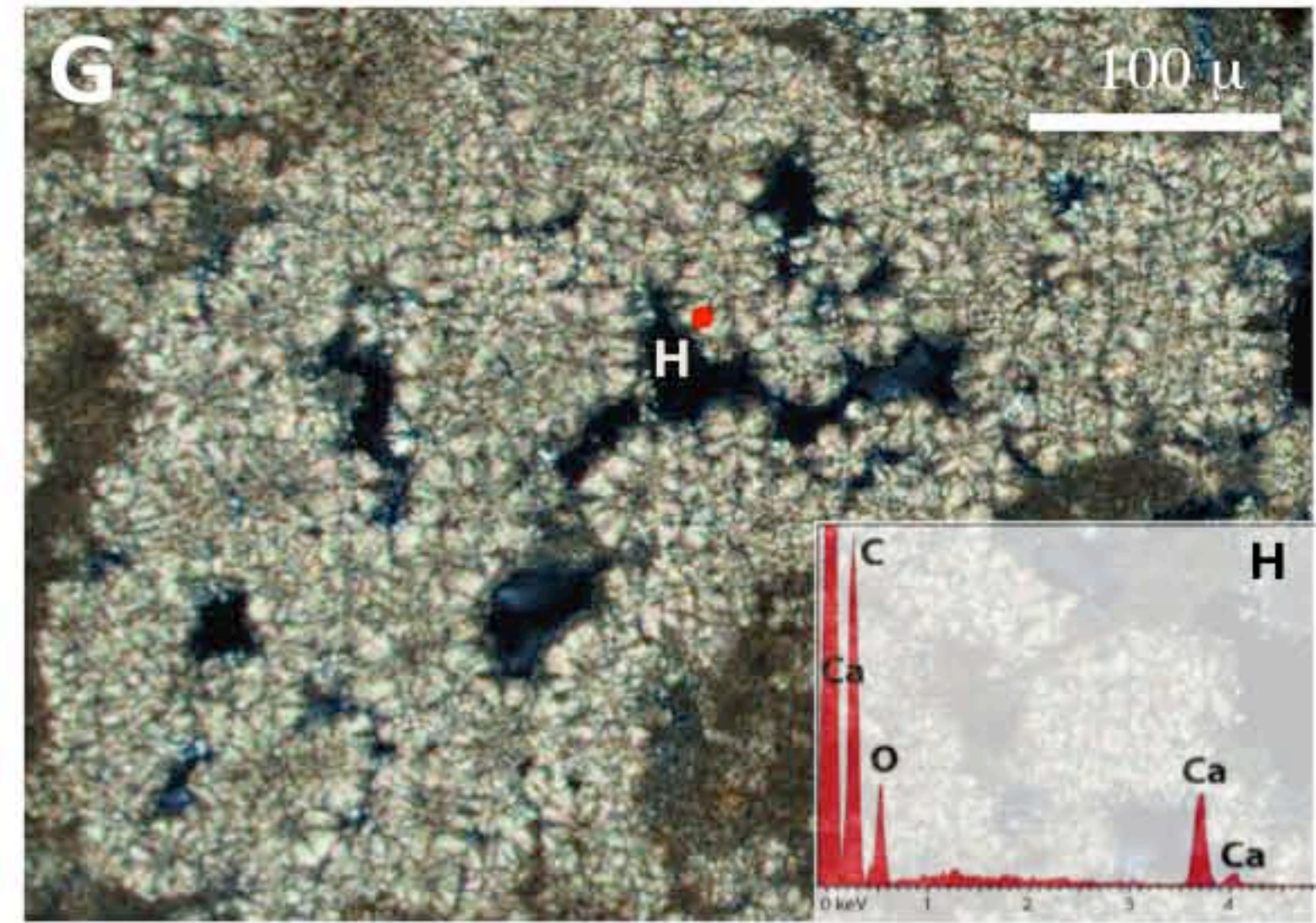
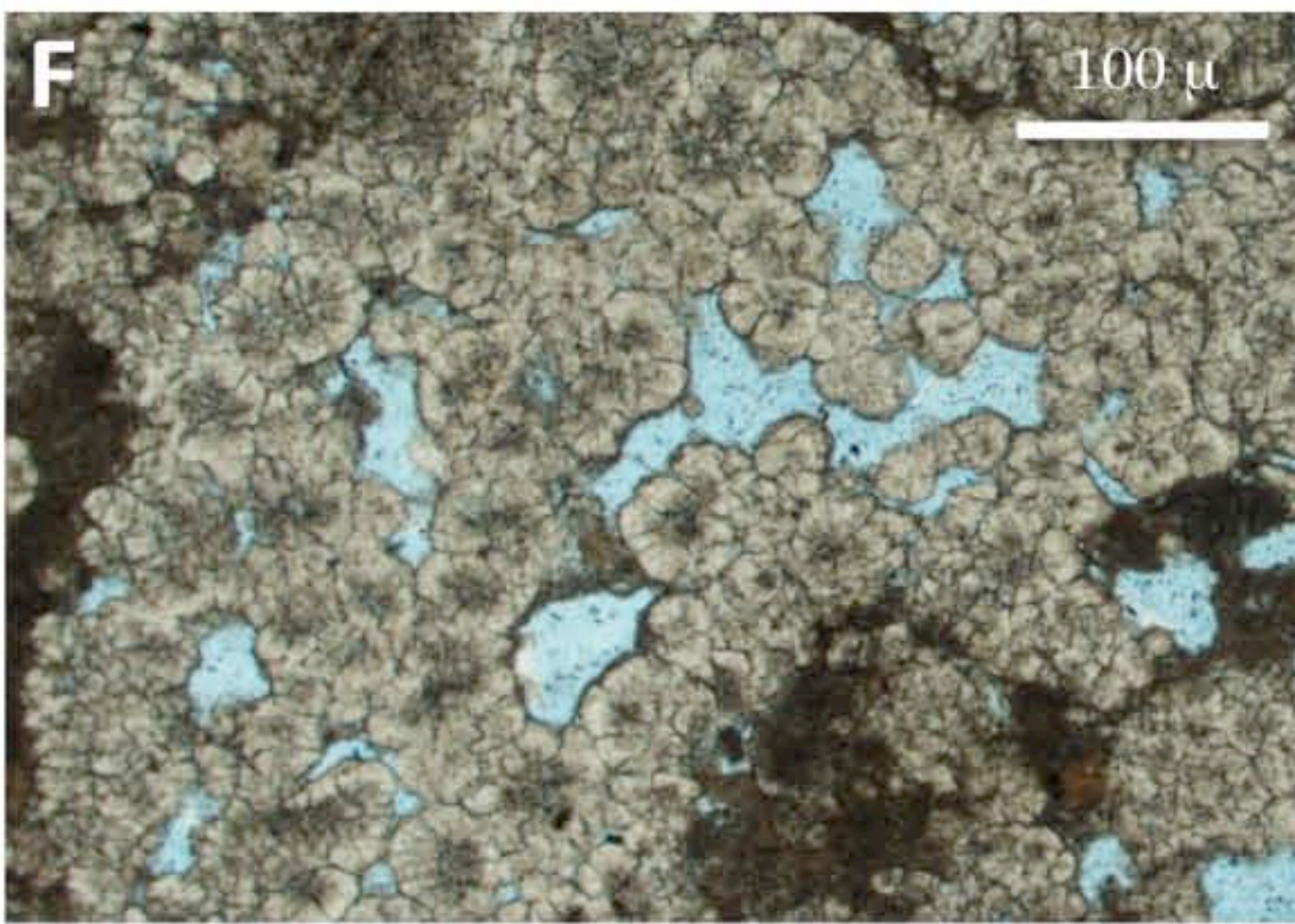
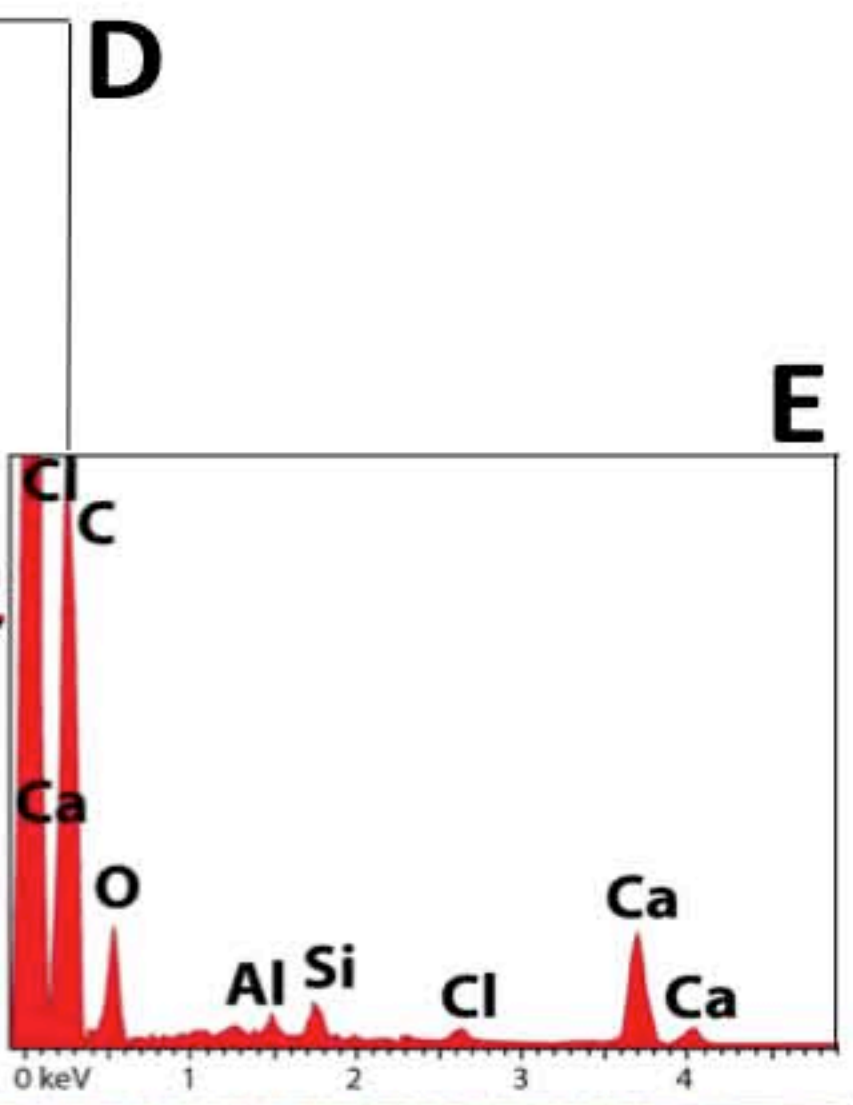
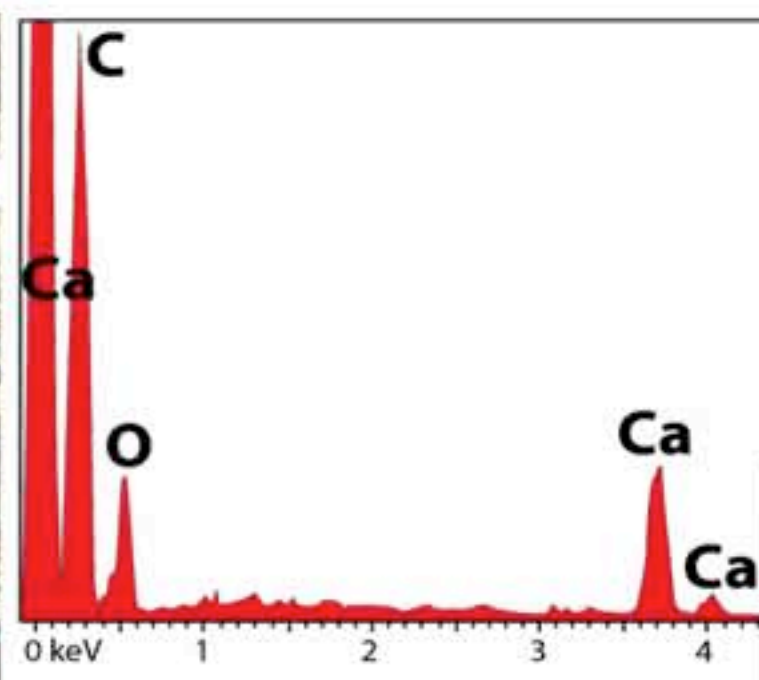
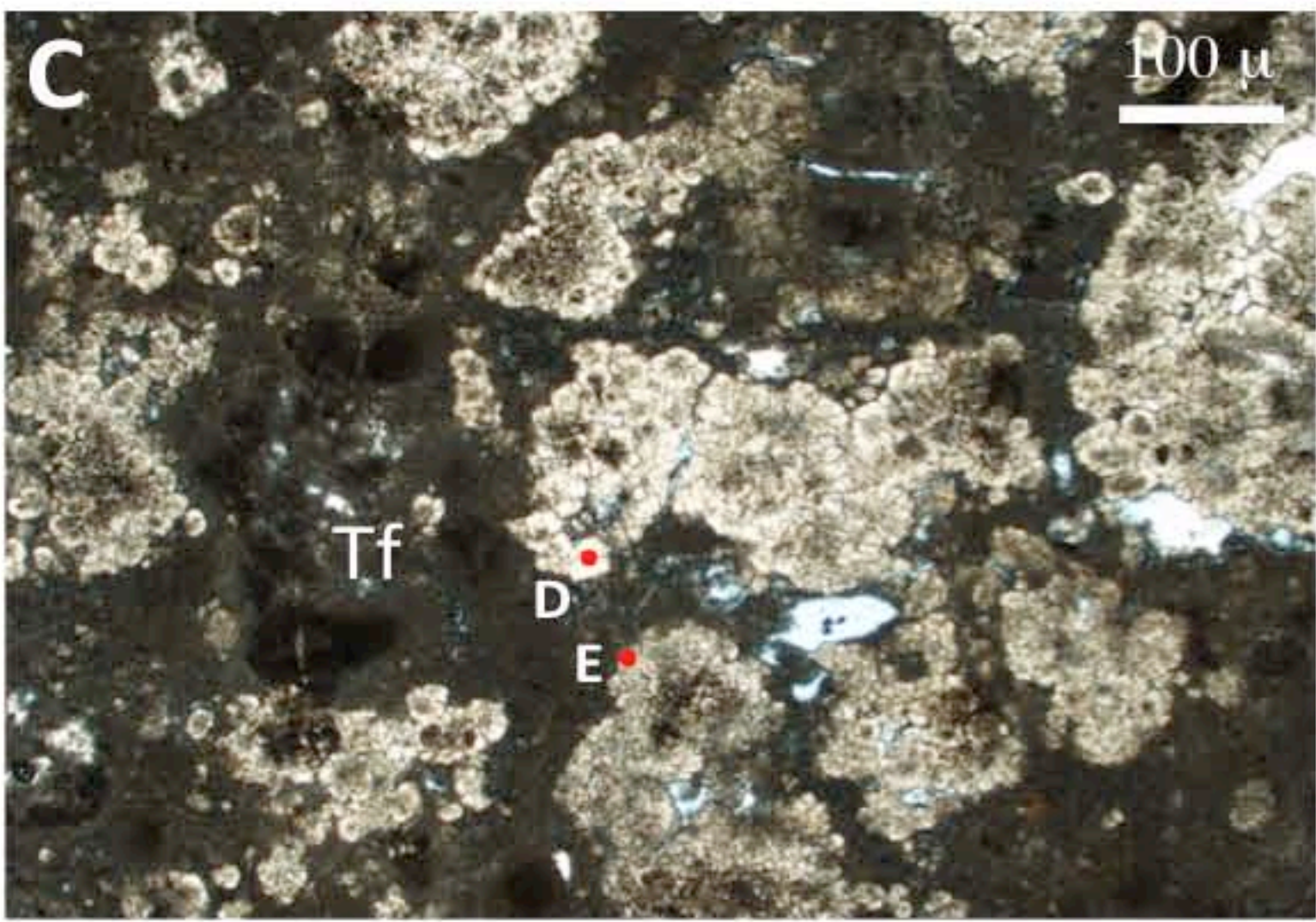
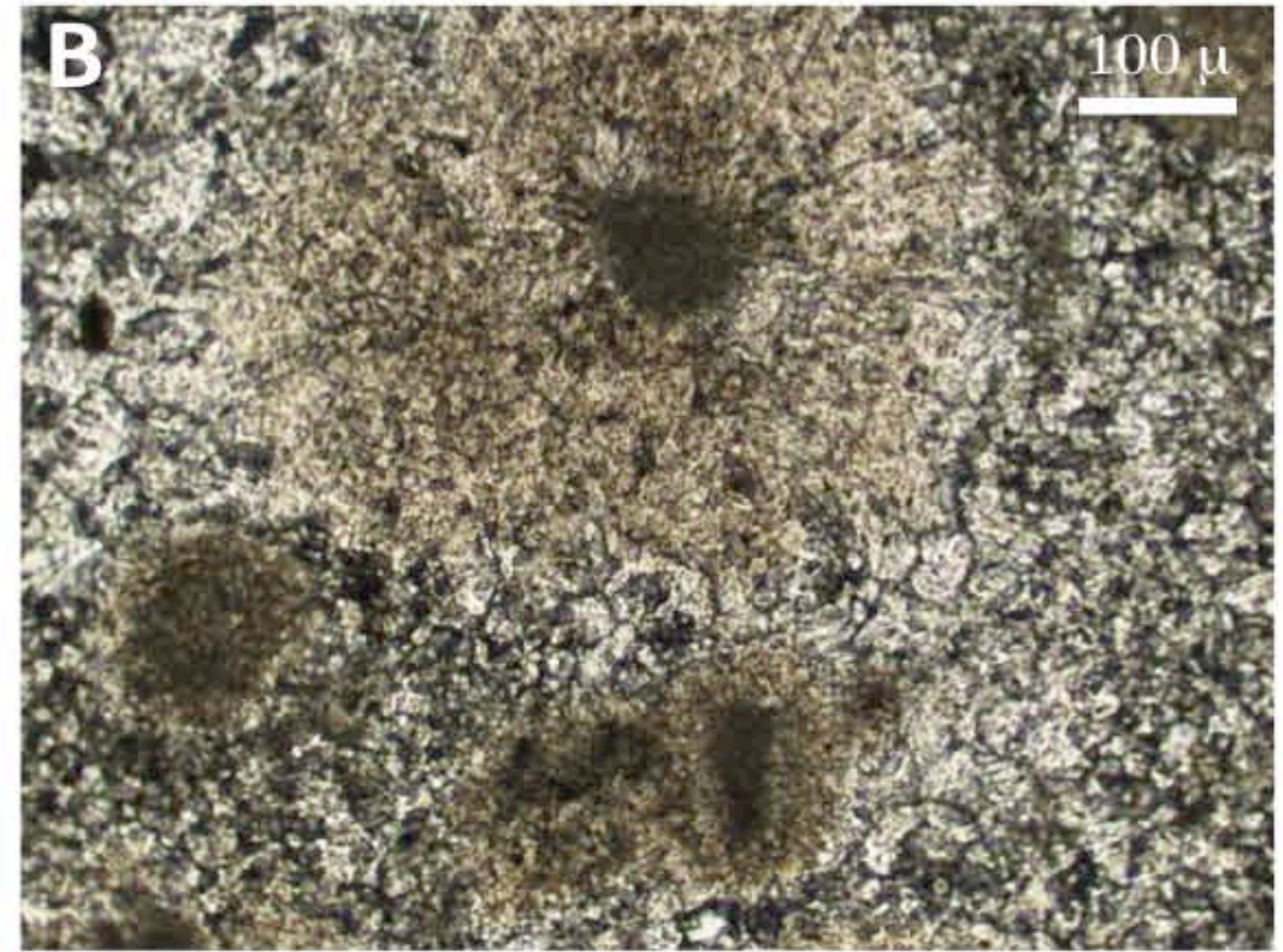
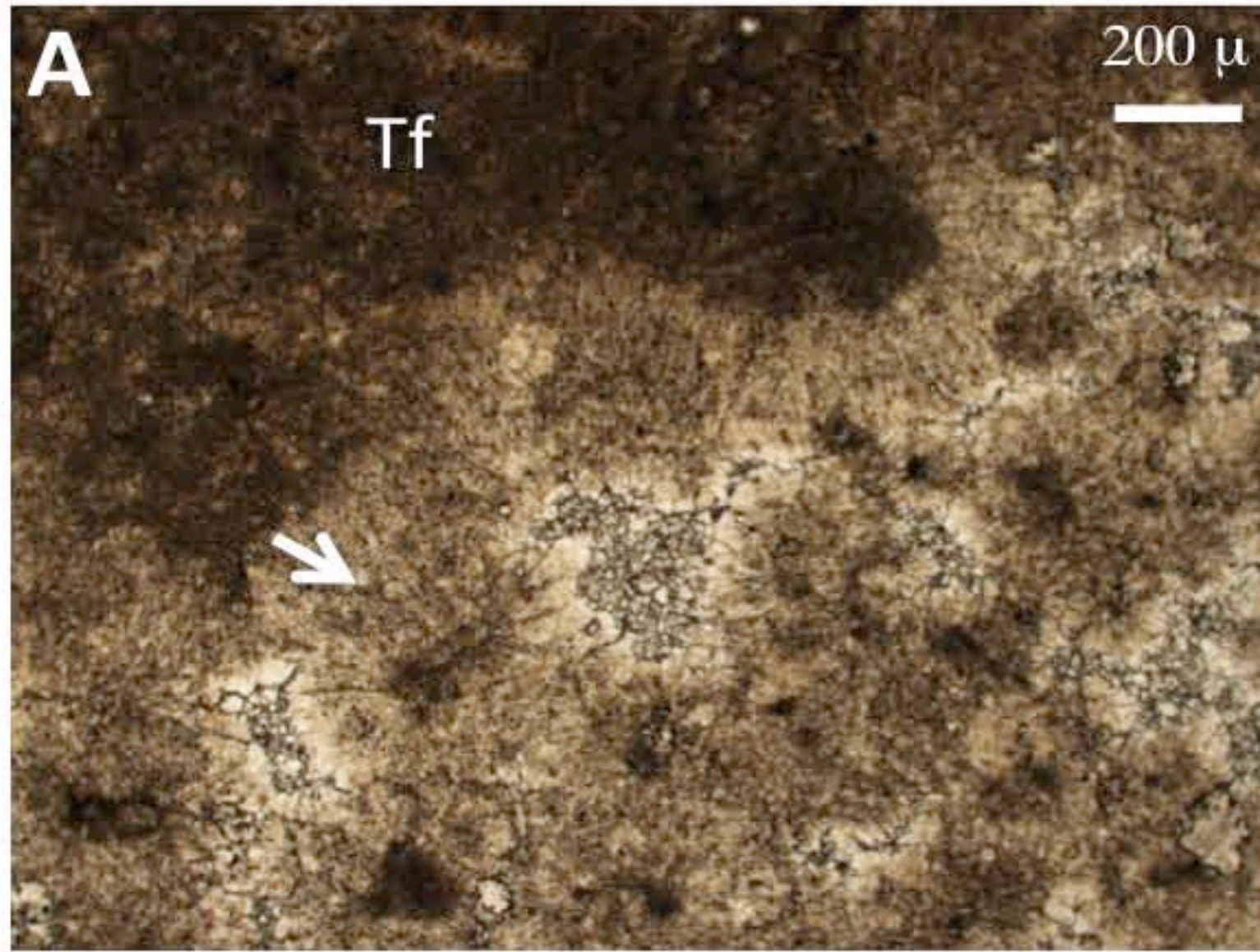


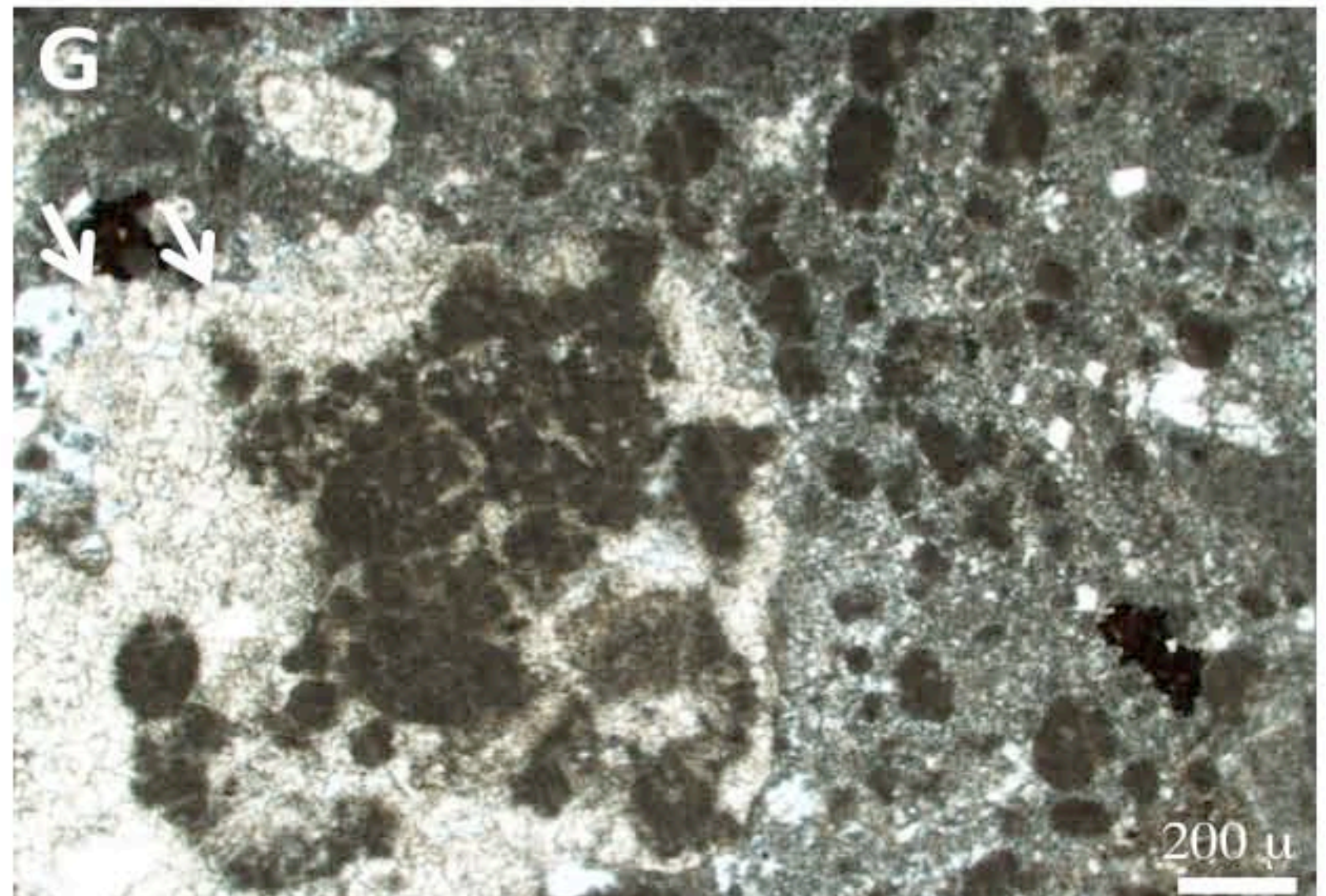
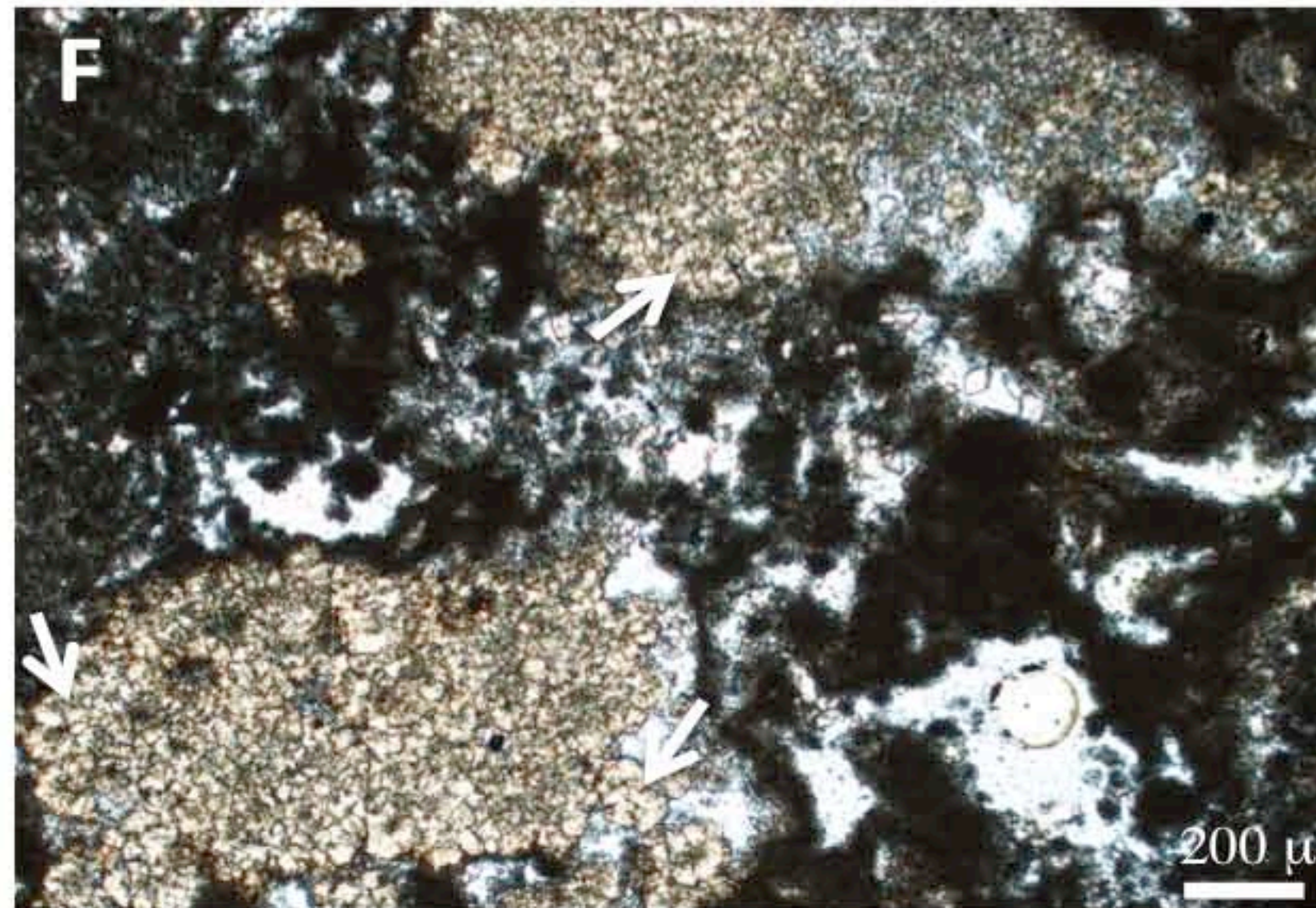
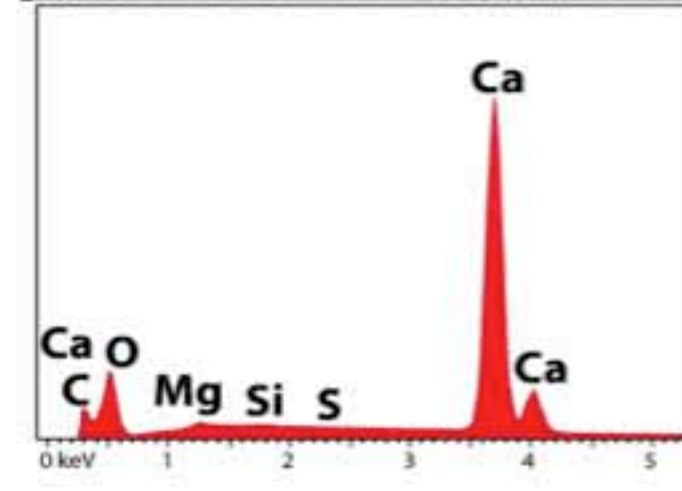
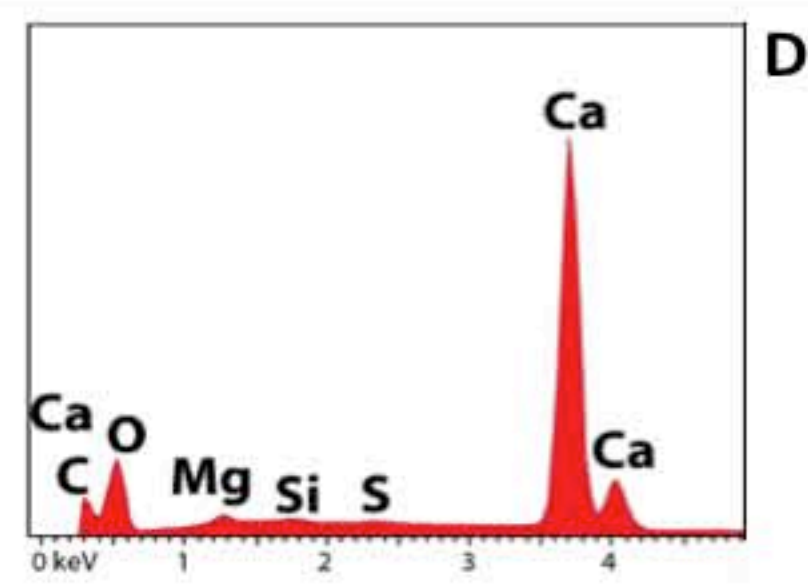
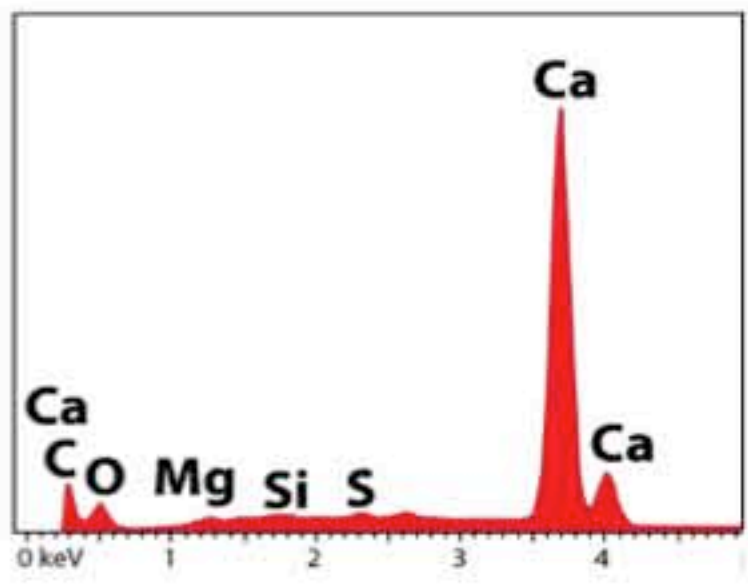
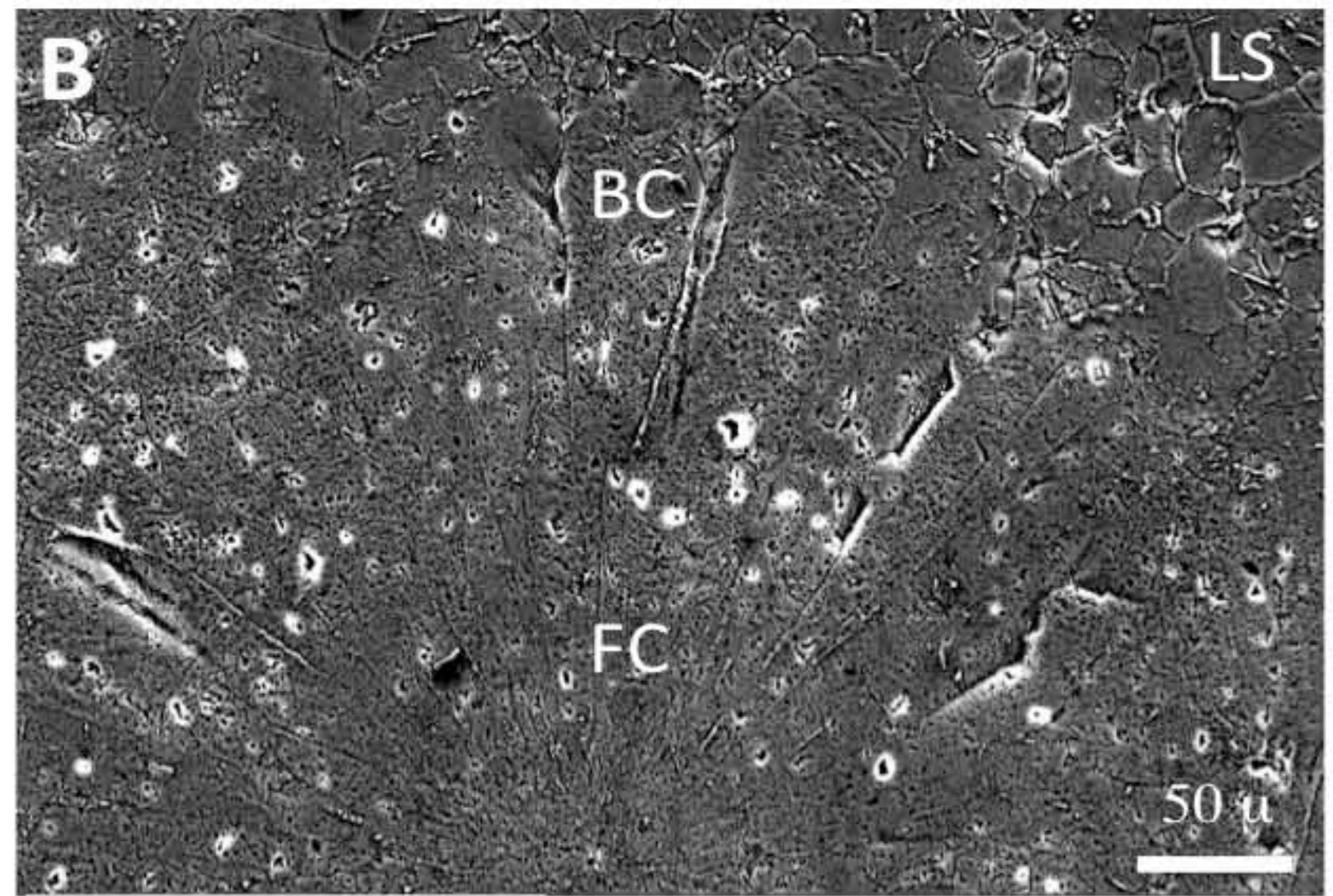
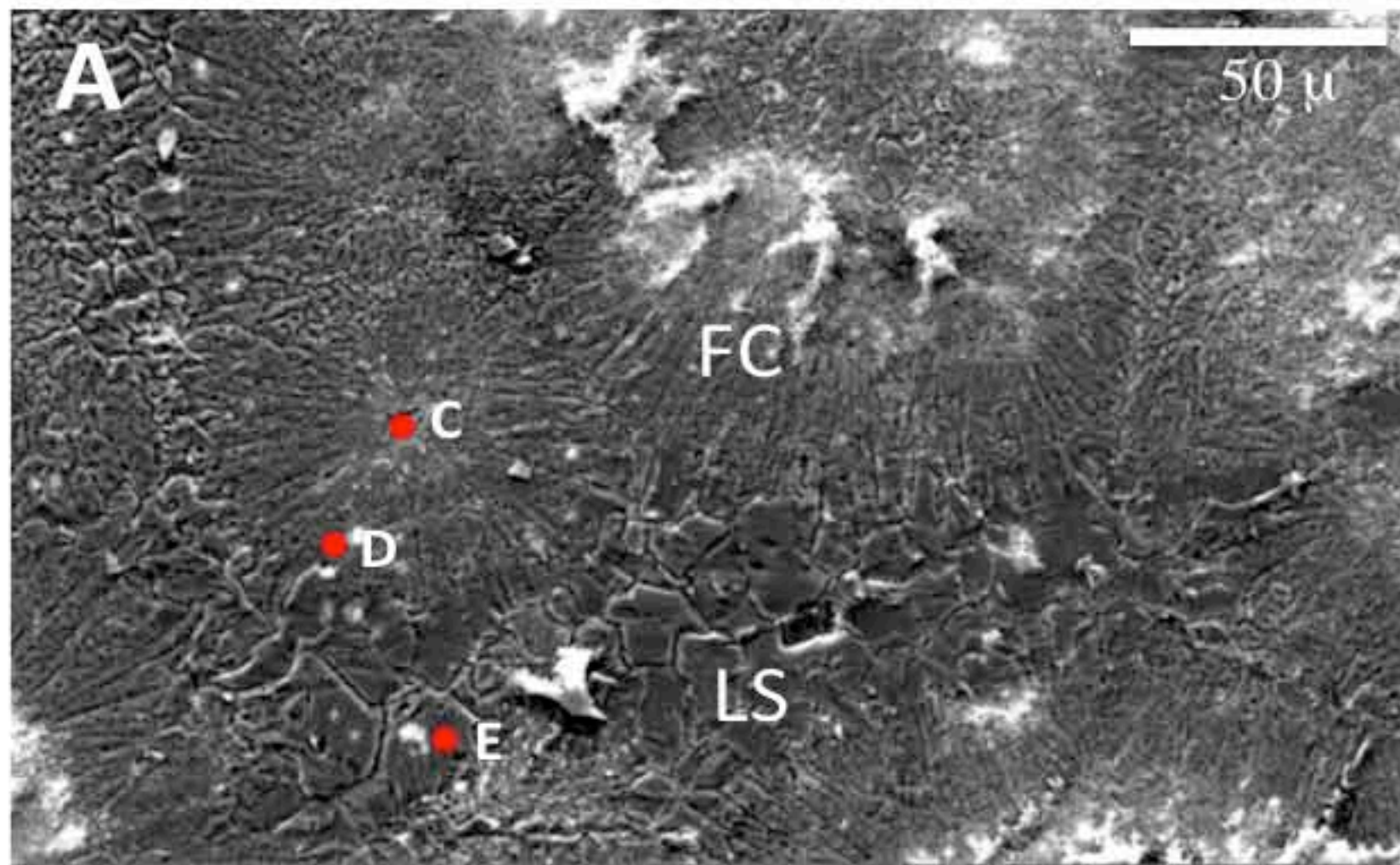


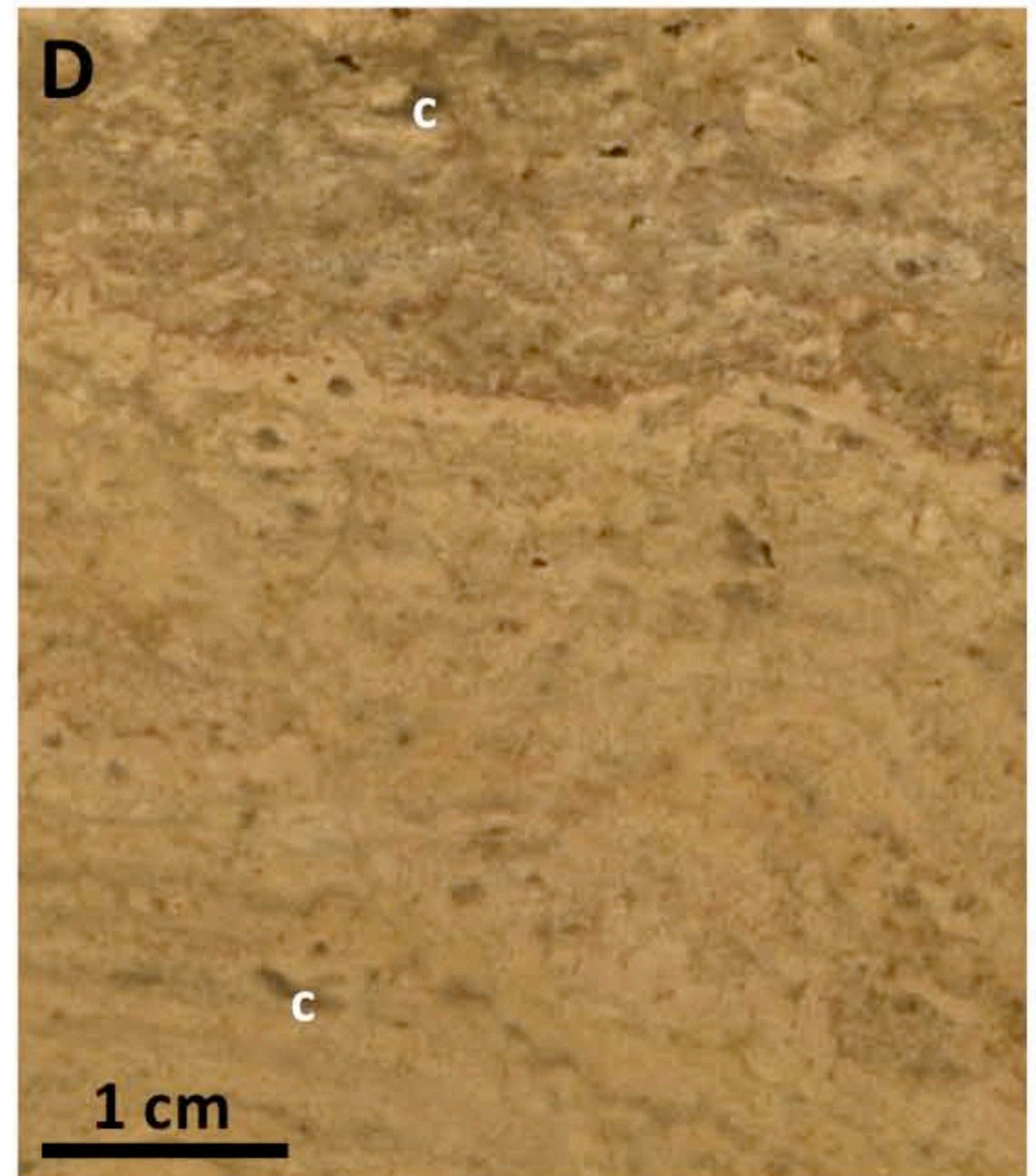
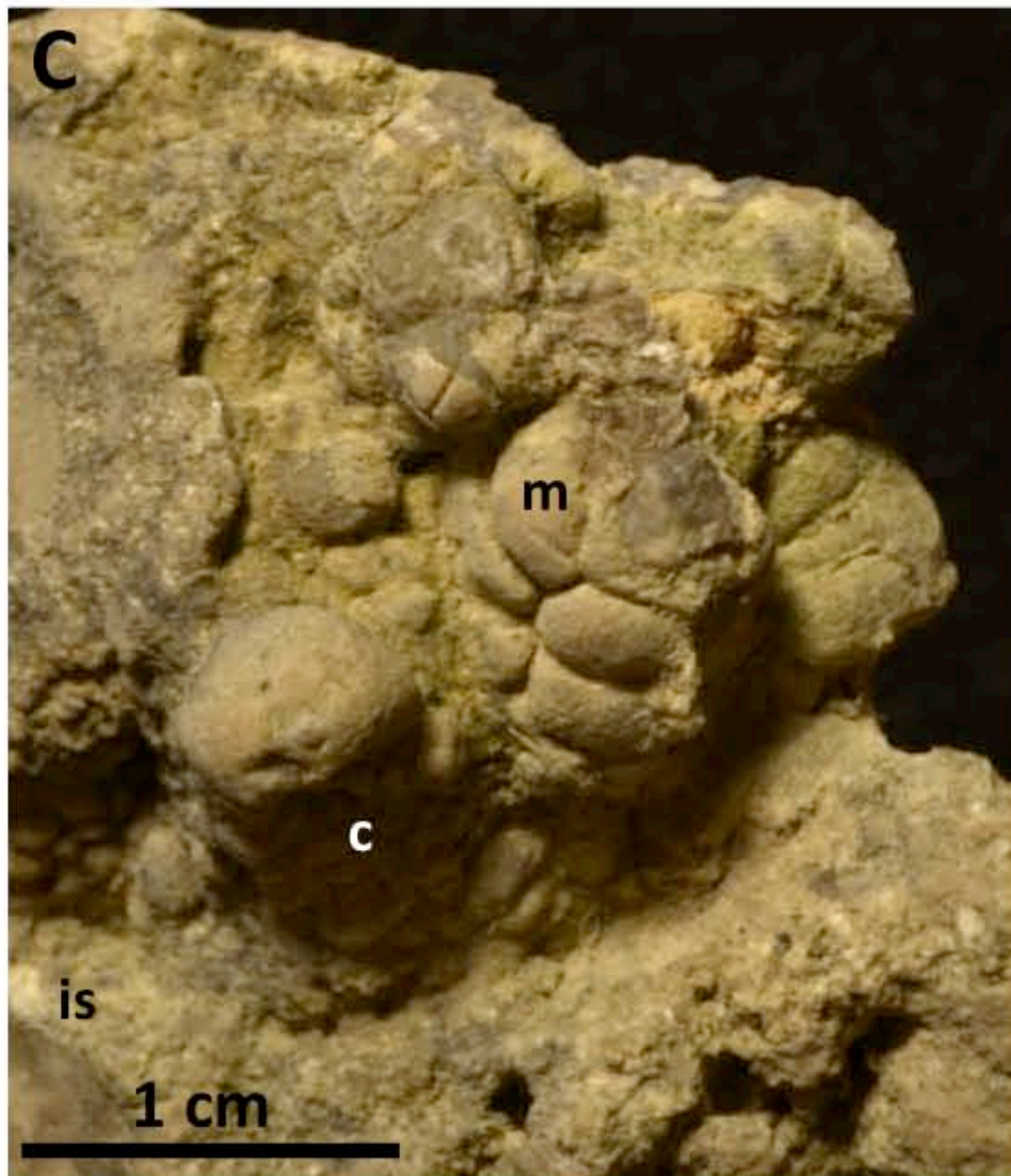
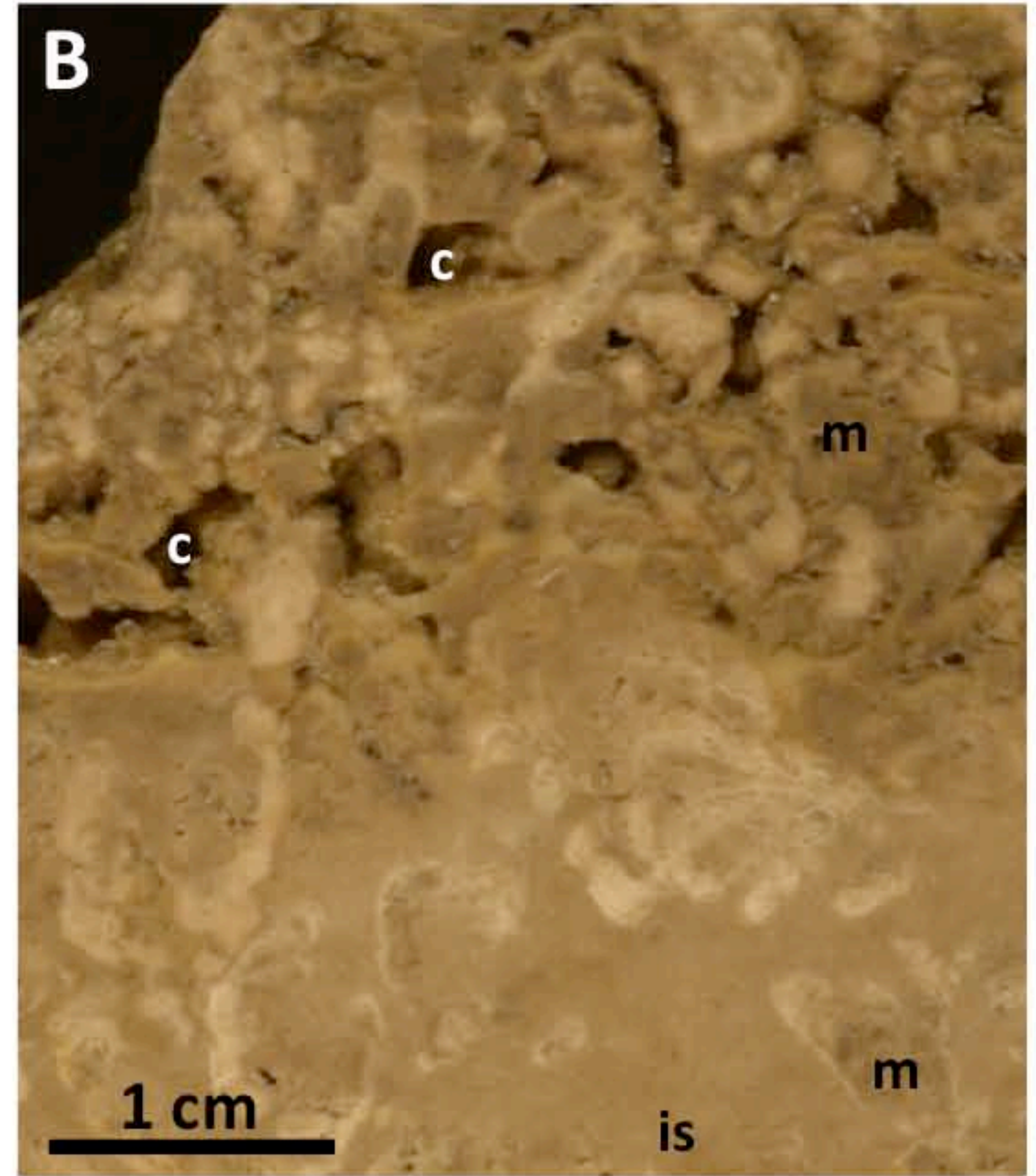
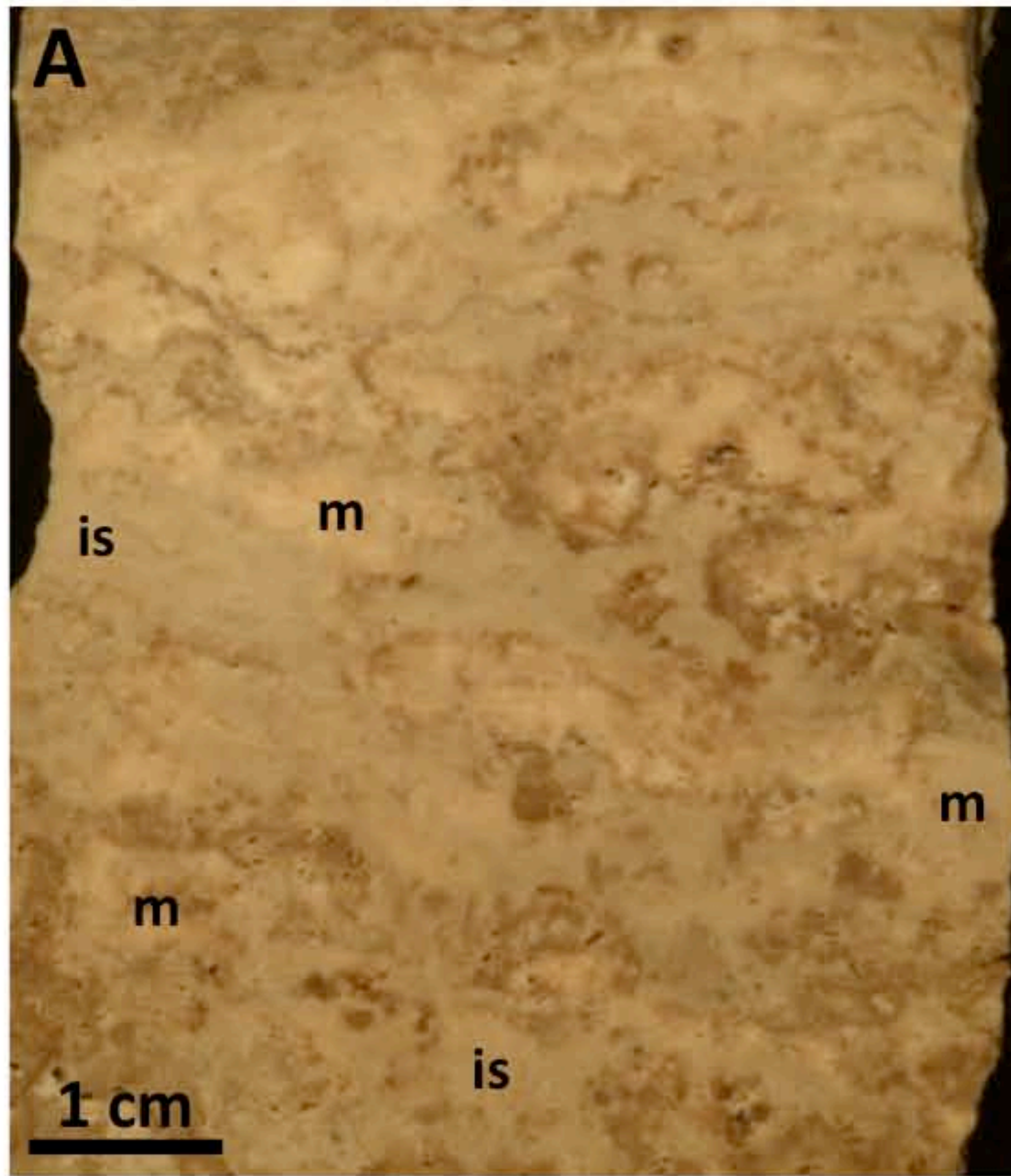


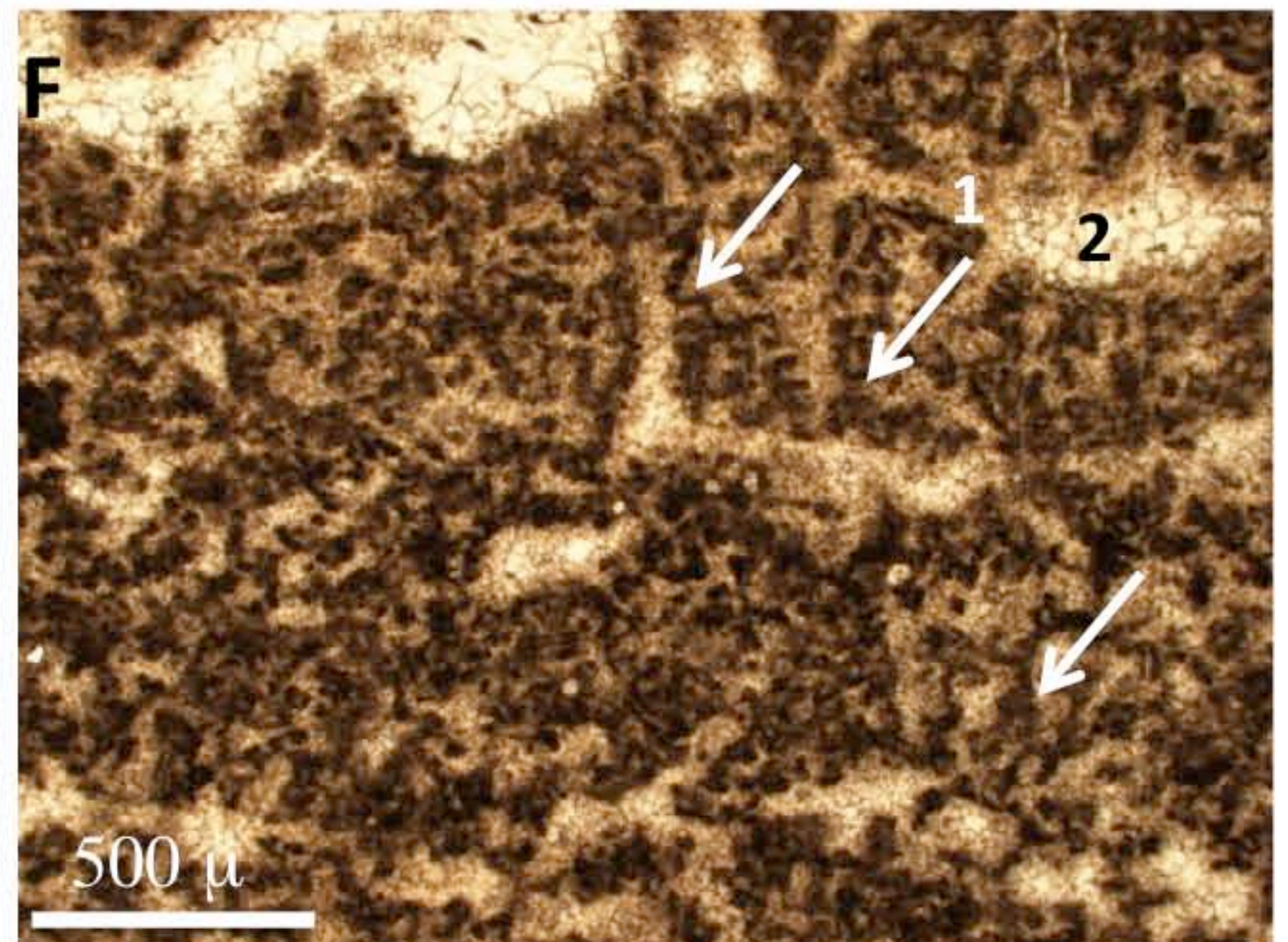
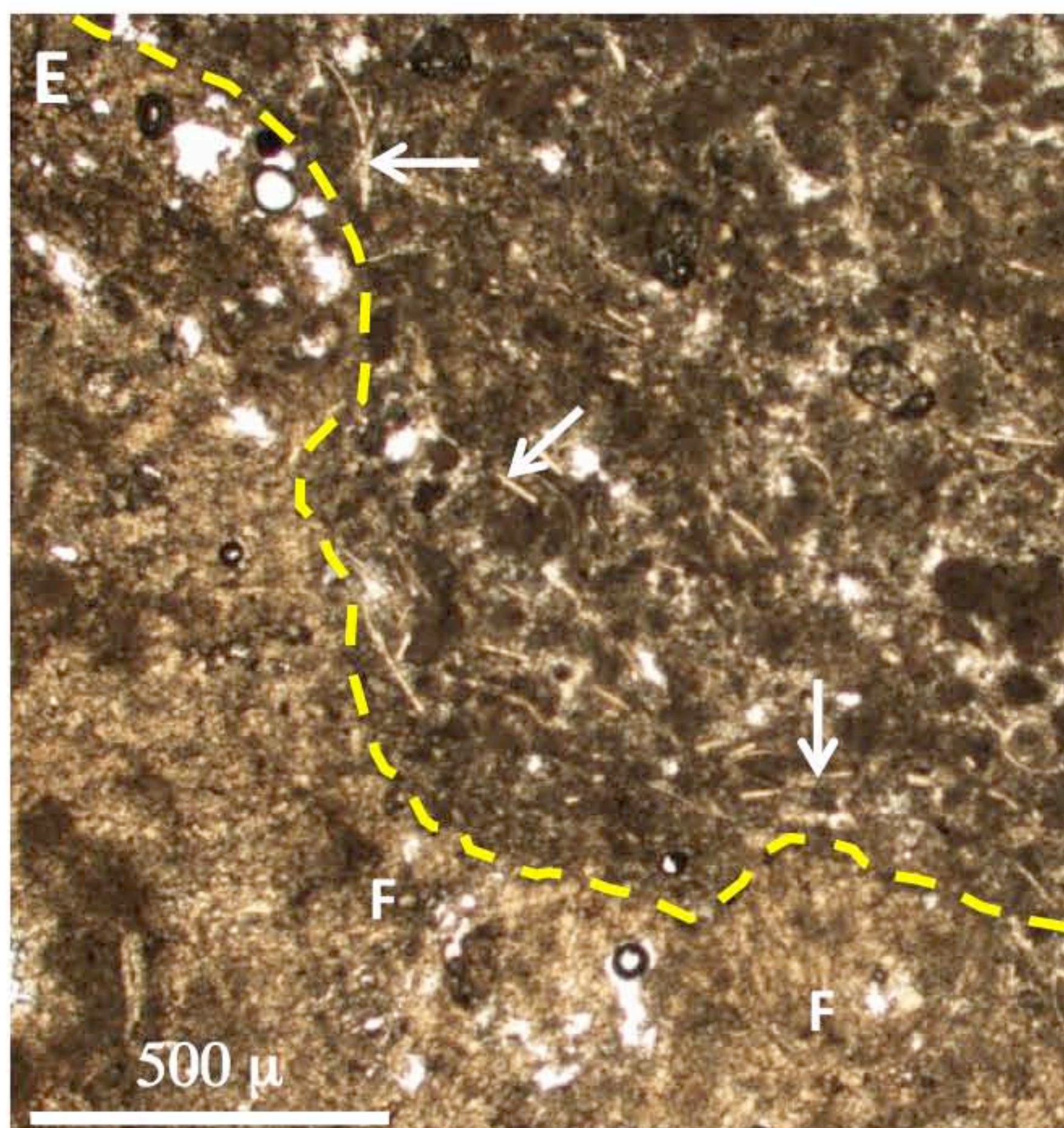
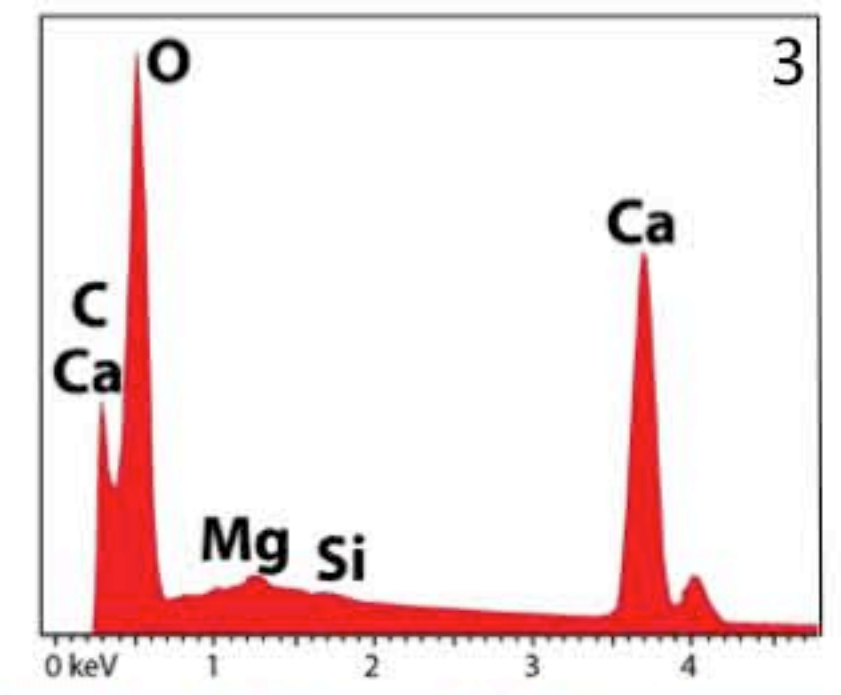
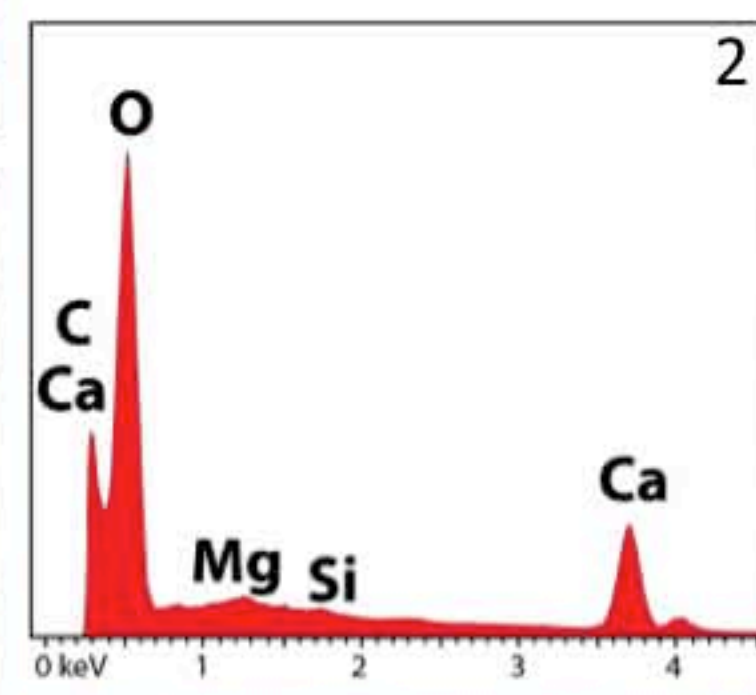
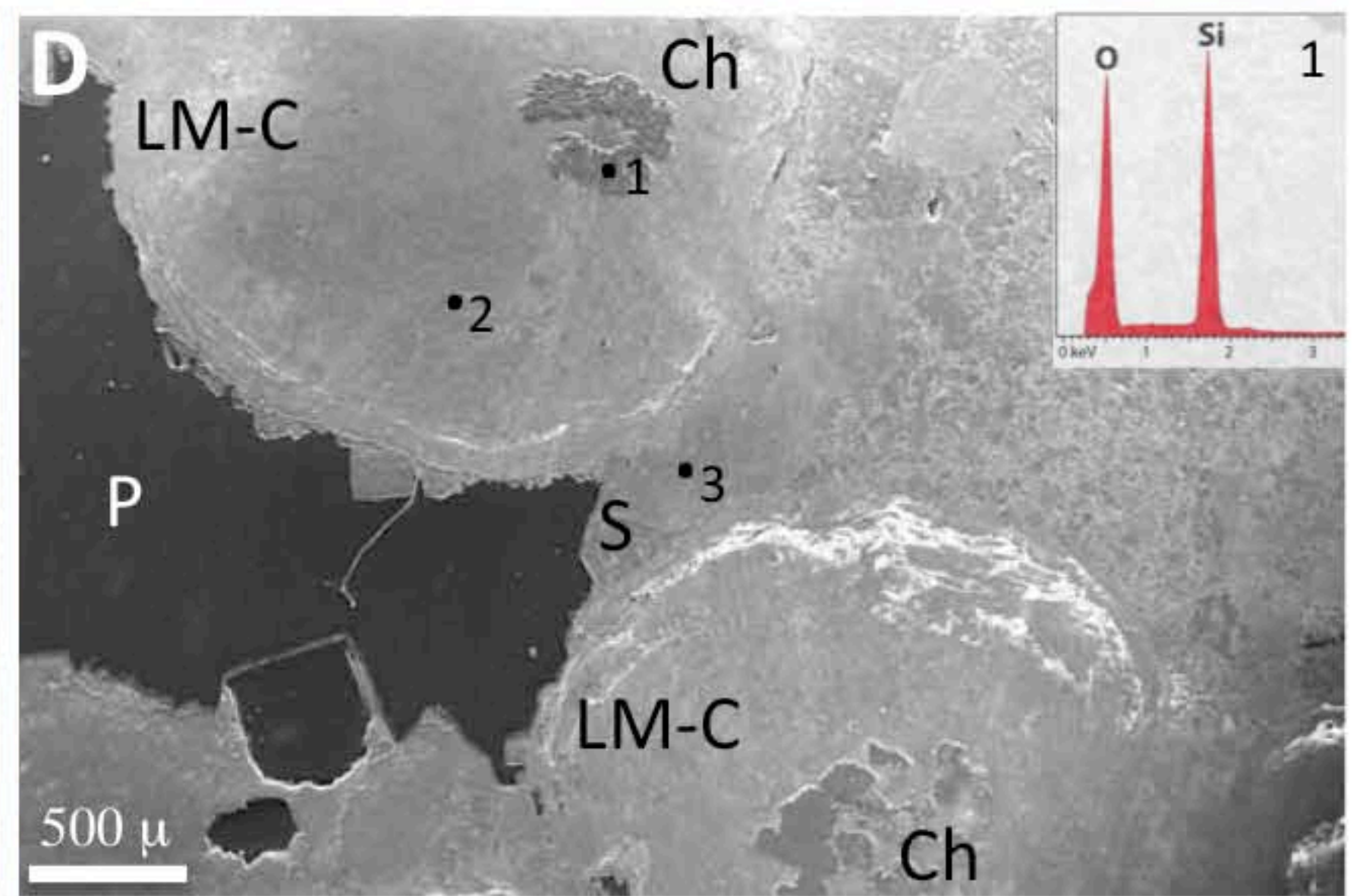
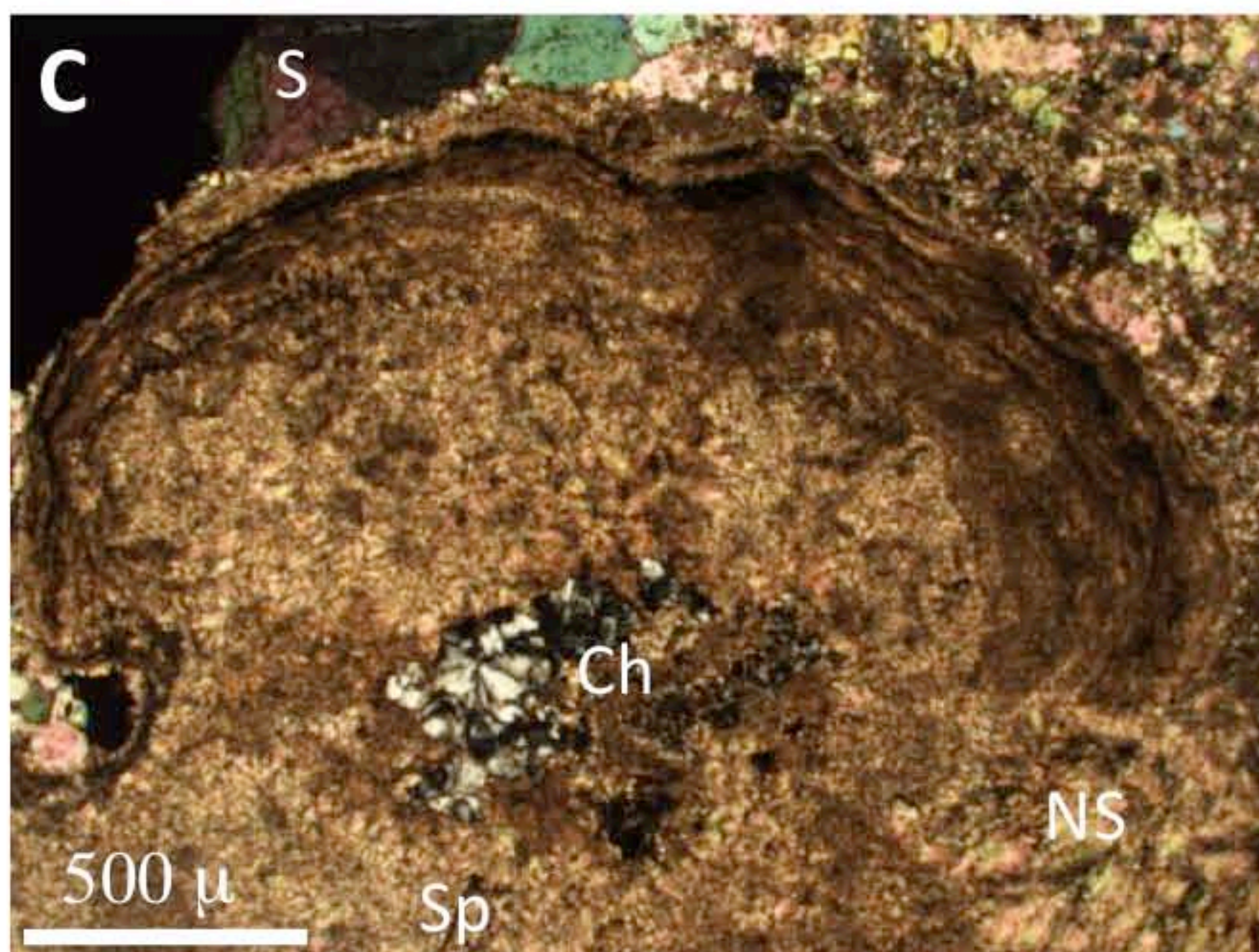
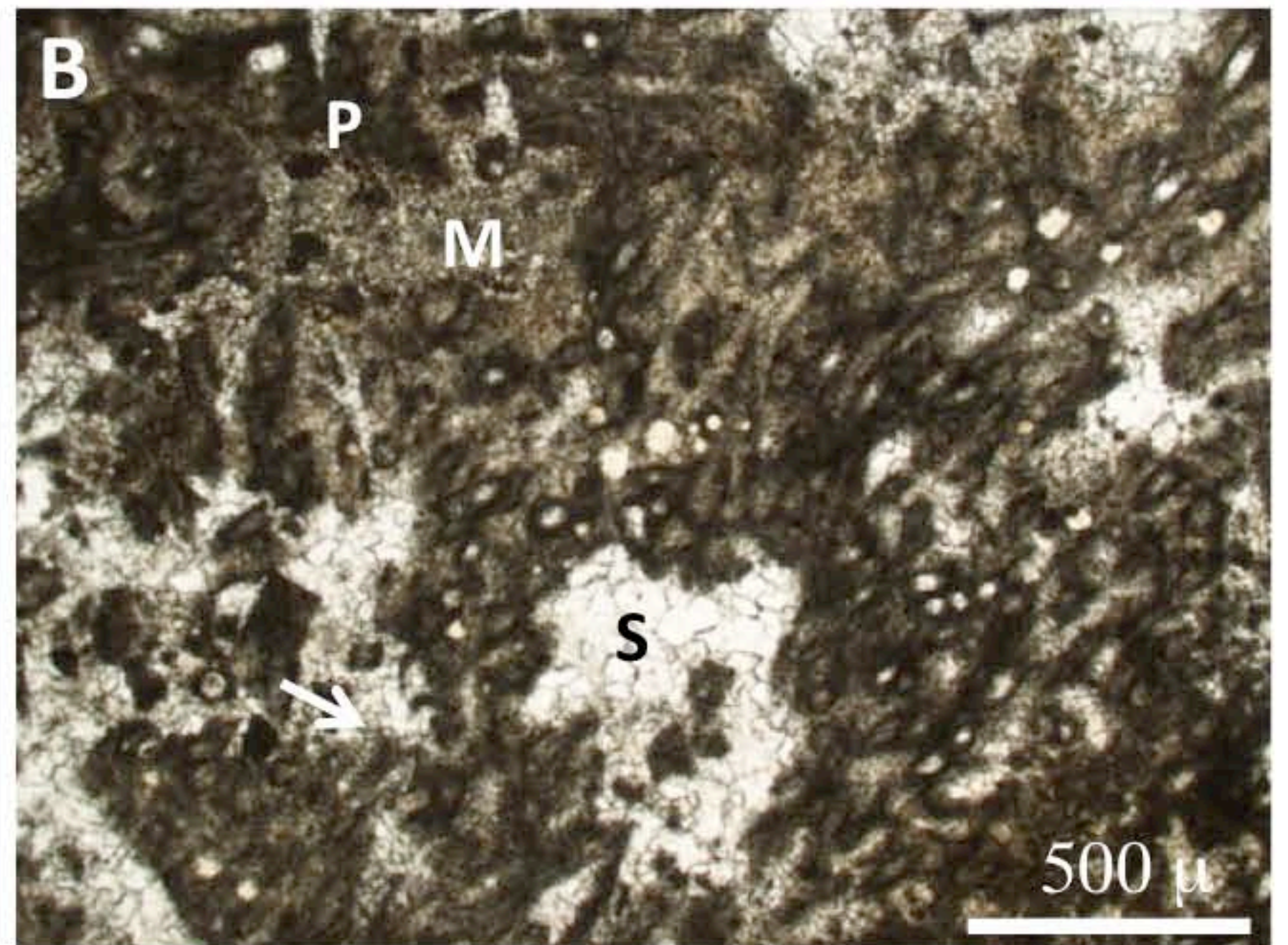
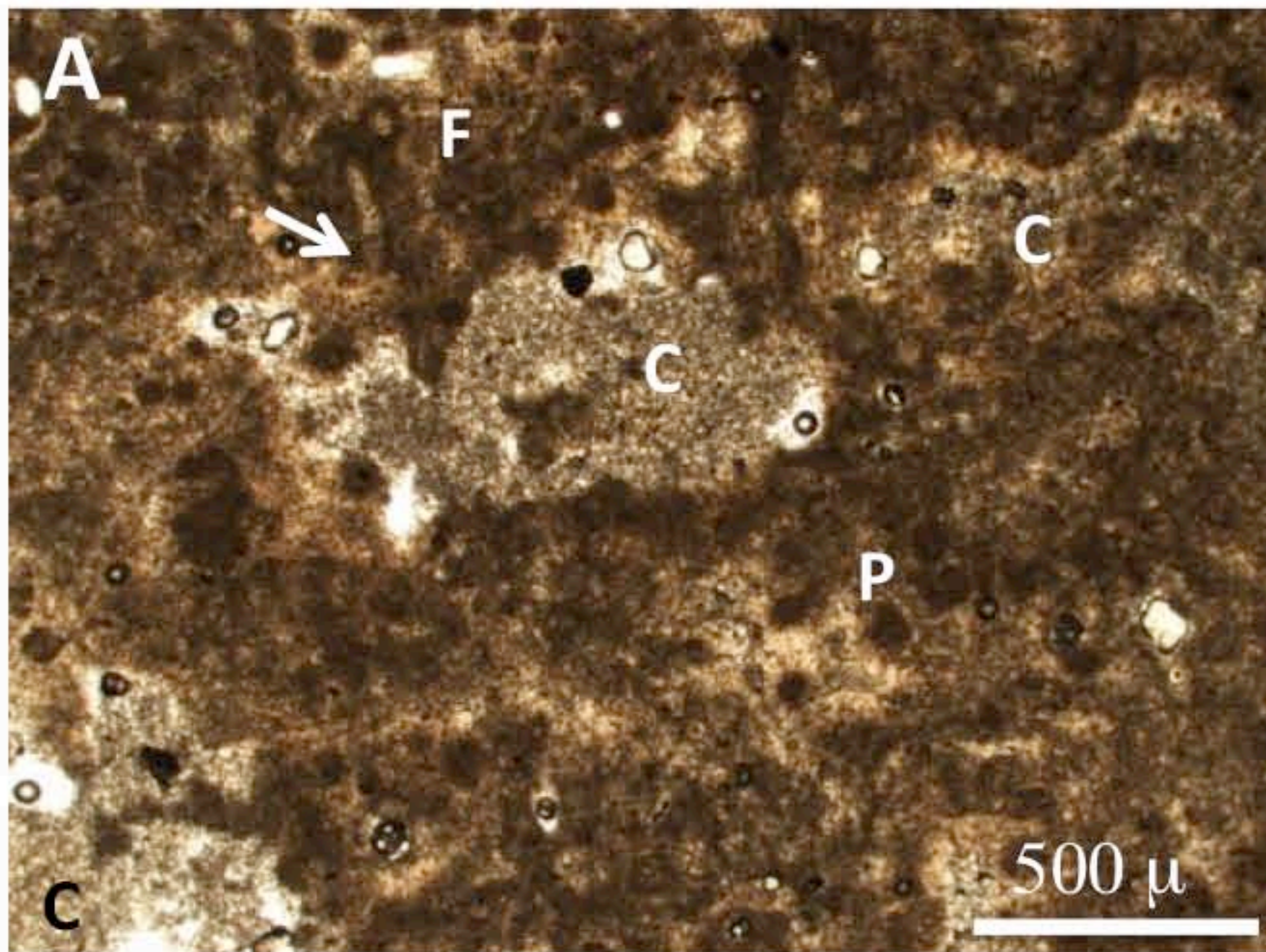


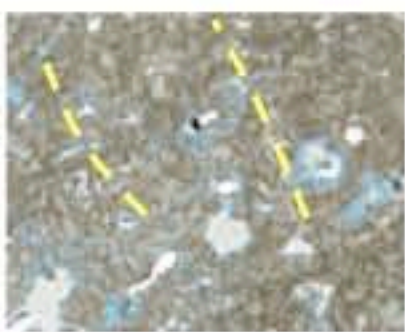




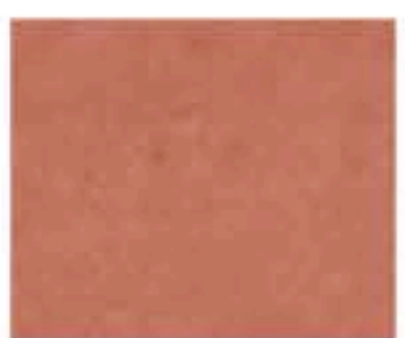




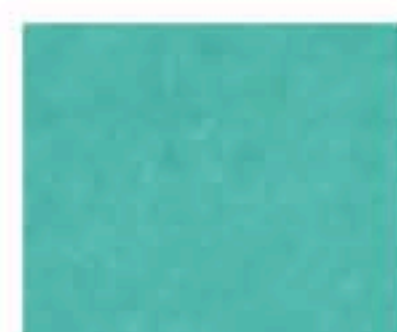




Cladophorites Thrombolite (CTh) with filament orientations (dashed lines) and spar filled framework cavities



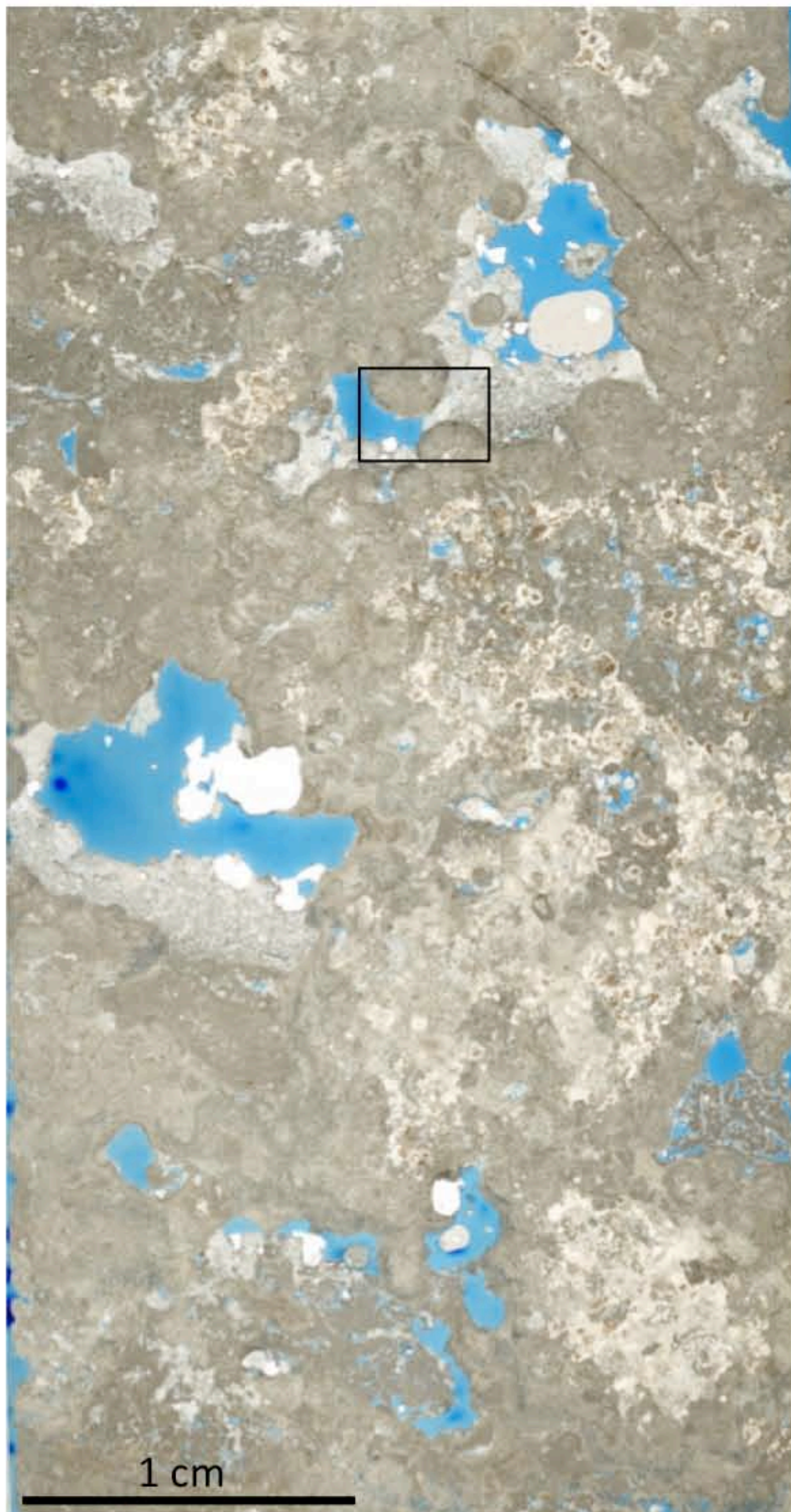
Dense Micritic Leolite crust (DMLc) with skeletal debris overgrowing CTh f



Peloidal Thrombolite (PTH) framework with filled and open fenestrae



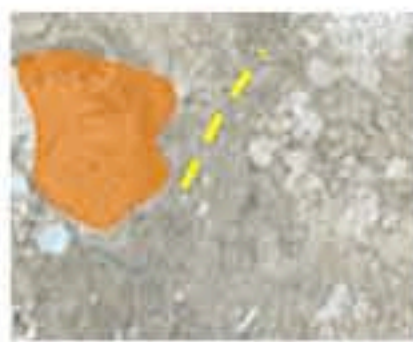
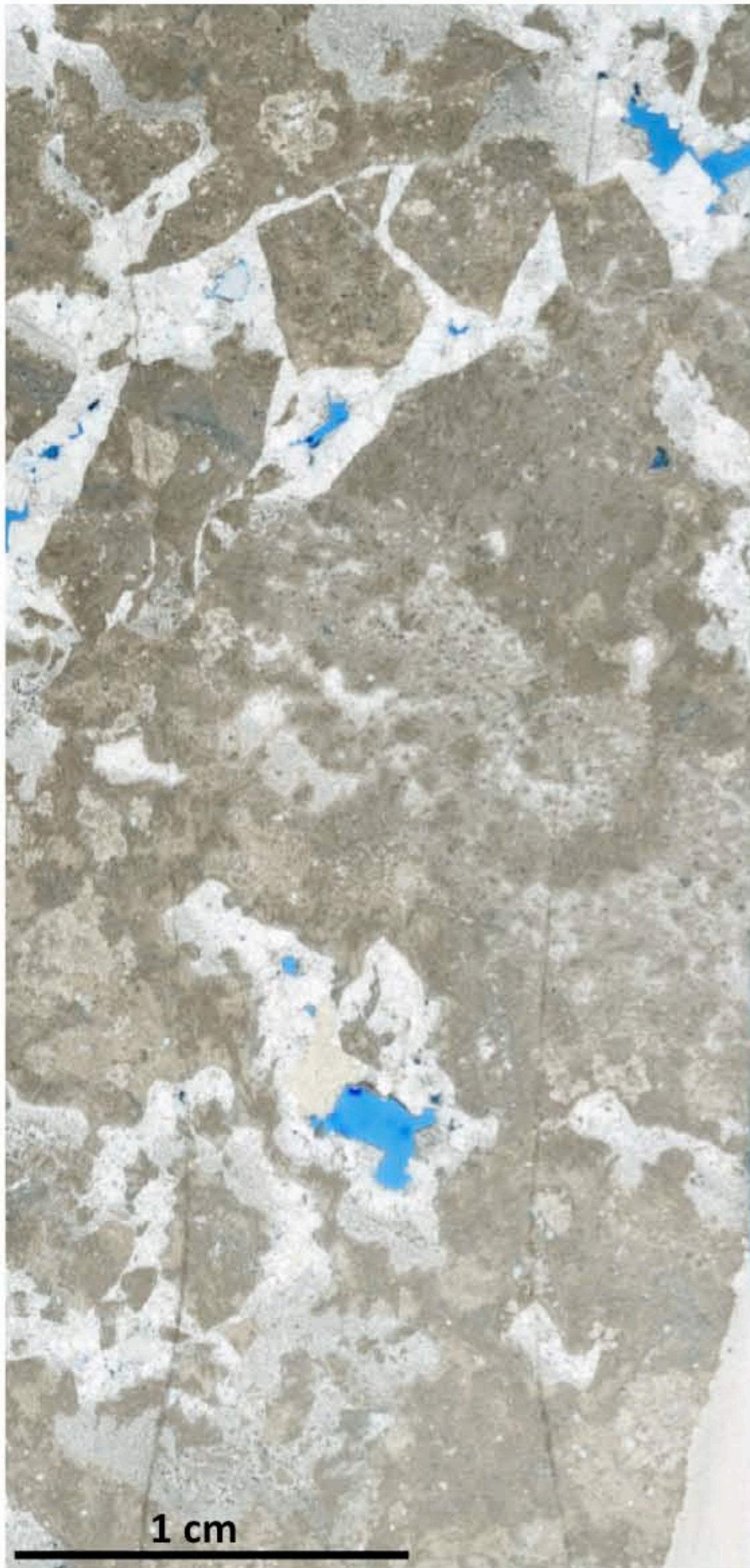
Packstone with peloids, thrombolite intraclasts and filament debris



Concentrically Layered Thrombolite (CLTh) with accretion layers (dashed lines) and replaced by clusters of quartz spherulites (brown)



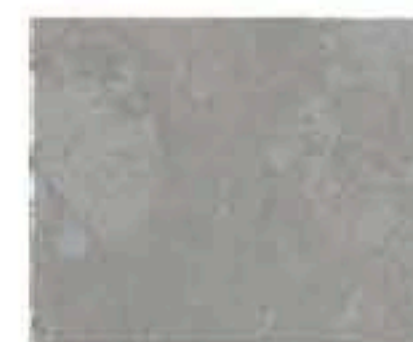
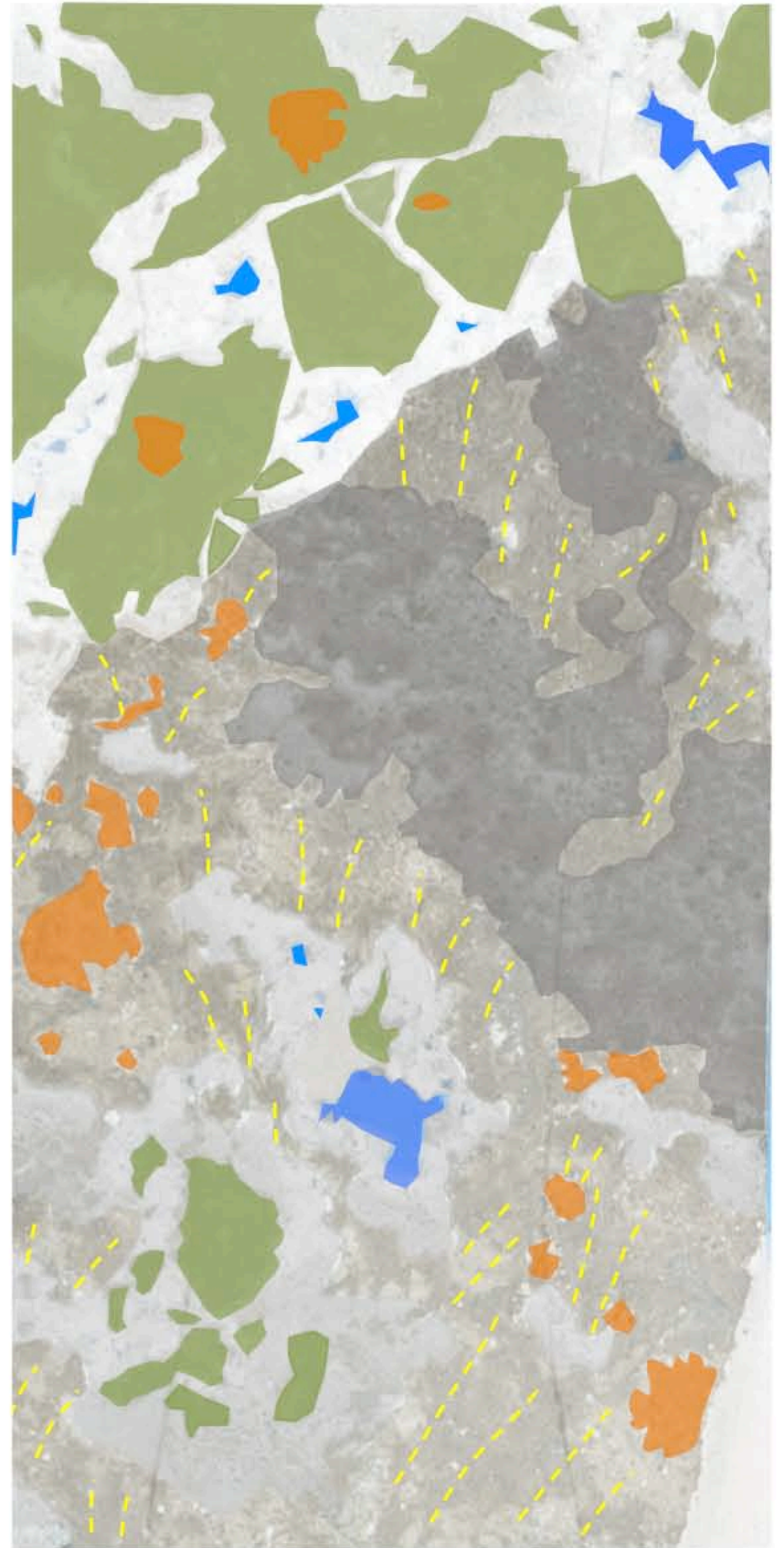
Primary framework cavities. Variously filled with fibrous cement fringe, geopetal sediment, spar and pore space.



Cladophorites Thrombolite (CTh) framework with filament orientations (dashed lines), quartz spherulites (brown)



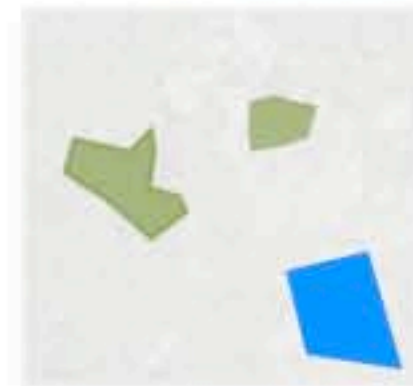
Thrombolite fragments/intraclasts



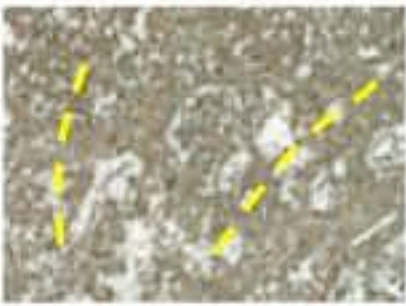
Cavity stage 1 infilled with fibrous fringe cement, intraclasts, peloids, spherulites and spar cement



Cavity stage 2 with fibrous fringe cement, geopetal infill, spar and some pore space (blue)



Cavity stage 3 with brecciated thrombolite (green), geopetal infill, spar and pores (blue)



Cladophorites Thrombolite (CTh) with filaments (dashed lines) and spar filled framework cavities



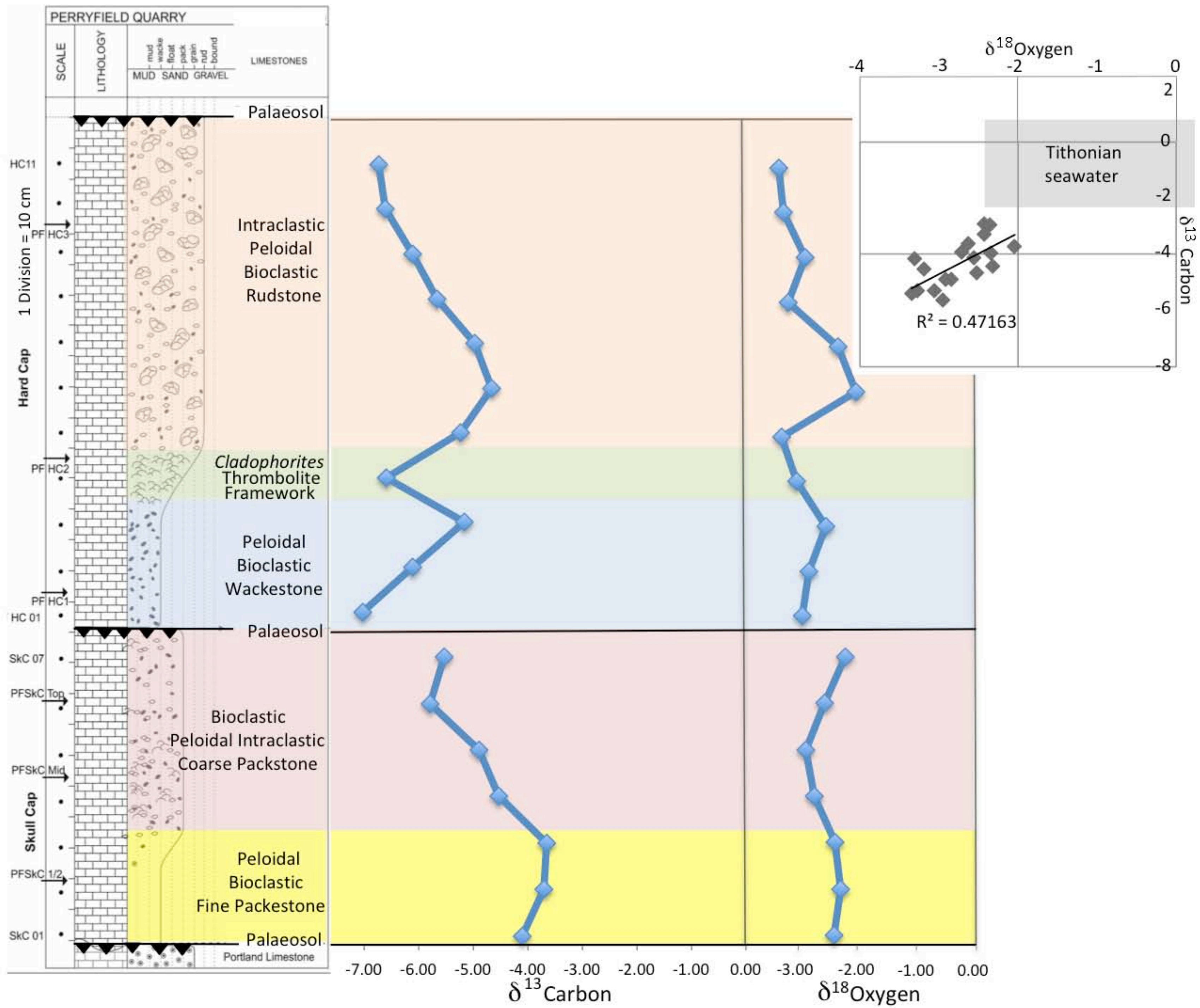
Intraclasts of Peloidal Fenestral Stromatolite (PFS) in matrix of small intraclasts, peloids, and spar cement

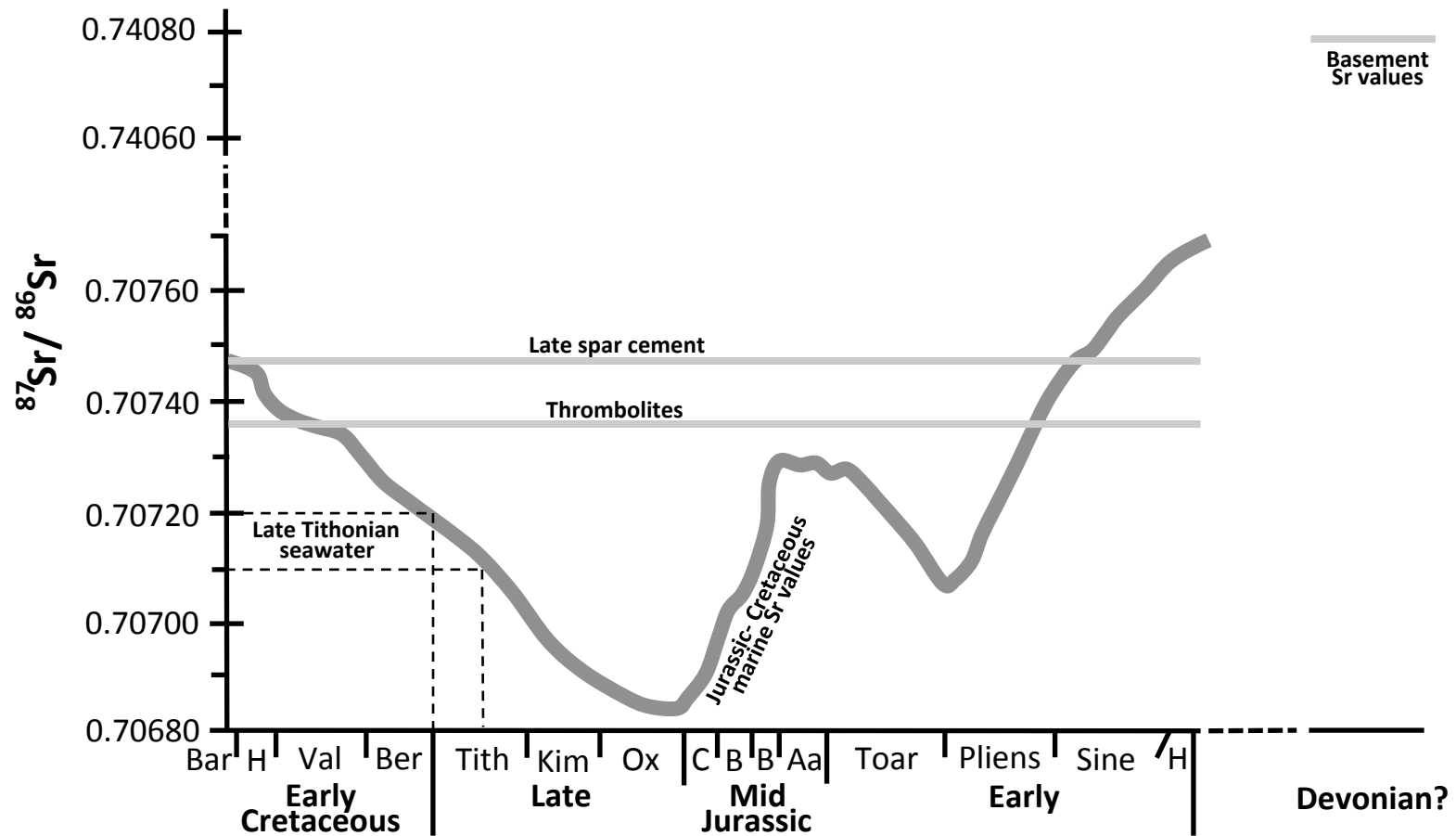


Thrombolite fragments/intraclasts in matrix of small intraclasts, peloids and spar cement

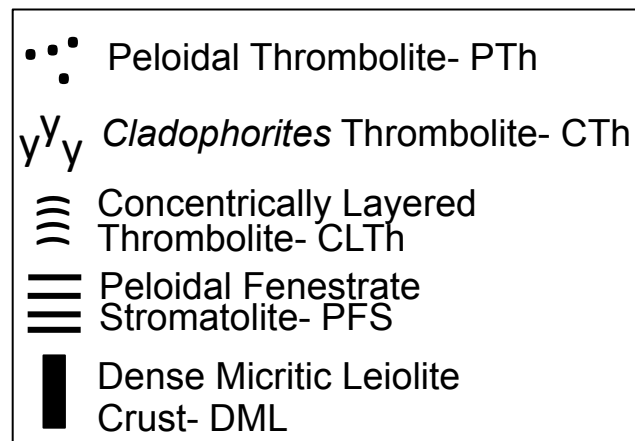
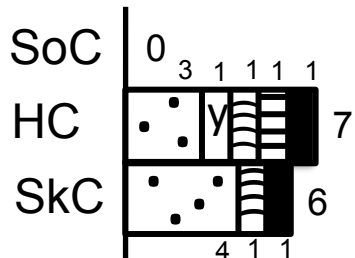


Packstone with peloids, thrombolite intraclasts and filament debris

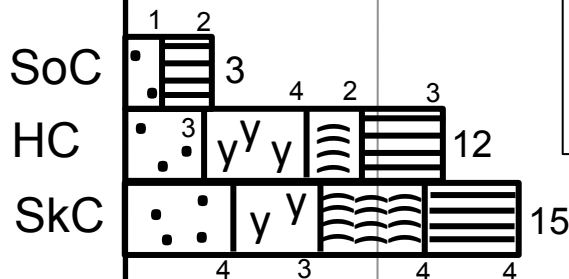




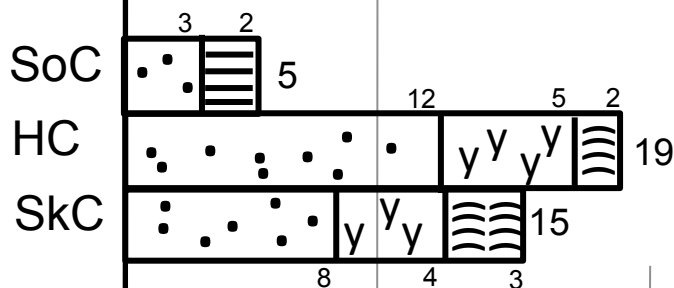
Western Area
(PQ, C, POQ)



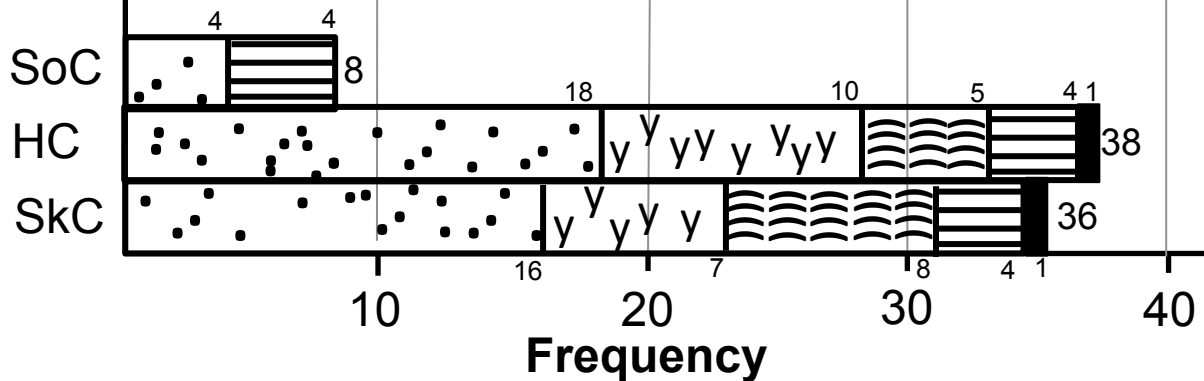
Eastern Area
(WLC, FF, MB, WT
HB, SQ, FL)

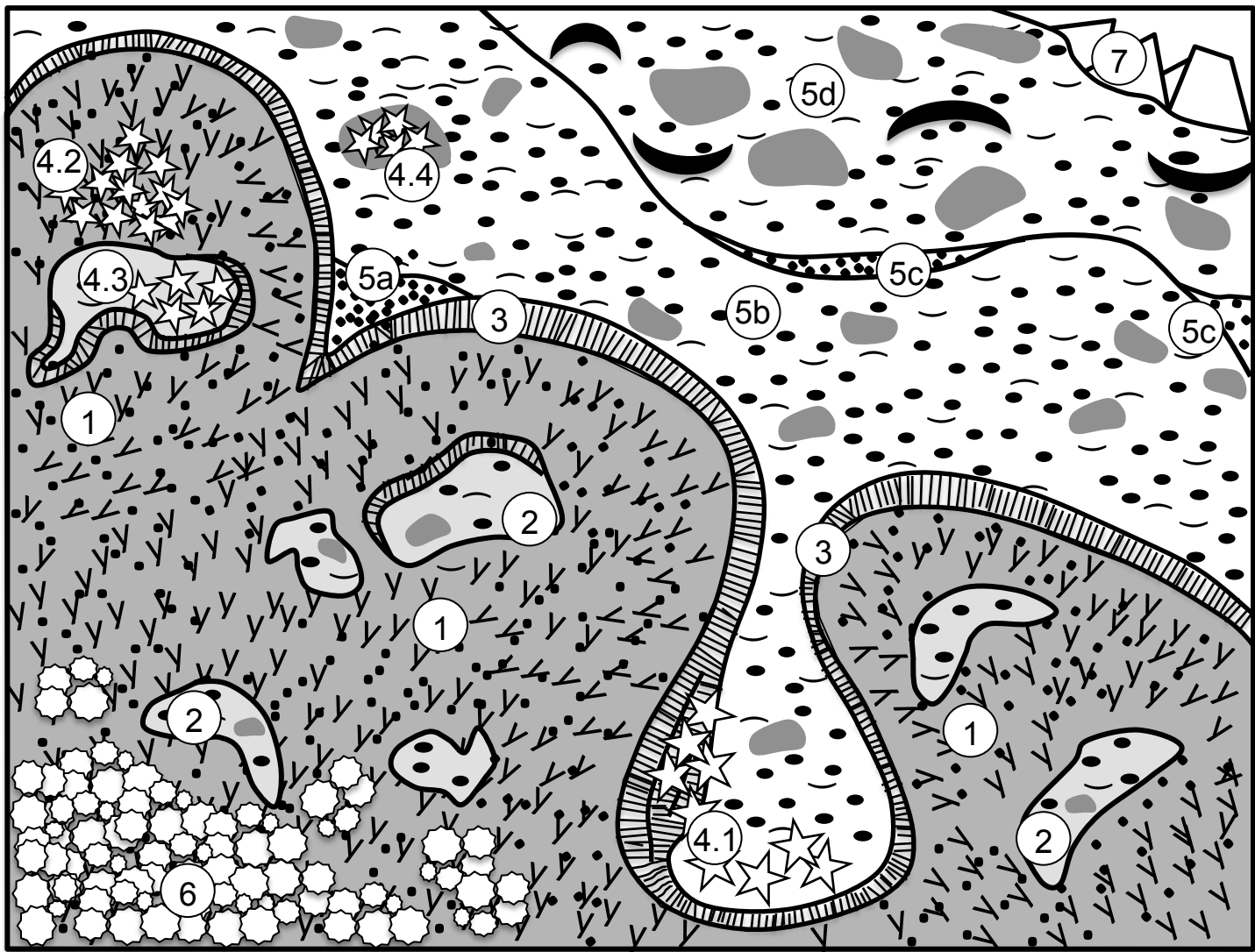












Isle of Portland
(CQ, GN, KB, LQ,
PB, SWB, SQ, TQ)



Totals (n=82)





- | | | |
|--|--|--|
| <p>① Thrombolite framework </p> <p>② Cavity </p> <p>③ Fibrous cement </p> | <p>④ ☆ Calcite spherulites</p> <p>④.1 type 1 to ④.4 type 4</p> <p>⑤a to ⑤d Internal sediments:</p> <p>peloid  microspar </p> <p>ostracod  mollusc </p> <p>intraclast </p> | <p>⑥ Quartz spherulite </p> <p>⑦ Coarse spar cement </p> |
|--|--|--|